Efficient Routing Algorithms in Vehicular Ad Hoc Networks

A thesis submitted in partial fulfillment of the requirements for the degree of Master of Science in Computer Science

Master Degree Candidate

Yashar Ghaemi

Supervisor

Dr. Hosam El-Ocla

Lakehead University

Department of Computer science

Thunder Bay, Ontario

September 2021

Abstract

During the last decade, the research on Intelligent Transportation System (ITS) has improved exponentially in real-life scenarios to provide optimized transport network performance. It is a matter of importance that the emergency messages being delivered in a timely manner to prevent vehicular traffic problems. The fact is an ITS system per se could be a part of a vehicular ad hoc network (VANET) which is an extension of the wireless ad hoc network. Therefore, similar to the other ad hoc networks, the nodes in the network can send data packets to each other through intermediate forwarding nodes. In all sorts of wireless ad hoc networks, the network topology is subjected to change due to the mobility of network nodes; therefore, an existing explored route between two nodes could be demolished in a minor fraction of time. When it turns to the VANETs, the topology likely changes due to the high velocity of nodes. On the other hand, time is a crucial factor playing an important role in message handling between the network's nodes. In this regard, we propose centralized ITS Multi-Path Routing Protocol for VANETs (MPRP) that effectively identifies an optimized path for packet delivery to the destination vehicle with a minimal time delay. Our algorithm gives a higher priority to the alert messages compared to normal messages. As a result, our algorithm would realize two goals. Firstly, speed up the data transmission rate and deliver data packets, particularly warning messages, to the destination vehicle promptly and therefore avoids vehicular problems such as car accidents. Secondly, the MPRP algorithm reduces the data traffic load, particularly of the normal messages, to alleviate the pressure on the network and therefore avoids network congestion and data collisions. This, in turn, lessens the packets' retransmissions. MPRP is a Road-Side Units (RSU)-enabled routing protocol in which RSU plays the rule of the central routing unit on each road section. In this regard, each road segment is equipped with an RSU node with a limited coverage spectrum. Moreover, during this study, we discovered several metrics impacting the performance of the network. The vehicular mobility speed has a crucial impact on the performance of the data communication through the VANET. However, in VANETs, nodes' mobility speed could be higher than other forms of ad hoc network. The mobility of nodes is more predictable due to the roads' structure and constraints; therefore, mobility speed is not the only reason behind the topological changes. Nodes density has another influential factor on the network topology and scalability so that a highly dense environment is

susceptible to having data collision and congestion. On the contrary, a lowly dense environment is vulnerable to having low nodes connectivity. Having network congestion itself is an essential factor in network performance. Therefore, we consider these factors and propose a new routing protocol based on MPRP discussed earlier. The main objective of the proposed protocol is to introduce a robust routing protocol to improve the route selection mechanism by considering the metrics such as nodes mobility speed, nodes density, and potential data congestion at intermediate nodes. In this regard, we introduce a new fitness function (FFn) as the optimization base for the genetic algorithm (GA) and hence propose two mechanisms which are MPRP-FFn and MPRP-GA. To demonstrate the effectiveness of the proposed protocol, the MPRP has been compared with the other protocols such as Ad hoc On-demand Multi-Path Distance Vector (AOMDV), Energy Efficient Multi-Path Routing Protocol for Mobile Ad-Hoc Network Using the Fitness Function (FF-AOMDV), Efficient Geographic aware Source Routing (EGSR), Q-learning based Multi-objective optimization Routing protocol (QMR). The results of the proposed protocols of MPRP-GA and MPRP-FFn are compared with two recent protocols of Topological change Adaptive Ad hoc On-demand Multipath Distance Vector (TA-AOMDV) and Elephant Herding Optimization Ad Hoc On-Demand Multipath Distance Vector Routing Protocol (EHO-AOMDV) as well as MPRP. The performance evaluation of proposed protocols took place on parameters such as simulation time, the number of nodes, maximum allowance mobility speed, variant number of application sinks (number of nodes sending packets), and variable packet sizes to calculate different quality of service (QoS) metrics like throughput, end-to-end delay, packet Loss Ratio (PLR), and routing overhead. Simulation results demonstrate that our proposed protocol proves its excellent performance compared to other protocols.

Acknowledgement

I am honored to express my gratitude to my supervisor, Dr. Hosam El-Ocla, for his patience, guidance, and support. I have significantly benefited from his wealth of knowledge and meticulous editing. I am incredibly grateful that he took me on as a student and continued faith in me throughout this thesis. I also appreciate faculty members of the Computer Science department for their support.

Dedication

I want to dedicate this dissertation to my wife (Zahra), who accompanied me through this journey with patience and hard work. I am so grateful to my parents (Bahram and Kaynoosh) for their support and presence, without whose I never had this chance.

Contents

List of Figures

List of Tables

Acronyms

AODV . . . . Ad-hoc On-demand Distance Vector

AOMDV . . . . Ad hoc On-demand Multi-Path Distance Vector

AOMDV-FFn . . . . On-demand Multipath Distance Vector by employing fitness function

AOMDV-GA . . . . On-demand Multipath Distance Vector by employing genetic algorithm

AOMR-LM . . . . Ad-hoc On-Demand Multi-Path Routing with Life Maximization

ARWO . . . . multi-objective auto-regressive whale optimization

BP . . . . back-pressure

BRFD . . . . Bayesian-based Receiver Forwarding Decision

C-V2X . . . . cellular Vehicle-to-everything

CCN . . . . content-centric networking

Congestion-aware FMLB . . . . congestion-aware fibonacci multi-path load balancing

CRL . . . . certificate revocation list

CS . . . . content store

D-LAR . . . . Directional-Location Aided Routing

DD-LAR . . . . Distance and Direction based Location aided routing

DSDV . . . . destination-sequenced distance-vector

DSR . . . . dynamic source routing

DSRC . . . . Dedicated short-range communication

e2e . . . . end-to-end

EE-LB-AOMDV . . . . load-balanced multi-path routing protocol with energy constraints

EGSR . . . . Efficient Geographic aware Source Routing

EHO-AOMDV . . . . Elephant Herding Optimization Ad Hoc On-Demand Multipath Distance Vector Routing Protocol

FD-AOMDV . . . . Fault-Tolerant Disjoint Multi-Path Distance Vector Routing Algorithm

FF-AOMDV . . . . Energy Efficient Multi-Path Routing Protocol for Mobile Ad-Hoc Network Using the Fitness Function

FFn . . . . fitness function

FIB . . . . Forwarding Information Base

GA . . . . genetic algorithm

GFR . . . . greed forwarding routing

GIS . . . . geographic information systems

GPS . . . . Global Positioning System

GPSR . . . . greedy perimeter stateless routing protocol

GSR . . . . geographical source routing

GTLQR . . . . greedy traffic light and queue aware routing protocol

I2V . . . . infrastructure-to-vehicle

ISR . . . . Improved Road Segment-Based Geographical Routing Protocol for Vehicular Ad-hoc Networks

ITS . . . . Intelligent Transportation System

LBMMRE-AOMDV . . . . Load balancing maximal minimal nodal residual energy ad hoc on-demand Multi-Path distance vector routing protocol

LENC . . . . low-latency and energy-efficient routing based on network connectivity

LFPM . . . . link failure prediction mechanism

LLECP-AOMDV . . . . link lifetime and energy consumption prediction Ad hoc On-demand Multi-Path Distance Vector

LOA . . . . lion optimization algorithm

LORP . . . . Lion optimization routing protocol

M-GEDIR . . . . Multi-metric Geographic Routin

M-GOR . . . . multilevel-scenario-oriented greedy opportunity routing protocol

MANETs . . . . mobile ad hoc networks

MM-GPSR . . . . Maxduration-Minangle GPSR

MPR . . . . multipoint relays

MPRP . . . . centralized ITS Multi-Path Routing Protocol for VANETs

NDN . . . . Named Data Network

NFD . . . . NDN forwarding-daemon

NOLSR . . . . new optimized link-state routing protocol

OBU . . . . On-Board Units

OLSR . . . . optimized link-state routing protocol

PDR . . . . packet delivery ratio

PIT . . . . pending interest table

PLR . . . . packet Loss Ratio

PVARR . . . . Parked Vehicle Assistant Relay Routing

QMR . . . . Q-learning based Multi-objective optimization Routing protocol

QoS . . . . quality of service

RCER . . . . Reliable Cluster-based Energy-aware Routing

RPSPF . . . . Reliable Path Selection and Packet Forwarding Routing Protocol

RREQ . . . . route request packet

RSU . . . . Road-Side Units

RTT . . . . round trip time

SA-RSU . . . . standalone RSU

STB . . . . sojourn time backlog

STBP . . . . delay-optimal back-pressure routing algorithm for multihop wireless networks

SUMO . . . . Simulator of Urban Mobility

TA-AOMDV . . . . Topological change Adaptive Ad hoc On-demand Multipath Distance Vector

TCP CERL+ . . . . TCP congestion control in wireless networks with random loss

TIHOO . . . . An Enhanced Hybrid Routing Protocol in Vehicular Ad-hoc Networks

TMED . . . . spider-web-like transmission mechanism for emergency data

TNS . . . . tabu node search

TORA . . . . temporally ordered routing algorithm

V2I . . . . vehicle-to-infrastructure

V2V . . . . vehicle-to-vehicle

VANET . . . . vehicular ad hoc network

VID . . . . vehicle ID

VTDF . . . . vehicle tracking data forwarding

WBANs . . . . Wireless Body Area Networks

ZRDM . . . . zone-based route discovery mechanism

Chapter 1

Introduction

In recent years, Intelligent Transportation Systems (ITSs) in Vehicular ad hoc networks (VANETs) have become a popular and vital research topic in the transportation industry [1]. ITS is an advanced application that facilitates nodes mobility in a network at high velocity. In ITS, vehicles interact and communicate with each other to deliver messages for various purposes such as alerts, traffic jams, and accident zones on the road. Vehicular ad hoc networks are established with mainly two types of communication, i.e., vehicle-to-vehicle (V2V) communication and vehicle-to-infrastructure (V2I) communication [2]. V2I communication is used among the deployed vehicles with On-Board Units (OBU) in the system. V2I communication is used for the interaction between vehicles and Road-Side Units (RSU) [3]. Both V2V and V2I communications consist of two types of messages, viz., normal messages, and emergency messages. The normal messages are sent to the RSU and other vehicles in the same range, and these messages include the speed and Global Positioning System (GPS) information. The emergency messages contain collision details and must be sent to other responders to act promptly. As a result, the accident notification is sent before the normal message to the concerned destination vehicle. VANET communicates with high-speed moving nodes and alongside RSU, where packet delivery should be maximized with the least tolerance for data loss [4, 5]. In the event of an accident, the data must be sent to all nodes in the network as soon as possible since time plays a major role in avoiding vehicle collisions, particularly on the highway. A Multi-Path routing protocol is capable of handling high loads of data, balancing the data traffic, and managing time better than a single path routing protocol. In the case of having a node or link failure, Multi-Path protocols provide alternative routes without going through the route discovery phase and this enhances the network performance compared to the single route mechanisms such as the Ad-hoc On-demand Distance Vector (AODV) protocol. In [6], the authors describe VANETs are being categorized as a sub of mobile ad hoc networks (MANETs). Routing in VANETs must be able to improve the efficiency of the traffic and provide an infotainment facility as well.

Because of having data traffic problems, including data congestion and packet collisions, the data transmission time increases. As a result, this would magnify the possibility of having vehicle traffic problems and car accidents when warning messages are not arriving at their destinations on time. It should be noted that data congestion and collision are two reasons for having packet loss in a wireless network in addition to random loss. In all these cases, data packet retransmission increases the traffic load on the network and hence the chance of having more traffic problems [7]. This, in turn, would degrade the performance in terms of the end-to-end delay and the throughput leading to have vehicle traffic problems that should be avoided.

Based on the minimum number of hops, Ad hoc On-demand Multi-Path Distance Vector (AOMDV) provides alternative routes in case of having a channel disconnect. However, it does not consider the status of the nodes in the sense of having traffic problems. In this thesis, we propose a centralized ITS where vehicles can send data to RSU, which in turn would convey to other vehicles. RSU will use centralized ITS Multi-Path Routing Protocol for VANETs (MPRP) for data communication in an infrastructure-to-vehicle (I2V) mode in case of emergency messages. The main aim of MPRP is to deliver data messages by selecting the most optimized path in the network. MPRP is a reactive protocol where round trip time (RTT) measurement is utilized to select the shortest path. Whenever the RSU needs to send a message to the destination vehicle, the optimized route is found based on the least RTT to transmit a message to the destination. Minimum RTT implies passing through nodes with the least traffic data. Additionally, MPRP algorithm lessens the amount of data packets to avoid network congestion and data collisions of data packets. Therefore, MPRP will speed up the data transmission needed particularly to be less than the vehicle speed and hence avoid any delay of the alert messages. This would certainly alleviate the possibility of vehicle traffic problems. In doing this, a dynamic threshold should be met to find a route; otherwise, RSU should wait a backoff time before repeating the discovery phase, and hence the intermediate vehicles are getting closer with less traffic. Therefore, our proposed routing MPRP algorithm can achieve the following contributions:

- Prioritize ITS emergency messages compared to normal packets. As a result, deliver both emergency warning and data packets in VANET environment in a timely manner to avoid vehicular traffic problems,
- Select the shortest route that has the minimum time delay and, therefore, speed up the data transmission,

- MPRP uses the minimum RTT to select the optimized route, and as a result, it can adapt to the topological change,
- Our protocol reduces the traffic problems through using a threshold value where it should be higher than the RTT value to add its route to the efficient routes array.
- Minimize the data traffic load through reducing the retransmission data packets and therefore enhance the network performance.

The analysis of MPRP proves promising results and works better under different network performance metrics such as end-to-end delay, packet delivery ratio, packet loss ratio, throughput, and routing overhead compared to other protocols like AOMDV, Energy Efficient Multi-Path Routing Protocol for Mobile Ad-Hoc Network Using the Fitness Function (FF-AOMDV), Q-learning based Multi-objective optimization Routing protocol (QMR), Efficient Geographic aware Source Routing (EGSR) and Improved Road Segment-Based Geographical Routing Protocol for Vehicular Ad-hoc Networks (ISR) which represented in chapter 4.

There are several characteristics that distinguish a VANET from a MANETs such as high nodal mobility speed, shared wireless spectrum and channels, dynamic topological change [8] and having various nodal densities. Therefore, to design an efficient data routing protocol for a VANET network, we need to include some of the given features in our design. In this regard, we consider nodal mobility speed and density in addition to network congestion to optimize the routes in the network.

In chapter 5, we propose a routing protocol in which the first challenge we considered is the vehicular mobility speed. A higher speed causes having a faster topological change in the network which results in a link failure [9–12]. To combat this challenge, we propose a route selection method in which a route with a limited nodal mobility speed is likely to be selected. Also, we assign the number of intermediate vehicular nodes in the sender's region is considered as a metric to measure the network connectivity. It should be noted that the chance of having a data collision and congestion is increased when the density of nodes in one region increases. On the other hand, when we have an environment with a lower nodes density, the chance of a link failure increases due to a lack of nodes connectivity [13–15]. Our algorithm provides a compromised performance between these two extremes.

Having network congestion is a crucial incident impacting negatively on the network performance. Hence, another challenging metric we have considered in our routing protocol is data congestion to avoid data loss, particularly in urgent situations such as reporting vehicular accidents on the highways. Additionally, our mechanism would delimit the bottleneck queuing delay that occurs in case of data congestion. For this purpose, we use the TCP congestion control in wireless networks with random loss (TCP CERL+) [16] to select paths with the least congested nodes.

Chapter 5 introduces a new fitness function (FFn) as our route optimization mechanism and it is employed on MPRP (MPRP-FFn) to obtain the route with the best weight within the discovered routes. Also, we combined MPRP with the genetic algorithm (MPRP-GA) based on the proposed FFn. MPRP protocol selects the routes based on the minimum RTT and hence the FFn is employed to produce a pool of the selected routes that have the highest fitness weight. MPRP-GA goes through the crossover and mutation phases to discover more efficient paths. The contributions of our proposed routing protocols are noted briefly as follow:

- A new fitness function is introduced and engaged as the optimization mechanism. The fitness function contains three important metrics of data network congestion, nodes (vehicular) connectivity, and vehicular mobility.
- Proposing two complementary protocols to MPRP introduced through employing FFn: (MPRP-FFn) and (MPRP-GA).

1.1 Thesis organization

The remaining chapters of the thesis are structured as follows: Chapter 2 presents a literature review. The simulator tool, QoS metrics definitions and implemented classes are introduced in chapter 3. Chapter 4 proposes MPRP routing protocol and provides results comparison of different network scenarios. Chapter 5 discusses the MPRP-FFn and MPRP-GA characteristics. A brief conclusion for this thesis is noted in chapter 6

Chapter 2

Background and Literature Review

A variety of algorithms and protocols have been proposed over the years to improve the data communication performance in VANETs. To overcome different challenges in VANET, various researchers proposed and improved different approaches.

2.1 Topological approach:

In [17], the authors proposed a new protocol named Load balancing maximal minimal nodal residual energy ad hoc on-demand Multi-Path distance vector routing protocol (LBMMRE-AOMDV) which is an extended version of the AOMDV protocol. The protocol consists of two phases. The first generates disjoint link paths and maintains them in case of having one or more path failures. The second phase balances the data load among the generated link-disjoint paths. Through these phases, the protocol evaluates the generated paths to determine the maximal nodal residual energy and the actual number of packets that can be transmitted over that path without depleting the nodes' energy. Results achieve better performance in terms of packet delivery ratio, and energy consumption while taking into account the number of dead nodes [18]. However, it suffers from a long end-to-end delay. Thus, the authors recommend using this protocol in applications such as banking and online shopping than generic applications.

In [19], the author proposed a protocol based on nodal connectivity. The advantage of the work is that the given protocol is independent of the global network information. Every node relies on the data collected by itself to calculate the connectivity factor, which is used to avoid broadcast storming of the routing packets during the route discovery phase. This protocol solely studies the proposed connectivity factor on a single path routing protocol. In case of having a faulty node in the selected route, the route discover process has to start over again and this in turn would degrade the performance of the network in the sense of throughput and latency.

In [20], the authors presented a hybrid protocol that is based on the AODV algorithm using fuzzy logic named An Enhanced Hybrid Routing Protocol in Vehicular Ad-hoc Networks (TIHOO) to restrict the phase of route discovery. This algorithm is efficient and improves performance. However, it is rather a complex algorithm and unrealistic as it obviously consumes energy and therefore reduces the node's lifetime.

On the other hand, the authors in [21] focused on reducing energy consumption using FF-AOMDV protocol with dragonfly topology. FF-AOMDV uses the fitness function to find the optimal multi-path routing. It has been proven that the FF-AOMDV algorithm produces better results in terms of energy consumption, packet delivery ratio (PDR), throughput, end-to-end delay, and routing overhead ratio when compared to AOMDV and Ad-hoc On-Demand Multi-Path Routing with Life Maximization (AOMR-LM). However, the fitness function spends a long processing time and therefore enlarges the end-to-end delay.

In [22], the authors presented a traffic-aware routing protocol in VANET by introducing multi-objective auto-regressive whale optimization (ARWO) algorithm. ARWO selects the best path from multiple paths by considering multiple objectives such as end-to-end delay, link lifetime and node distance in the fitness function. However, it suffers from network overload when there is high traffic and congestion on the routes since all the vehicles try to choose the best path to reach the destination.

In [23], Fault-Tolerant Disjoint Multi-Path Distance Vector Routing Algorithm (FD-AOMDV) was introduced. This algorithm finds the shortest path based on the residual energy of the intermediate nodes at the expense of the number of nodes of that selected path and, therefore, the transmission delay.

In [24], the authors presented a novel V2V-enabled resource allocation scheme based on cellular Vehicle-to-everything (C-V2X) technology to improve the reliability and latency of VANETs. The main challenge with this cellular-based V2V technique is how to allocate spectrum resources and broadcast opportunities properly in the V2V communication, so the network performance can be improved without causing disturbing interference to cellular users.

In [25], it was suggested a hierarchical failure detection mechanism based on the architecture of VANETs. The failure detector can adapt to the dynamic network conditions and meet the different quality of service (QoS) requirements of multiple applications in VANETs. By sharing messages among vehicles, communication link failures can be overcome, and detection accuracy is further improved. The major shortcoming of this mechanism is its routing overhead which increases as the number of detection messages increases.

In [12], the author proposed QMR routing protocol, a method based on Q-learning with a Multi-objective optimization mechanism. In this protocol, the author tries to take advantage of both proactive and reactive routing protocols to optimize the delay and the efficiency of the network. Each node in the network is equipped with GPS. Based on the measured distance and residual energy, each node can determine to forward the data packets. This protocol imposes a high load of routing overhead.

In [26], authors proposed a protocol named Lion optimization routing protocol (LORP). Firstly, this protocol selects the most maximized using lion optimization algorithm (LOA) routes by considering the three metrics of power efficiency, throughput and packet delivery ratio. Secondly, it uses LOA to minimize the routes based on the delay and hop count. Finally, it selects the optimized route considering minimized and maximized algorithms. However, the superiority of the multi-path scheme is proven [27]; this protocol overlooks this critical feature.

In [28], the authors proposed a protocol for Wireless Body Area Networks (WBANs) for monitoring a patient's vital signals. To establish a data transmission, the sensor node sends control packets to its neighbors. Neighbor nodes calculate a score based on the residual energy and the link state of neighbors and reply it back to the original sensor node with an acknowledgment. After receiving the acknowledgments, the sender forwards data packets to the neighbor node having the highest link weight. The link quality is being calculated based on the packet delivery ratio.

The authors proposed two protocols based on AOMDV by employing fitness function (AOMDV-FFn) and genetic algorithm (AOMDV-GA) [7]. The novelty of the study is the fitness function introduced as the optimization mechanism. These protocols optimize energy consumption, distance and network congestion. It also discriminates random loss from congestion. However, authors did not consider the impact of high density and speed of nodes on the data communication quality, particularly in VANETs.

The paper [29] introduces two mechanisms of zone-based route discovery mechanism (ZRDM) and link failure prediction mechanism (LFPM). The main objective of ZRDM is to indicate the threshold value of each zone, node classification, determine the minimum intermediate node. Regarding LFPM, the sender node constantly checks the connectivity by considering the distance, density and link stability. Its main objective is to use topological information such as mobility and mobility speed information, region node density and destination to end of the coverage area to utilize the network connectivity. ZRDM results in having lower routing overhead where LFPM increases the packet delivery ratio. This protocol is not showing significant improvement in end-to-end delay due to overlooking network congestion; therefore, this protocol is not suitable for time-sensitive environments such as VANETs.

The authors in [30] propose EHO-AOMDV. The main objective of this protocol is to increase the lifetime of the network. To achieve this aim, the protocol introduces a node classification mechanism. Every node in the network is placed in a clan according to its residual energy. This protocol fails to provide superiority in simulation results in end-to-end delay with the larger packet size.

In [31], the authors propose a protocol named low-latency and energy-efficient routing based on network connectivity (LENC). The LENC considers two metrics of latency and energy efficiency for every single route with the help of fuzzy logic. This protocol has a high complexity which needs high processing resources such as memory and CPU.

The AOMDV based protocol of link lifetime and energy consumption prediction Ad hoc On-demand Multi-Path Distance Vector (LLECP-AOMDV) is proposed in [32]. This protocol introduces a new energy consumption and prediction model. Additionally, it comes up with a link lifetime prediction mechanism. This mechanism brings the distance, mobility speed and direction of each two adjacent nodes into consideration. It is a probabilistic protocol that works based on network prediction. Despite the superior performance of this technique, it uses probabilistic models which is not always valid in real-world applications.

The main drawback of the topological approach is that mobility is an overlooked challenge in the design of routing protocols. In topological routing protocols, the network is being considered as a graph of nodes in terms of vehicles and edges, which are the connectivity between adjacent nodes. On account of the fact that the mobility in VANETs is fast, the constructed graph is subjected to change frequently. With the occurrence of a link failure, the graph needs to be reconstructed, which imposes a high cost in terms of routing overhead and end-to-end delay.

2.2 Road and traffic awareness approach:

In [33], the authors proposed a Multi-metric Geographic Routin (M-GEDIR) algorithm to select the next hop. The next node vehicle is selected from the dynamic forwarding region based on the probability of the area whether being safe or unsafe. It is a V2V communication where the roadside unit is not considered. This is an unrealistic approach as the processing time is long to determine the optimal path.

In [34], a mechanism was developed based on a combination of the intersection-based routing technique with the shortest path-based traffic light-aware routing protocol. The protocol was named Reliable Path Selection and Packet Forwarding Routing Protocol (RPSPF) by authors. Data packets are transmitted based on the traffic patterns and the traffic light signals along the intersection. The protocol could provide a high delivery ratio and throughput but has connectivity issues like the end-to-end connectivity among vehicles will be broken when one node goes away, leaving the network. Thus, vehicles should reconnect to communicate.

In [35], a Parked Vehicle Assistant Relay Routing (PVARR) algorithm was proposed to guarantee vehicle-to-vehicle communication in VANETs. Based on this algorithm, practical cooperation between stationary and moving vehicles prevents the network from having broadcast storms, increases resource utilization rate, and effectively diminishes load on the network. Results prove that the packet delivery ratio for the proposed protocol is high. This mechanism does not use RSU as intermediate nodes while the communication is rather running through parked vehicles in that network. Having parked vehicles on the road, particularly highways, is not always common. Therefore this protocol is not applicable if no parked vehicles are available on the road. On the contrary, using RSU can reduce the number of hops (because there is a range for each RSU), which simultaneously reduces the delay when compared to parked vehicles.

To enhance geographical source routing (GSR) protocol, research [36] proposed an efficient GSR (EGSR). This protocol has been designed mainly for urban areas, and it is assumed that every node in the network is equipped with a GPS and digital map. Additionally, it is assumed that the clocks of all nodes are synced. The proposed protocol uses the ant-colony optimization algorithm to find the optimum path between nodes in the network. Each node can calculate the weight of the road segments by a small packet called ant, which is generated by vehicles at the intersections. On the basis of the weight of every road segment, the sender selects the best road route to the destination. The road segment is constituted by distance and the delay between intersections. This protocol relies on the delay, which requires an accurate synchronization to be calculated. In addition, routing tables are updated using ant packets generated in a timely fashion on the basis of a constant value of t_{ant}. When t_{ant} is short, routing overhead load is high, causing network instability and performance degradation.

In [37], it was introduced a new mechanism called Distance and Direction based Location aided routing (DD-LAR), which is an extended version of the existing Directional-Location Aided Routing (D-LAR) Protocol. In this protocol, the sender node first checks for the locational information of its nearby neighboring nodes in the request zone within its transmission range. The neighboring node that is positioned at the minimum angular deviation and a maximum distance from the sender node will be selected as the next-hop forwarding node. However, in case of having a conflict in which the node has the minimum angular deviation while not having the maximum distance, then the algorithm prefers the previous version because the relative distance of all the nodes from the source node is negligible. Moreover, the previous version (D-LAR) gives a better hop count in a dense environment like the city traffic conditions.

In [38], the authors proposed ISR protocol. This protocol uses segments for data transmission in urban VANET. The road map is divided into different segments, and routing takes place based on the information of the next segment. This protocol has been designed based on parameters such as node position information, direction, vehicular congestion density, and link quality between the communicating nodes. The protocol is highly dependent on GPS accuracy and availability. Therefore in case of GPS absence, like tunnels, where having a network connection is crucial, the protocol does not function properly.

In the intersection-aware approach, the main challenge is its high end-to-end delay. This approach is practical to confront physical obstacles such as buildings. Data are forwarded through intersections which are selected one by one. As a result, this mechanism imposes a high processing delay. In return, a lower cost is generated in terms of routing overhead. On the other hand, protocols in the traffic density aware sub-category consider vehicular congestion as a metric to evaluate the connectivity [39]. However, a highly congested road is vulnerable to having data congestion problems.

2.3 Clustering approach:

The paper [40] presents a moving-zone-based architecture and routing protocol for data transmission in vehicle-to-vehicle communication. A head vehicle is assigned for each area, and it is in charge of managing the information of other member vehicles as well as the message dissemination. This mechanism does not work with vehicle-to-infrastructure (vehicle-to-RSU) communication because the captain vehicle itself acts as a centralized unit. Clusters are formed by vehicles having similar moving patterns. In each cluster, one vehicle is elected as the section captain. The captain node is responsible for managing other nodes' information and handle data transmission. The sender node forwards its data to the captain. If the captain node detects that the receiver end is outside its zone, it forwards the data to a member node that is the nearest to the destination end. The chance of bottleneck occurrence for the captain node is high, which could result in having longer end-to-end delay and a higher chance of packet loss. Additionally, this scheme imposes high energy costs on the captain node.

To conquer the issues of the traffic-aware approach, authors in [41] proposed a delay-aware grid-based geographical clustering method. The novelty of this work is to address desirable performance in both scenarios of dense and spare vehicular congestion. Different backbone nodes compose backbone links in each street segment. Inter-grid and intra-grid mechanisms have been proposed to accommodate the data transmission in all traffic models. In addition to the dependency of protocol on online maps and GPS, the method requires complicated calculations.

In [42], the author proposed a clustering technique to transmit emergency messages such as road accidents with a minimum possible delay. This clustering technique handles broadcast storm problems to reduce network congestion. Simulation of this mechanism provides better results only at low speed. When the vehicle speed increases, it results in poor performance of the system as the network connectivity decreases.

Many clustering protocols overlook the road structure in their design. In [43], the proposed method tries to overcome the possible upcoming issues at the intersections related to change of direction and mobility speed with the assistance of RSU nodes. Two adjacent intersections and the corresponding road is considered as a road segment. The connectivity of each road segment is studied based on the average end-to-end delay in both scenarios of high and low-density road traffic. In this paper, the sender node decides the next forwarding RSU positioned at a nearby intersection. Then the data load is forwarded to the next intersection, which is close to the destination node through intermediate nodes in the next adjacent road sections until it reaches the destination vehicle.

The protocols under the category of clustering mainly provide a high rate of packet delivery. Additionally, scalability is another feature of this group. These protocols can adapt to different environments with different predictable mobility patterns. However, clustering approach protocols increase the latency in consequence of the communications involved between the sender node and the cluster head, and this consumes a processing time.

2.4 Time delay-based approach:

In [44], authors propose a routing protocol named congestion-aware fibonacci multi-path load balancing (Congestion-aware FMLB). This protocol discovers routes based on the minimum RTT. The data packet distributes through different routes based on the Fibonacci sequence number; therefore, the route with the smallest RTT is used more often. The analysis of results in this paper shows the superiority of RTT over the number of hops routing mechanisms. This protocol's main issue is the high chance of finding lengthy routes due to the absence of a mechanism to restrict the route lengthiness. These lengthy routes participate in the practice of data transmission according to the load balancing mechanism.

An RTT-based probabilistic routing protocol for content-centric networking (CCN) known as a receiver-driven network architecture is proposed in [45]. This method selects the paths based on the message content; therefore, one packet may pass to multiple servers, and accordingly, the RTT measurement is not accurate.

Authors in [46] proposed a novel delay metric named sojourn time backlog (STB) employed with the back-pressure (BP) algorithm. The delay-optimal back-pressure routing algorithm for multihop wireless networks (STBP) protocol was introduced to overcome the problem of having long end-to-end delays in BP scheme. STB considers queuing delay instead of queue length to selects the routes. However, this method is not yet a loop-free routing method; therefore, the provided delay is unsuitable for real-time network applications.

In [47, 48], two different routing protocols of Reliable Cluster-based Energy-aware

Routing (RCER) protocol and load-balanced multi-path routing protocol with energy constraints (EE-LB-AOMDV) were proposed to optimize the routes based on the three metrics of residual energy, hop count and RTT. RCER mainly aims to maximize the network lifetime by clustering the network into the geographical segments based on the nodes' residual energy and the node neighboring. This protocol is suited for a network with low nodes mobility to avoid frequent cluster reconstruction. EE-LB-AOMDV load-balances the data over different discovered routes based on the route score to increase the lifetime of the network. Due to the absence of a restriction mechanism for the lengthiness of routes in this protocol, it is likely to send data through routes with high end-to-end delay.

2.5 Greedy-Perimeter forwarding approach:

In simulation scenarios, researchers may overlook many real-life constraints. Road structure urban VANETs contain several levels such as viaducts, tunnels, and ramps. These road structures act as an obstacle during the data transmission. In [49], the authors study the impacts of different road structures and propose a new technique named multilevel-scenario-oriented greedy opportunity routing protocol (M-GOR). The method introduces a connectivity prediction model and employs it on GOR. This paper scrutinies the impacts of signal propagation on multi-level roads and use them in routing algorithm mechanism. This protocol relies on GPS; therefore, it is not applicable for environments such as tunnels where GPS is unavailable.

The paper [50] states two main limitations of greedy perimeter stateless routing protocol (GPSR) and proposes and new protocol to overcome the given constraints. The GPSR selects the closest neighbor node to the destination as the next node to forward the data load in greedy mode. The selected nodes' positions are mainly at the verge of the communication range. Therefore the chance of link failure increase with this scheme for long-range communications. When the greedy scheme fails, the node goes through the perimeter mode, which may cause redundancy of intermediate nodes in data transmission. The Maxduration-Minangle GPSR (MM-GPSR) employed two "cumulative communication duration" and "the allowed communication area" factors to overcome the next-hop instability problem. Additionally, in the perimeter mode, the next hop is selected based on the angle of the source node and the next hop to the destination to avoid intermediate node redundancy. In a low-density environment, the perimeter mode fails due to a lack of network connectivity.

Paper [51] introduces A novel spider-web-like transmission mechanism for emergency data (TMED). The mechanism spider-web-like model is a combination of geographic information systems (GIS) and electronic maps. The objective of this method is to minimize the end-to-end delay and packet loss ratio. Additionally, this paper introduces a dynamic multi-priority message queue. After determining the destination intersection, the current node transmits the data packet to the closest node to the next selected intersection. Data transmission may take place via vehicular nodes or intersection nodes. A forwarding node with no neighbor node may carry the node until it approaches a forwarding node. This study only emphasizes the data forwarding mechanism and overlooks other impacting factors such as mobility speed, density and congestion. Additionally, it produces a massive amount of routing overhead.

In [52], authors propose a greedy traffic light and queue aware routing protocol (GTLQR) to overcome the urban road constraints such as un-even car distribution as the result of the traffic signals and traffic congestion in rush hours. As to the neighbor discovery, this method introduces a mechanism for HELLO packet based on the mobility speed of each node. It also proposed various mechanisms to evaluate street connectivity, channel prediction and queueing delay.

In [53], the authors propose a greedy forwarding method of routing based on nodes position, neighbor angle, residual energy and link quality. They named it routing based on greed forwarding routing (GFR) protocol. The GFR is not taking network density into account; therefore, the network's connectivity could be susceptible to data congestion and data collision.

2.6 Named Data Network (NDN) approach:

The enhancement of the driving assistant and emergency systems for vehicles requires new data communication techniques and technologies [54]. NDN is one of those technologies proposed for VANETs and the future of the internet. In NDN, instead of using the old IP base routing techniques, the nature of a data packet is the primary concern of data communication [55]. However, NDN is not the case of this paper, considering the architectural change is inevitable to propose an adaptive protocol.

In [56], the authors proposed a routing protocol for NDN based on standalone RSU (SA-RSU). The proposed protocol introduces a broadcasting model of emergency messages. To avoid the broadcasting storm, the RSU selects the next forwarder for ITS message data broadcasting. This protocol is highly dependable on the GPS. Also, it should be considered that the communication range in the real world is subjected to many external constraints.

In [57], the authors introduced Bayesian-based Receiver Forwarding Decision (BRFD) for NDN-VANETs. This protocol is designed based on the caching of received and forwarded data. Additionally, every node stores a table of interests for the data type request is received from other nodes. With the help of Bayesian decision theory as the learning technique, each node decides whether to cache a data packet or not.

To achieve a universal ad hoc network in [58], the researchers combine LoRa [59] and wifi networked employed NDN forwarding-daemon (NFD). During the processing of a data packet, the NFD uses three data structures: content store (CS), pending interest table (PIT) and Forwarding Information Base (FIB).

The authors used the optimized link-state routing protocol (OLSR) to propose a new protocol (NOLSR) [60] for NDN-MANET. In this protocol, they used the concept of multipoint relays (MPR) introduced by OLSR to manage the interest packets. This concept prevents the network from having broadcast storms. As the OLSR is a proactive protocol, the network is prone to flood with the routing load.

In [55], the authors introduce a data forwarding scheme for Vehicle Tracking (VTDF) in NDN-VANETs. The authors introduce a new node search (TNS) algorithm based on tabu search theory to track consumers in the complex urban environment. It also introduces a quick handover method to mitigates the handover issues during the data transmission.

An efficient routing algorithm in VANETs that considers multiple challenges such as congestion avoidance, vehicle energy, and end-to-end delay is desired. In this thesis, we propose a routing algorithm called MPRP in chapter 4 used to reduce the time taken by the packets to transmit from source to destination. To improve the performance of MPRP in chapter 5, we introduce two algorithms of MPRP-FFn and MPRP-GA based on the proposed fitness function considered the characteristics of VANETs.

Chapter 3

Implementation

3.1 Thesis tools

We have implemented the proposed protocols in two phases. For developing MPRP in stated chapter 4, we used network simulator NS-3 (version 3.30.1) on Ubuntu 20.04.2 LTS as the operating system. On the same version operating system, we used network simulator NS-3 (version 3.32) to develop the MPRP-GA and MPRP-FFn discussed in chapter 5. These two chapters have been studied at different times; therefore, we used the most recent distribution for each of them. SUMO is the tool used to generate the mobility model for these simulations. Additionally, we used Gnuplot to illustrate the results.

3.1.1 Network simulator 3 (NS-3)

NS-3 network simulator is an open-source project started in 2006. It is a discrete event network simulator developed in C++. NS-3 simulation is more close to the real-time environment. There are several libraries available that implemented different network layers protocols. One of the most important features of NS-3 for developing VANETs excelling over previous versions is its complete IEEE802.11 model.It also supports visualization by the NetAnim tool. The coding languages in NS-3 are C++ and Python; however, it can work only with C++, making it more robust [61]. There are some tools in NS-3 which work only with python. In this regard, we used "create-module.py" located in the "utils" folder to initiate our routing protocols. All the protocols are coded in C++.

3.1.2 Gnuplot

Gnuplot is a portable plotting tool available for Windows, Linux and many other platforms. It is a command-driven tool that plots data in different graphical models, including graphs, histograms and more. Additionally, it provides various output files extension such as pdf, png, eps and many others.

3.1.3 SUMO

Simulator of Urban Mobility (SUMO) is a traffic and mobility simulator developed for different platforms, including Windows and Linux. It is a microscopic, space-continuous and time-discrete traffic flow simulation platform [62]. Sumo is compatible with many network simulators such as NS-2, NS-3 and OMNeT++. Sumo provides a trace exporter tool named "traceExporter.py" to generate trace files compatible with NS-2 and NS-3. The road map can be exported from the open street map using the "osmWebWizard.py" module or generate by XML files. The "randomTrips.py" as a SUMO tool is used to generate the random trips for our mobility simulation model. The output is stored in the .trips.XML file. Using trip file, we developed a route file for each generated trip using the duarouter command. This tool stores discovered routes in a .rou.xml file.

3.2 Routing protocol implementation

All the protocols implemented in this thesis, either proposed or used for comparison, are inherited the base class of "Ipv4RoutingProtocol". Figure 3.1 shows the hierarchy of data flow at the receiver end node. Ipv4Listrouting class is used to assign the routing protocols to the nodes. Additionally, we used the ns2-mobility model to connect the traffic model generated by SUMO to our simulation scenario. "Ipv4RoutingProtocol" sends packets (data/routing) to routing protocol by calling "RouteInput()" method. The routing protocol call "Sendout()" to send packets to "Ipv4RoutingProtocol" class in "RouteOutput()" method.

Two helpers of "Wifi80211pHelper" and "NqosWaveMacHelper" are used to constitute the network interface layer of the simulations. We assigned energy resources to the network nodes using BasicEnergySourceHelper class. Also, we used "radioEnergyHelper" to define an energy consumption model for the network nodes.

We used NS-3 "FlowMonitor" module to study the QoS metrics of the network. This module keeps track of each packet in the network. At the end of the simulation, it provides a result for the simulated scenario. The results are stored in CSV space-delimited files.

Due to diversity of simulation scenarios an adequate explanation is provided in 4.3.1, 4.3.2 and 5.3 where the simulation results are presented.

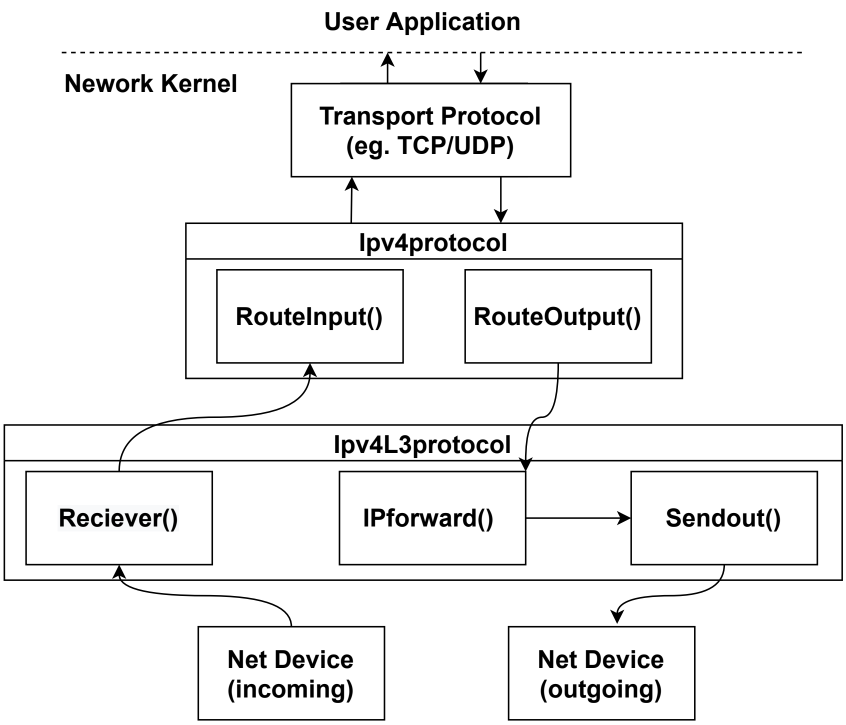

Fig. 3.1: hierarchy of packet processing in a network node.

3.3 Performance Metrics

Hereafter, we present the formulas used to measure the performance metrics [21, 63]:

1. End-to-end Delay (E2E): End-to-End Delay refers to the time taken by the packet to be transmitted across the network from source to destination. It is generally represented in seconds.

$$E2E\,(\text{in Seconds}) = \frac{\sum_{i=1}^{n}(R_i - S_i)}{n} \tag{3.1}$$

The R_i represents the simulator time at the receiving end when the packet delivered. Accordingly, S_i represents the time on which the packet is sent out, and, Finally, n is the number of packets delivered successfully.

2. Packet Loss Ratio (PLR): Packet Loss Ratio is the percentage of packets failed to deliver to the destination end by a total number of packets sent.

$$PLR\,(\text{in}\,\%) = \frac{\sum P_l}{\sum P_g} \times 100 \tag{3.2}$$

where P_l denotes the number of lost packets and p_g represents the number of generated packets.

where P_d denotes the number of delivered packets and p_g represents the number of generated packets.

3. Throughput: Throughput is the number of packets successfully received by all nodes in the unit of time and is represented in Mbps

$$G\,(\text{in Mbps}) = \frac{\sum B_r \times 8}{T} \times 10^{-6} \tag{3.3}$$

In the given equation, G represents the throughput, B_r is the total number of bytes delivered successfully, and T is the time network has been engaged in data transmission.

4. Routing Overhead (RO): It is the number of routing packets required for network communication that is measured as a percentage (%).

$$RO\,(\text{in }\%) = \frac{R_p}{R_p + D_P} \times 100 \tag{3.4}$$

Where R_p is the number of routing packets, D_p is the number of data packets delivered successfully.

Routing overhead reveals the amount of control required for the protocol to works. It should be noted that the control packets impose a cost to the network as time, energy and occupy medium; therefore, the more control packet can impact network performance.

5. Energy consumption (EC): The total amount of energy is being used during simulation by all nodes despite their state.

$$EC\,(\text{in Joules}) = \sum_{i=1}^{n}(I_i - E_i) \tag{3.5}$$

where, I_i is the initial existing energy of node i , E_i is the remaining energy of node i at the end of simulation and n represents the number of nodes

6. Error bar: The error bar margin is calculated as follow:

$$\sigma = \sqrt{\frac{\sum (x_i - \mu)^2}{N}} \tag{3.6}$$

where σ represents the deviation, x_i is the cumulative result of each run, μ is the average of results for each simulation setup and N is the number of runs.

$$error\_margin = \mu \pm \frac{\sigma}{\sqrt{N}} \tag{3.7}$$

$error\_margin$ represents the upper and lower boundaries of the error bar.

7. Gain and Saving function (GS): We use this function to calculate the percentage of

gain or saving of a simulation.

$$GS\,(\text{in}\,\%) = \left|\frac{(y_{1i} - y_{2i})}{y_{2i}}\right| \times 100 \tag{3.8}$$

where y_{1i} is the primary value and y_{2i} is the value we compared with.

Chapter 4

Multi-Path Routing Protocol in VANETs (MPRP)

4.1 Proposed Protocol

4.1.1 Problem Statement

VANETs use pre-existing proactive and reactive routing protocols like Ad-hoc On-demand Distance Vector (AODV), destination-sequenced distance-vector (DSDV), dynamic source routing (DSR), optimized link-state routing protocol (OLSR) [6]. Path selection in these protocols is based on various parameters such as hop count, end-to-end reliability, energy, etc. The major problem in data routing among vehicles is the link failure as a result of node mobility, particularly with high speeds. It is desired to propose a protocol that considers this mobility problem and also to avoid the network congestion to alleviate the traffic load in the network and therefore enhances its performance.

4.1.2 Proposed solution

In this thesis, we present our Multi-Path Routing Protocol (MPRP) running in a VANET environment. MPRP utilizes the RTT measurement to select the shortest path rather than using the minimum number of hops. If one path fails, an alternative path with the next least RTT is used to transfer data messages. MPRP sets a threshold value that caps a measured instant RTT to consider a potential route. This threshold is the average RTT that is set to avoid overwhelming the network with data packets when RTT is large or when nodes' mobility is high. MPRP is designed based on the node-disjoint mechanism in which routing protocol avoids intermediate nodes overlapping for different routes as

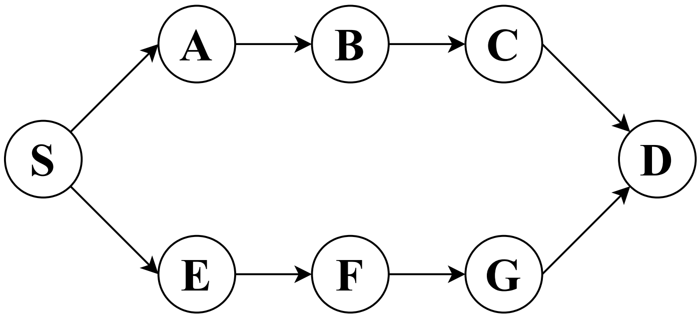

Fig. 4.1: Node-disjoint mechanism.

it is depicted in Figure 4.1. Our protocol is designed to differentiate the emergency and normal message. Emergency messages are sent to the destination without delay, whereas normal messages are pushed in the queue following the FIFO queuing mechanism to reach the destination using MPRP protocol.

4.1.3 System model

For a better understanding of the routing protocol, we first explain the system model as follow:

The node-set of N is constituted by the vehicles-set of $V = \{v_1, v_2, \cdots v_n\}$ and the RSU-set of $I = \{rsu_1, rsu_2, \cdots rsu_m\}$. The node-set N is defined as $N = V \cup I$ where $V \cap I = \emptyset$. Therefore each node can be placed only in one set. The set of wireless links between RSUs and OBS is denoted by $E = \{l_1, l_2 \cdots, l_k\}$. The network graph is represented by $G(N, E)$ for all nodes $s \in N$ and for all links $(x, y) \in E$.

Dedicated short-range communication (DSRC) is the wireless technology supporting communication in VANETs [64, 65]. The DSRC is referred to a set of standards, including IEEE 802.11p [66]. Therefore, the routing protocols utilize data propagation through a DSRC using relay nodes to obtain successful data communication in ad hoc networks, including VANETs. Due to the coverage range limitation of DSRC, the network relies on the multi-hop forwarding mechanism in which packets are forwarded through the intermediate nodes. Every road segment is equipped with an RSU with a limited coverage range which is not covering the entire dedicated road segment.

4.2 Methodology

MPRP is a Multi-Path routing protocol that is based on the RTT that mainly focuses on reducing end-to-end time delay. Figures 4.2 to 4.4 show the components used to implement the MPRP algorithm using routing path selection, message handling, and RTT concepts. In below, we explain the main components of the message handling in the VANET shown in Figure 1. Figure 4.3 explains the flow of data transmission at On-Board Unit (OBU).

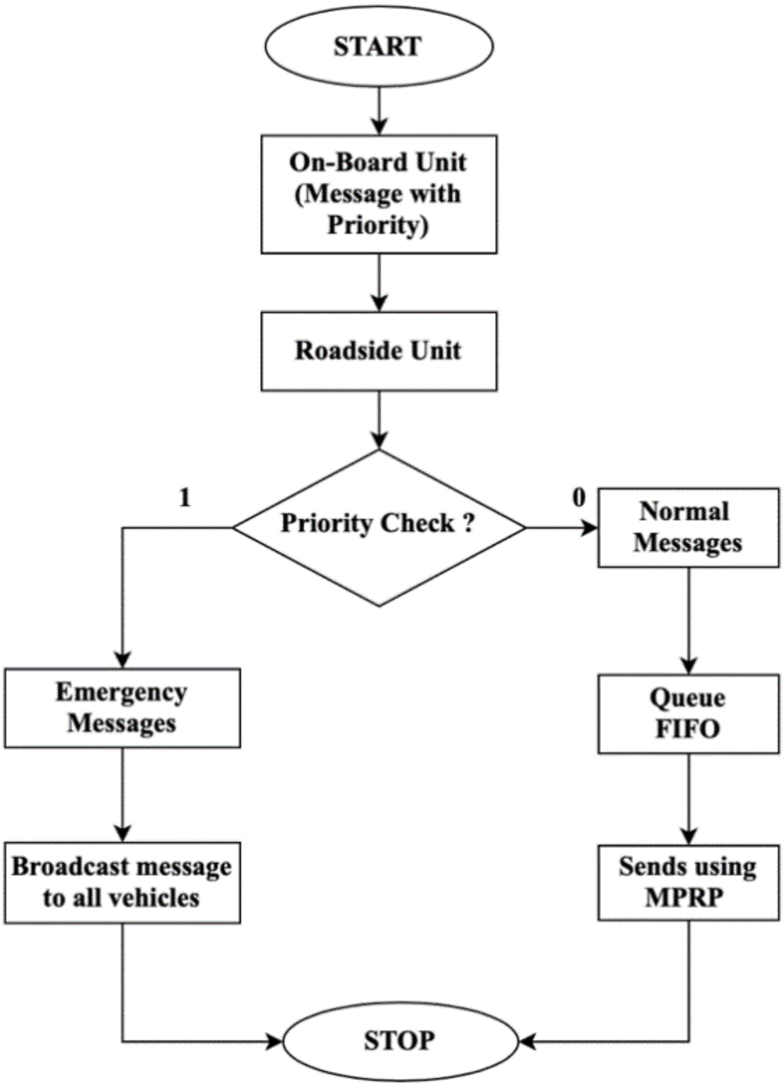

Fig. 4.2: Flow diagram of message handling.

4.2.1 Flow Methodology

1. OBU: This unit present in the source vehicle is used to send data messages to other vehicles through RSU. Messages produced in the OBU consist of the source vehicle ID (VID) and are assigned a priority value that decides the type of messages.

2. Roadside Unit (RSU): The messages received at RSU are checked for the priority value (0 or 1) to decide which message should be sent first [3]. RSU is the centralized routing unit presents on each road segment.

3. Priority Check: The priority check happens once the messages are received by RSU. If the priority value is 0, then it is considered as a normal message, whereas if the

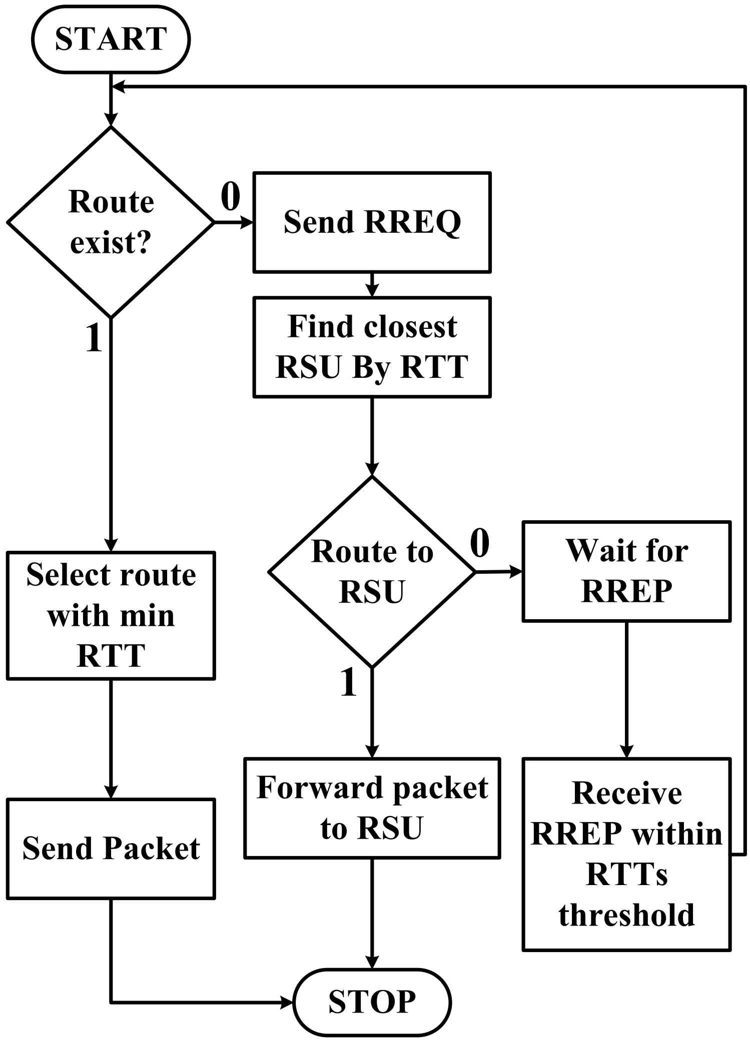

s

Fig. 4.3: Flow diagram of packet forwarding.

priority value is 1, this is considered as an emergency message and is given the most priority among all the messages received from the OBU.

4. Messages: The messages have information regarding the sender's vehicle. Based on the content of the message, the priority is determined. These messages are transmitted in the VANETs to disseminate network state or emergency incident information to other vehicles in the network.

   (a) Normal message: Normal message consists of general information about the sender's vehicle such as the speed of the vehicle, the time at which the message is sent, direction, and location of the vehicle. The normal messages are sent through unicast communication and are given less priority. These messages are pushed into the queue following the FIFO mechanism to be transmitted to the destination using MPRP.

(b) Emergency message: This message type is given higher priority compared to the normal message because it has the information regarding emergencies (i.e., a collision of vehicles or functional disorder of the vehicle which leads to traffic problems). These messages are immediately transmitted among all the vehicles in the network within the RSU range without any delay. So, the approaching vehicles in that range can avoid traffic jams and advance to take a detour.

5. Broadcast: The emergency messages received by RSU are broadcasted immediately to all other vehicles in the network [67]. These are alert messages aimed to provide road safety for vehicles of any possible risk.

6. Queue: Queue consists of a list of normal messages to be transmitted sequentially following FIFO.

7. Routing Protocol (MPRP): This protocol was implemented to transfer the messages from the source to the destination. The normal message goes through routing protocol which uses the path with the minimum RTT among multiple paths generated. Alternative paths can be used in case if there is a link failure.

The unicast transmission also happens in some cases where there is no need to interfere with the entire network in the range of an RSU, even if these messages are somewhat emergency. For example, unicast communication is needed when two cars traveling in different streets are about to meet each other in a blind corner [20]. In such a scenario, vehicles cannot see the other side of the intersection due to hindrance caused by high buildings or trees. At such an instance, the source vehicle communicates with the RSU which in turn sends a message to another vehicle in the opposite direction which is likely to get collided. Each road segment is equipped with RSU nodes acting as cluster head. All communications between OBU nodes take place via RSU. In this case, MPRP protocol is utilized to avoid this collision for a message from RSU to the other vehicle(s) in danger in a specific road zone. Another scenario is when a vehicle needs to be aware of the turns and lane change made by a front vehicle. When the ahead vehicle turns on an indicator to change direction, a message is sent to the behind vehicle to inform about this direction change to avoid an accident. RSU sends frequent information messages to all vehicles in its range, informing them about its MAC address. If the vehicle joins newly to the network and does not receive such a message promptly, it can solicit through sending ICMP messages. Normal and emergency messages are sent from vehicles to RSU, which in turn would convey to other vehicles. MPRP algorithm is used by RSU to send unicast messages to vehicles. Communication between RSU and OBU of vehicles are explained below:

1. All vehicles present in the range of RSU send and receive messages that can be either emergency or normal messages such as vehicle accidents, fire alerts, car speed limits, snow alerts, etc.

2. Initially, OBU sends a message to the RSU using the MPRP protocol with assigned priority based on the content in the message. If the message is an emergency, it is assigned 1; whereas, the normal message is assigned 0.

3. If the message is for an emergency case, RSU broadcasts to all vehicles, in its range, without any delay.

4. The normal message is pushed into the queue where it follows the FIFO mechanism. RSU sends these normal messages to vehicles in the network using MPRP protocol in that RSU range.

5. Once the RSU receives a message from an OBU; it adds the sending vehicle ID (VID) to the certificate revocation list (CRL) if it does not exist.

6. RSU checks the routing table for the destination vehicle. If the routing table is empty, RSU broadcasts an RREQ message to all vehicles in that RSU range, and it contains a vehicle ID (VID) of the intended vehicle as being its destination address.

7. The intermediate vehicle OBU adds the VID in the RREQ message to its CRL list if it is not there.

8. If the intermediate vehicle OBU has a path to the destination, it returns RREP, and the RSU, in turn, would calculate the RTT_{ij}. If there is no path, OBU will send other RREQ messages to other nodes.

9. RTT_{ij} is measured for every request in all the paths and is stored in an array.

10. The average RTT will be calculated using the following formula.

$$RTT_{ia} = \sum_{j=0}^{n} \frac{RTT_{ij}}{n}$$

    where,
    i = Id of a specific path
    j = Id of requests per path
    n = Total number of requests
    a = Average of RTT

11. Instant round trip time (RTT_{ij}) is compared with a threshold value which is the average round trip time (RTT_{ia}). If RTT_{ij} is greater than the average RTT_{ia} then drop the route with that instant RTT_{ij}.

12. If the instant RTT_{ij} is less than or equal to the average RTT_{ia}, the instant RTT_{ij} route will be added into an array. Then the array is sorted in ascending order. Accordingly, the routing table will be updated using Dijkstra's algorithm. If the routing protocol fails to find at least one route within the RTT threshold, the MPRP goes through the route discovery phase again.

13. RSU sends the packet using the first minimum RTT path in the array and waits for the acknowledgment from the destination vehicle.

14. If the time out occurs before receiving an acknowledgment, MPRP uses the next minimum RTT path to resend the data packets.

15. This loop performs till the packets are successfully delivered to the destination vehicle.

Steps 1 to 4 are summarized in Algorithm 1. Steps 5 to 8 are summarized in Algorithm 2. Steps 9 to 15 are summarized in algorithm 3.

MPRP-LF (Multi-Path routing protocol – Link Failure) uses the same concept of the minimum RTT as MPRP protocol, but it provides only a single path. In case of having a link failure, this protocol has to restart the route discovery process to find an alternative path in a similar way to the AODV protocol.

Algorithm 1 Message Handling

```
procedure 1:                                        ▷ At OnBoard Unit
Input: Message
if (type == emergency) then
 |  assign weight = 1
else
 |  assign weight = 0
end
end procedure
procedure 2:                                        ▷ Priority check at RSU
Input: Message
if weight == 1 then
 |  broadcast Message;
else
 |  push Message (FIFO Queue)
 |  send data message using MPRP in Algorithm 3
end
end procedure
```

OBU would send a message to RSU, which, in turn, will send the message as a broadcast (emergency) or unicast (message to a specific vehicle) [20] to another vehicle OBU. Figure 4.4 shows the frame format in the case of unicast transmission. The format

Algorithm 2 Routing Path Establishment

procedure 1: ▷ At RSU upon receiving a normal message.
Input: Normal_Message
Look Up Routing Table
if (path to destination == null) **then**
  Produce RREQ (VID)
  Broadcast RREQ (VID) to all nodes (vehicles) in the range
else
  Follow algorithm 3
end
end procedure

procedure 2: ▷ Receiving RREQ message at OBU and RSU
Input: RREQ
if (new VID == old VID) **then**
  Drop RREQ
else
  Add new VID to CRL
end
end procedure

procedure 3 ▷ Receiving RREQ message at OBU
Input: RREQ
Look Up Routing Table
if (there is a path to the destination) **then**
  Send RREP to the RSU
  RTT is measured at the RSU
else
  Broadcast RREQ (VID) to other neighboring nodes
end
end procedure

mainly consists of six categories: Sequence, Type, Source ID, Destination ID, Timestamp, and Data.

1. Sequence number: It is the frame number that helps to avoid redundancy.

2. Type: This indicates the type of a message, i.e., emergency or normal message.

3. Source ID: This contains the sender's VID to inform the destination (OBU or RSU) from which ID the message is received, an acknowledgment is to be sent.

4. Destination ID: This contains the VID of the destination (OBU or RSU) to which the message should be sent.

5. Timestamp: It can be used in the priority ordering in the FIFO in the case of

Algorithm 3 MPRP Routing Protocol

```
at RSU:
While (RREP = true)                                  ▷ RREPs received from Algorithm 2
procedure 1:                                         ▷ Calculating average RTT_ij
Input: Array of routes for destination i
RTT_ia = (Σ_{j=1}^{n} RTT_ij) / n
end procedure
procedure 2:                                         ▷ Path Selection
Input: D_r[] ← Array of discovered routes for destination i
foreach route ∈ D_r[] do
    if route.RTT > RTT_ia then
        drop route
    else
        add route into an array A[]
    end
end
if A[]! = null then
    sort array A[] in an ascending order
    update the Routing Table
    Send a message using a route with the minimum RTT in A[]
    if (timeout) then
        send a message using a route with the next minimum RTT in A[]
    end
else
    Follow procedure 1 In algorithm 2
end
```

normal messages. Also, it can be used to reflect status, such as congestion on the road.

6. Data: This field holds the contents of a frame-like latitude, longitude, speed, direction, and the current time.

    (a) Latitude and Longitude: This field holds the exact location of the vehicle with specific latitude and longitude.

    (b) Speed: This field holds the speed of the sender's vehicle when the message is sent.

    (c) Direction: This field displays the direction in which the sender vehicle is moving.

    (d) Current Time: It displays the time at which the message is sent.

Messages are transmitted using VID as the MAC sublayer addresses. MPRP is used in the case of unicast transmission from the RSU to the OBU of a vehicle.

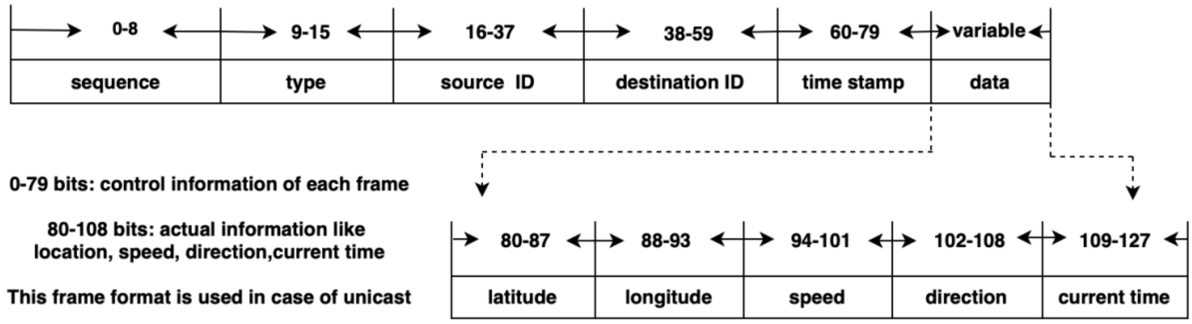

Fig. 4.4: Emergency packet format.

4.2.2 MPRP routing characteristics

Our algorithms filter those available paths to the final destination in which the instant RTT of a path should be less than or equal to the average RTT for a given route request. If this condition is not met for all available paths, this means that the data packets have no efficient route to the final destination. Therefore the RSU has to wait for a backoff time and later try again to find a route when the destination vehicle is closer. In this way, excessive data traffic, particularly normal messages, can be reduced to mitigate the pressure on the network and therefore avoid network congestion.

Vehicles' mobility might have a negative impact on the precision of the RTT calculation in terms of aberration, and this is one of the limitations of the algorithms that use RTT. Several techniques utilize RTT in various data communications systems as discussed in [68]. RTT variation relies on the communication model, whether being short-term or long-term transmissions. In VANETs, data communication between RSU and OBU is usually for a short term, where RTT will be updated quite often. This accordingly avoids the RTT inaccuracy happening when vehicles have high speed on the road. In [69], the effect of mobility speed has a limited effect on the RTT calculation as the data packets carrying information can travel back and forth at speeds that are much higher than the node speed. This is valid, particularly in small networks having a shorter path for data packets to traverse. On the other hand, and as in [70], RTT increases with wider networks as having more nodes in the network increases the queuing delay, and this, in turn, would reduce the data packets' transmission speed. In this case, the data packet traveling speed will be comparable with the vehicle speed, and as a result, RTT accuracy will reduce. To overcome such constraints, it is recommended to have more RSUs in crowded regions such as urban areas to have less distance where packets have to travel, and therefore RTT will reduce. On the contrary, in a high way, particularly between cities, having fewer RSUs can work efficiently as the number of vehicles is relatively small. Therefore RTT will be short, which in turn increases the data packets' transmission speed compared to the vehicle speed. RTT can be calculated through a few ICMP echo requests and response packets between the source node (RSU) and the destination node (vehicle) as suggested in [71].

4.3 Experiment Setup and Performance Analysis

To evaluate the performance of MPRP, we used NS-3 (version 3.30.1) on Ubuntu Ubuntu 20.04.2 LTS operating system to obtain simulation results. Performance is measured by quantitative metrics of end-to-end delay, packet delivery ratio, packet loss ratio, throughput, and routing overhead. During the simulations, we considered different network configurations with randomly distributed vehicular nodes in a square shape connected roads with 1km length bidirectional double lane in each direction. Different Network loads in terms of having various packet sizes, number of concurrent connections, and different environmental configurations, including mobility speed, number of nodes, and so forth, are considered to scrutinize the network's performance. Table 5.2 shows the simulation parameters. Experiments are all set to parameter assumptions in table 5.2 unless otherwise noted. The results indicate the efficiency of our protocol, even as the number of nodes increases.

As MPRP uses stationary RSU nodes in its network topology, there was an effort to implement a fair simulation environment for all the protocols. As the result of the same consideration, there was the same number of stationary nodes at the same position in the network for all the simulations.

Table 4.1: Simulation Parameters

Parameter Type	Parameter Value
Network Simulator	ns-3.30.1
Traffic Simulator	SUMO 1.7.0
Wireless Protocol	IEEE 802.11p
MAC and Physical Layer standard	OFDM rate (6Mbps, 9Mbps, 12Mbps, 18Mbps, 24Mbps, 36Mbps, 48Mbps, 54Mbps) 20 MHz
Protocols	AOMDV, MPRP-LF, FF-AOMDV, EGSR, QMR, MRPP
Number of runs	5
Simulation Time	10,20,30,**40**,50,60,70,80,90,100 seconds
Number of nodes	40, 50, 60, 70, 80, 90, **100**, 110, 120, 130
Mobility speed	**10**, 15, 20, 25, 30, 35, 40 m/s
Number of concurrent Connections	5, 8, **10**, 11, 14, 17, 20, 23, 26, 29
Data payload	256, 512, **768**, 1024, 2048 3072 bytes/packet
Transmission speed	1024 Kbps
Transmission Power	7.5 db
Initial Energy Source	100 Joules
Transmission Energy	0.2 watt
Receiving Energy	0.1 watt

4.3.1 The results of scenario 1

In the scenario depicted in Figure 4.5, we considered a situation in which data communication occurs between OBUs and the RSU close to it in one road segment. The study's objective in this scenario is to evaluate the effectiveness of each protocol within a road segment. Below are the simulation results of the MPRP protocol when compared with FF-AOMDV, QMR, and EGSR.

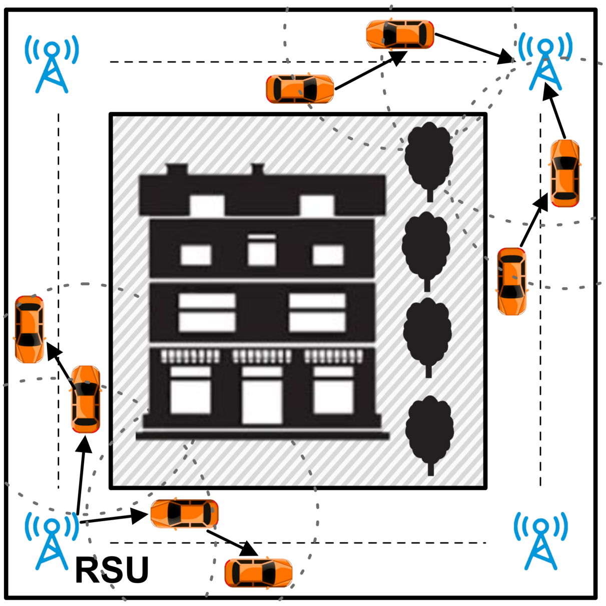

Fig. 4.5: Scenario 1: data communications in one road segment.

4.3.1.1 Assessment of the simulation results on the basis of time-variable:

With simulation time progression, more data communications among nodes take place and this in turn will increase the data traffic problems such as data congestion and collision. Accordingly, the performance of the network will degrade with the simulation time, as we see in the results below.

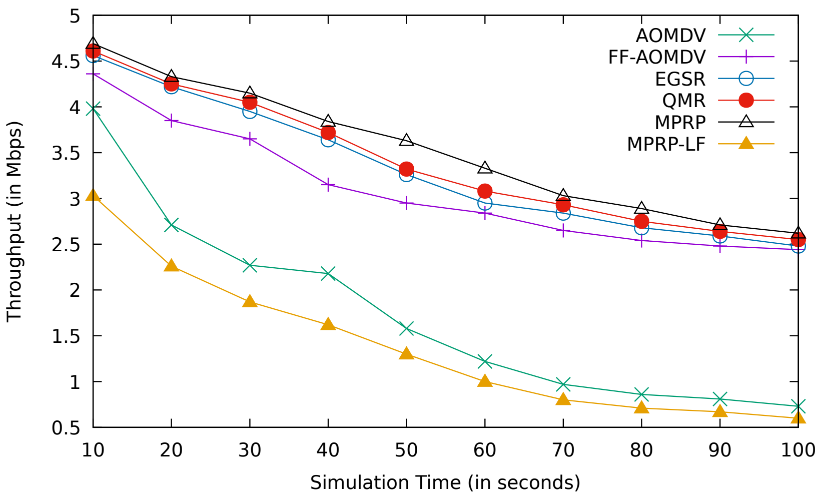

Fig. 4.6: Comparison between AOMDV, FF-AOMDV, EGSR, QMR and proposed protocol MPRP and MPRP-LF for throughput with simulation time.

Table 4.2: Simulation time vs. throughput

Time	MPRP-LF	AOMDV	FF-AOMDV	EGSR	QMR	MPRP
10	3.03	3.98	4.36	4.56	4.61	4.69
20	2.26	2.71	3.85	4.22	4.25	4.33
30	1.87	2.27	3.65	3.95	4.05	4.15
40	1.62	2.18	3.15	3.64	3.72	3.84
50	1.3	1.58	2.95	3.26	3.32	3.63
60	1.02	1.22	2.84	2.95	3.08	3.33
70	0.8	0.97	2.65	2.84	2.93	3.03
80	0.71	0.86	2.54	2.68	2.75	2.89
90	0.67	0.81	2.48	2.59	2.64	2.71
100	0.6	0.73	2.44	2.48	2.55	2.62
Sum	13.88	17.31	30.91	33.17	33.9	35.22
Gain (%)	153.74	103.46	13.94	6.18	3.89	

In Figure 4.6, MPRP enhances the throughput compared to other protocols. MPRP selects the route with the minimum RTT and, therefore, can deliver data to the destination vehicle quicker than other protocols. Furthermore, the minimum RTT implies that the selected route has less traffic and therefore avoids network congestion. In this case, other protocols provide multi-path routes, so alternative routes are available. AOMDV selects the shortest route based on less hop count, while FF-AOMDV concentrates more on the path with the highest residual energy rather than the path with less time to reach the destination node as MPRP does. MPRP-LF performance is poor in comparison with other protocols; because it is a single-path protocol, so whenever the link fails, they follow the same route discovery procedure to find a route. Table 4.2 represents the corresponding value for Figure 4.6. It also shows that how the MPRP's throughput improved in compare with the other protocols.

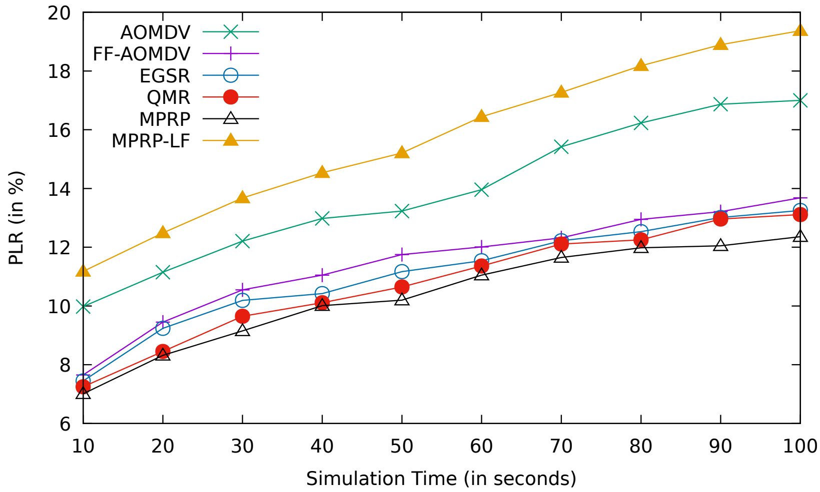

Fig. 4.7: Comparison between AOMDV, FF-AOMDV, EGSR, QMR and proposed protocol MPRP and MPRP-LF for PLR with simulation time.

In Figure 4.7, MPRP has a better PLR compared to other protocols. MPRP can deliver more data successfully to the destination vehicle, so according to equation (3.2), PLR improves. MPRP uses the threshold mechanism shown in algorithm 3, where the optimum routes have less RTT than the average RTT. This, in turn, reduces the PLR. EGSR and QMR protocols also consider the time factor in their route selection mechanisms, and that is why their performance is close to MPRP. Other protocols do not consider this time factor, so data packets likely are delivered in a long time, so PLR enlarges. Additionally, multi-path protocols, including MPRP, behave better than MPRP-LF, particularly when a link failure occurs. MPRP-LF has to re-compute the shortest path once there is a link failure, and this, in turn, would enlarge the processing time that flare-up the PLR. MPRP saved 3.8%, 6.5%, 9.5%, 25.5% and 34% of PLR in comparison with QMR, EGSR, FF-AOMDV, AOMDV and MPRP-LF, respectively.

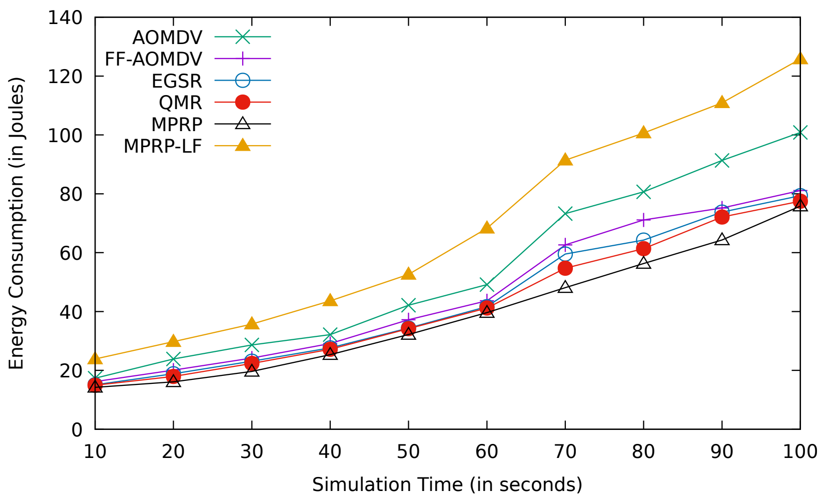

Fig. 4.8: Comparison between AOMDV, FF-AOMDV, EGSR, QMR and proposed protocol MPRP and MPRP-LF for energy consumption with simulation time.

A node consumes energy when it receives or forwards a message, including normal, emergency, or routing messages. In Figure 4.8, the consumed amount of energy by each protocol has been compared. Among all protocols, MPRP-LF devours more energy. In case of having a link breakage, MPRP-LF has to find an alternative route, so it restarts the route discovery phase. As route discovery is a broadcasting-based mechanism, more nodes are involved in this phase which causes more energy consumption. In contrast, MPRP relies on alternative routes discovered; therefore, it does not need to perform the route finding phase every time a link fails. Both FF-AOMDV and QMR consider residual energy as a metric of route evaluation. In addition to the residual energy, QMR considers end-to-end delay as well. The objective of these two algorithms is to increase the network's lifetime by distributing the data traffic load over nodes with more residual energy. However, MPRP is outperforming these protocols as the chance of having data traffic problems such as congestion and collision are minimal in the routes with shorter RTT time. Thus, the energy consumed during the queuing time (in the case of having data congestion) and the transmission time (in the case of having data collision) may reduce. Similar to the MPRP, AOMDV and EGSR, energy is not the metric of route optimization.

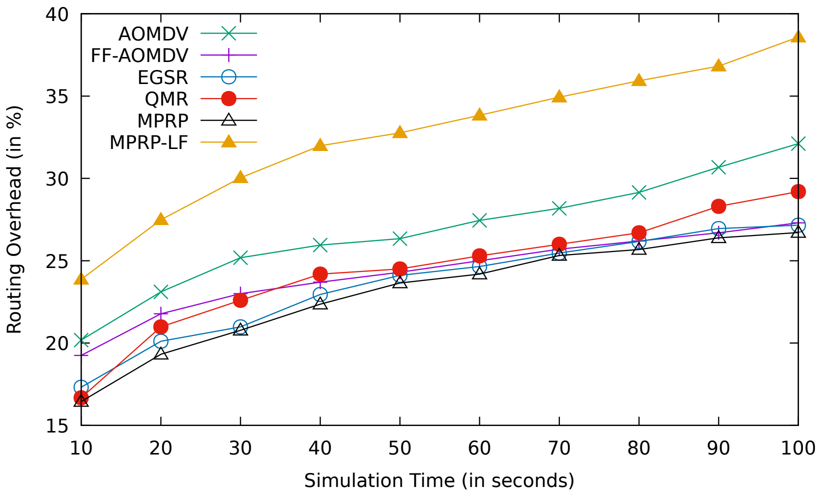

Fig. 4.9: Comparison between AOMDV, FF-AOMDV, EGSR, QMR and proposed protocol MPRP and MPRP-LF for routing overhead with simulation time.

Figure 4.9 shows the routing overhead for different protocols. In the case of MPRP-LF, the routing overhead is significantly higher than the other protocols as it is a single-path routing protocol. Despite the fact that the routing packets circulate through the network, only one route is used as the discovered route. In case of a route failure, the process of route-finding starts. In a fast-changing environment such as VANETs, where there is a high chance of topological change, the chance of route failure is also high. In this case, MPRP-LF will flood the network with RREQs messages adding excessive overhead loads to the network. On the contrary, MPRP keeps the record of all possible and optimized discovered routes in the routing table.

Pause time refers to the period on which the vehicle remains stationary. In the following simulation results with pause time, we considered the duration of the red light at the traffic signal as the pause time.

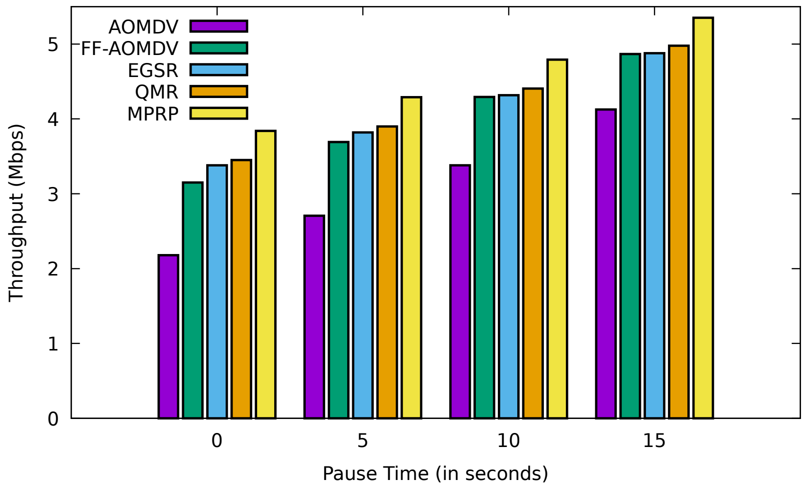

Fig. 4.10: Comparison between AOMDV, FF-AOMDV, EGSR, QMR and proposed protocol MPRP for throughput with pause time.

With a longer pause time, the chance of topological change occurrence reduces, which results in more network stability. With the given consideration, RTT as the metric of route selection, guarantees for the quality of the links and pause time bring more topology consistency. As a result; therefore, MPRP shows the highest performance where topological reformation is less likely as it is depicted in Figure 4.10. MPRP improves the throughput by 9.2, 11.5 14.2 and 47.5 percent in comparison with QMR, EGSR, FF-AOMDV and AOMDV, respectively.

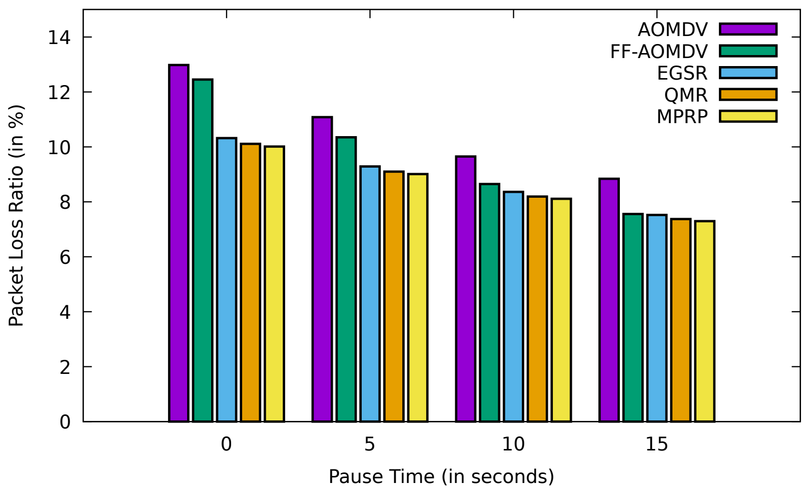

Fig. 4.11: Comparison between AOMDV, FF-AOMDV, EGSR, QMR and proposed protocol MPRP for PLR with pause time.

According to Figures 4.11, by increasing the pause time, the trend of PLR becomes down-warding. As getting a longer pause time, protocols get close to each other in terms of PLR. By increasing the pause time, the performance of FF-AOMDV shows significant improvement, which is the result of more topological consistency.

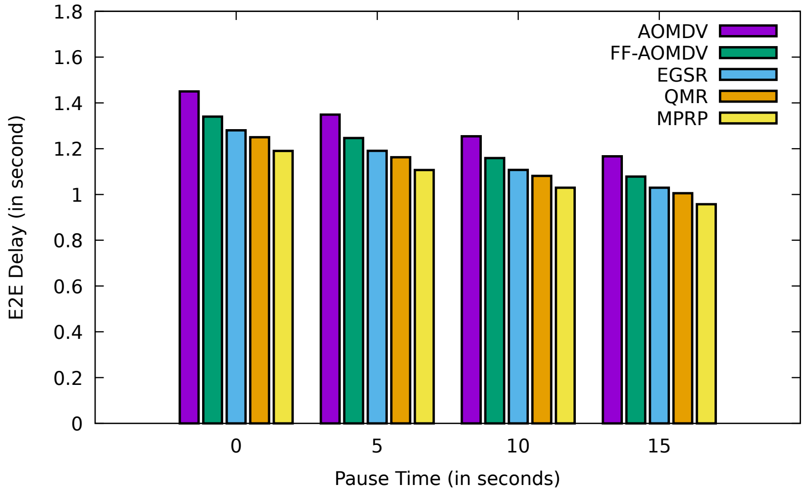

Fig. 4.12: Comparison between AOMDV, FF-AOMDV, EGSR, QMR and proposed protocol MPRP for PLR with pause time.

In Figure 4.12, with having a longer pause time, the end-to-end delay decreases. The reasoning behind this incident is that the number of link failures, which is the result of the topological change, has been reduced. With fewer link failure incidents, the time that the sender should be engaged in processing ICMP error messages is shorter. QMR prefers to forward the data packet through the neighbor nodes having mobility speed lower than average speed; therefore, with longer pause time, the performance is improved. MPRP lowered the end-to-end delay by 17.9, 11.2, 7.0 and 4.8 percent as it is compared with AOMDV, FF-AOMDV, EGSR and QMR, respectively.

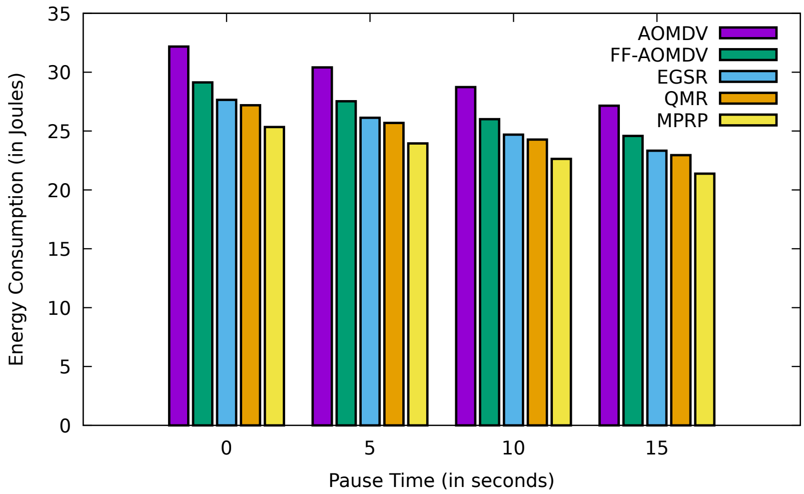

Fig. 4.13: Comparison between AOMDV, FF-AOMDV, EGSR, QMR and proposed protocol MPRP for energy consumption with pause time.

In Figure 4.13 shows that with increasing the pause time, the energy consumption is reduced in all protocols. This is owing to having less chance of a link failure, and the route discovery phase is not often needed. With increasing the pause times, all protocols would send less amount of data, and this reduces the needed energy.

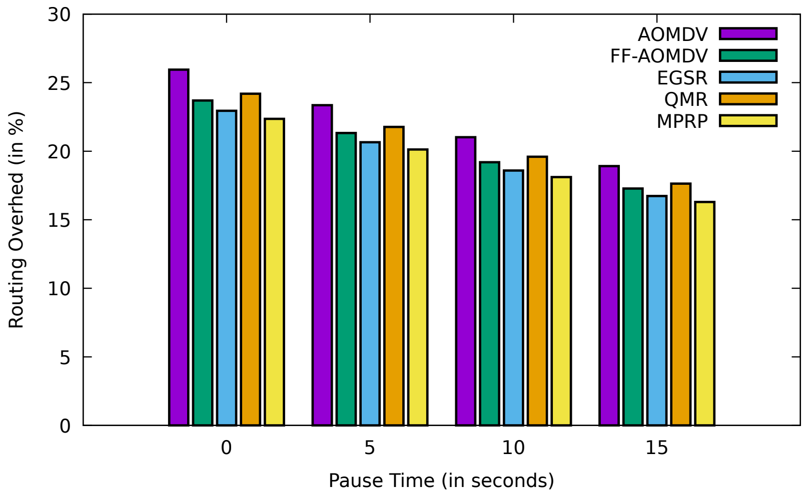

Fig. 4.14: Comparison between AOMDV, FF-AOMDV, EGSR, QMR and proposed protocol MPRP for routing overhead with pause time.

In Figure 4.14, the routing overhead ratio drops when pausing time increases. This is a result of having more link stability and less topological change. With a longer pause time, the topology is likely subjected to be consistent, which results in minimizing link failure and less need for the route discovery phase.

4.3.1.2 Assessment of the simulation results on the basis of concurrent connections:

The figures in this section illustrate the simulation result of two different scenarios in which different numbers of OBU nodes exchange data load with one RSU either as the sender or receiver.

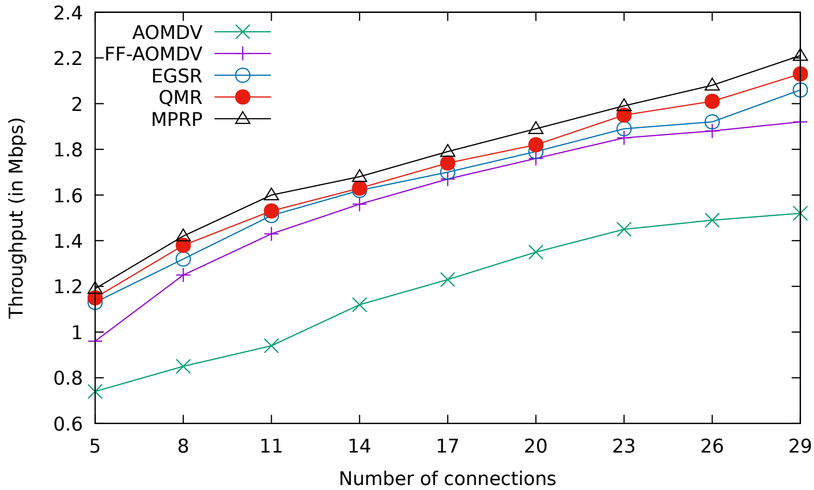

Fig. 4.15: Comparison between AOMDV, FF-AOMDV, EGSR, QMR and proposed protocol MPRP for throughput with different numbers of OBU nodes sending data to one RSU.

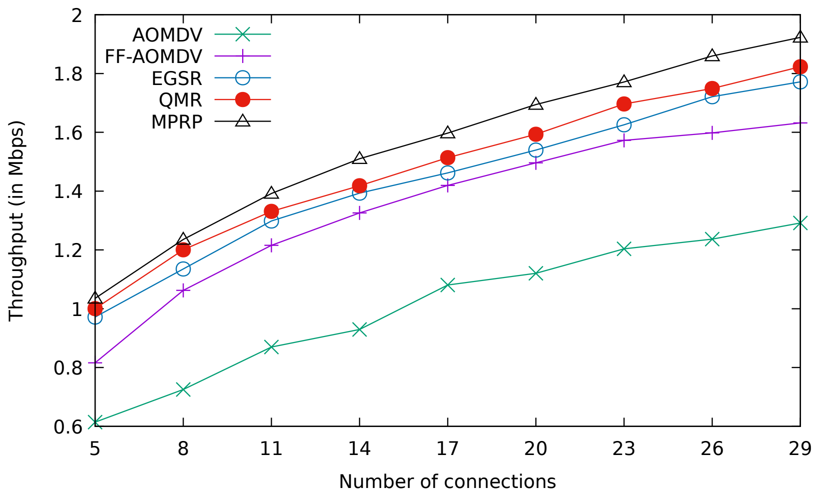

Fig. 4.16: Comparison between AOMDV, FF-AOMDV, EGSR, QMR and proposed protocol MPRP for throughput with different numbers of OBU nodes receiving data from one RSU.

Figures 4.15 and 4.16 depict the results of throughput for both the aforementioned scenarios. There is a slight difference between these two cases as a result of the amount of data produced. MPRP is performing better than other protocols as a result of the avoidance of the problematic routes having more traffic problems selected based on the minimum RTT.

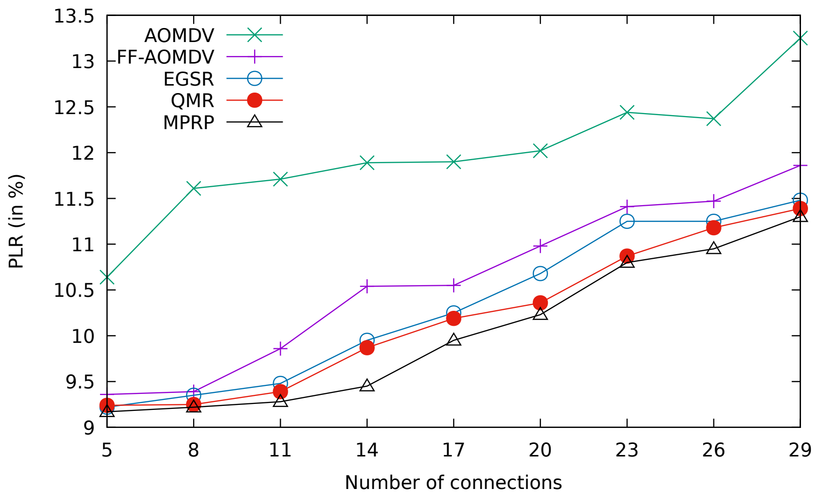

Fig. 4.17: Comparison between AOMDV, FF-AOMDV, EGSR, QMR and proposed protocol MPRP for PLR with different numbers of OBU nodes sending data to one RSU.

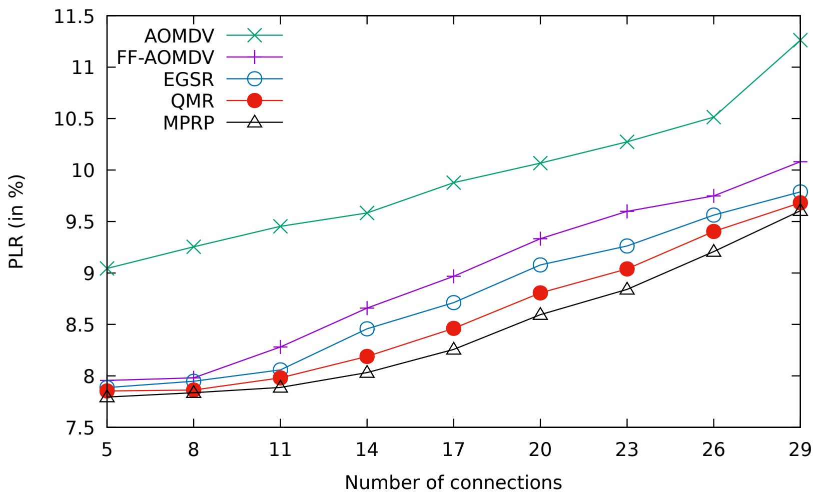

Fig. 4.18: Comparison between AOMDV, FF-AOMDV, EGSR, QMR and proposed protocol MPRP for PLR with different numbers of OBU nodes receiving data from one RSU.

In Figures 4.17 and 4.18, MPRP has less PLR than other protocols because of the threshold mechanism shown in algorithm 3, as explained earlier. There is a slight difference in terms of PLR. On the other hand, PLR increases with increasing the number of sending nodes which is the case in Figure 4.17 compared to having only one sending node in Figure 4.18. Similarly, as having more nodes involved in the transmission of the packets shown in Figure 4.19, the energy consumption is higher compared to Figure 4.20 for all protocols where MPRP has the least required energy.

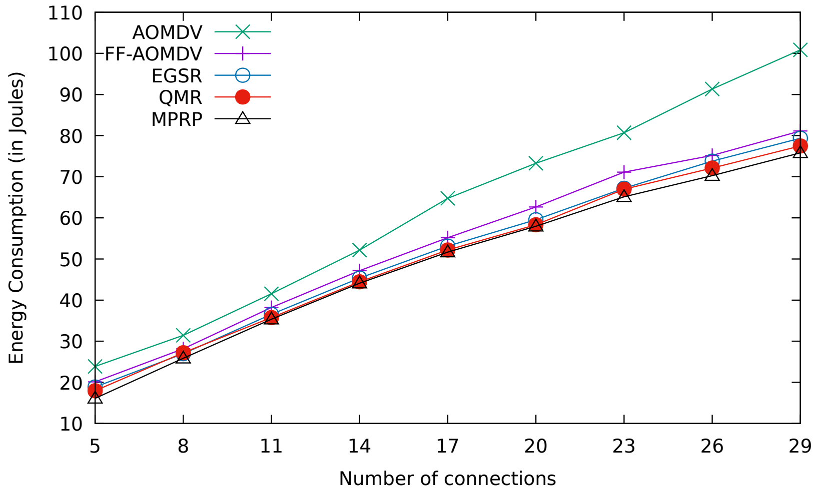

Fig. 4.19: Comparison between AOMDV, FF-AOMDV, EGSR, QMR and proposed protocol MPRP for energy consumption with different numbers of OBU nodes sending data to one RSU.

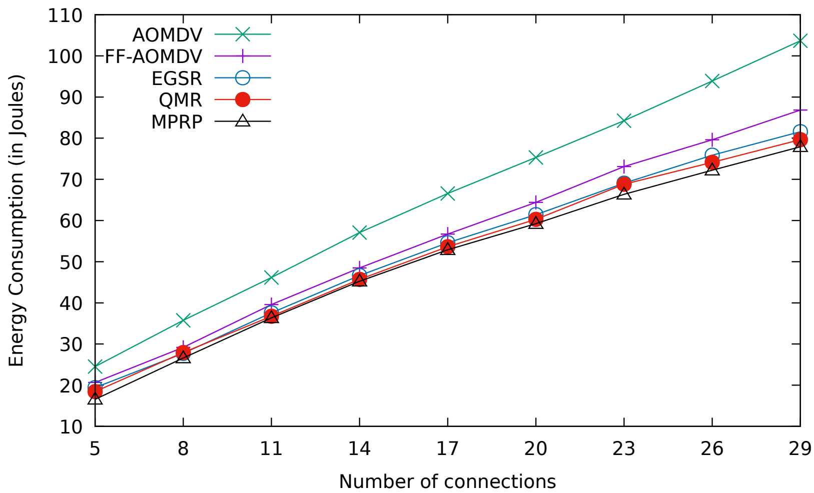

Fig. 4.20: Comparison between AOMDV, FF-AOMDV, EGSR, QMR and proposed protocol MPRP for energy consumption with different numbers of OBU nodes receiving data from one RSU.

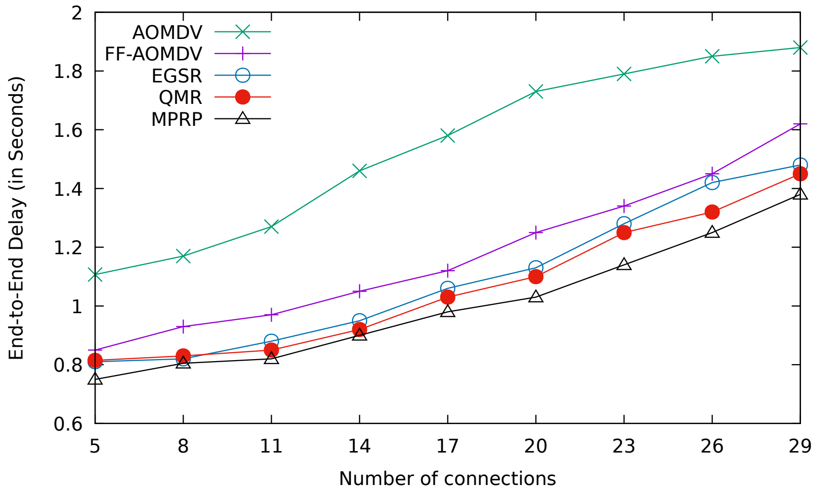

Fig. 4.21: Comparison between AOMDV, FF-AOMDV, EGSR, QMR and proposed protocol MPRP for end-to-end delay with different numbers of OBU nodes sending data to one RSU.

In Figures 4.21 and 4.22, the end-to-end delay shows an upward trend which happens as a result of data retransmissions associated with having network overload and data traffic problems (e.g., congestion and collisions) in the network. RSU mechanism is used to minimize the propagation time [72], and that is why E2E is less in Figure 4.22 compared to Figure 4.21.

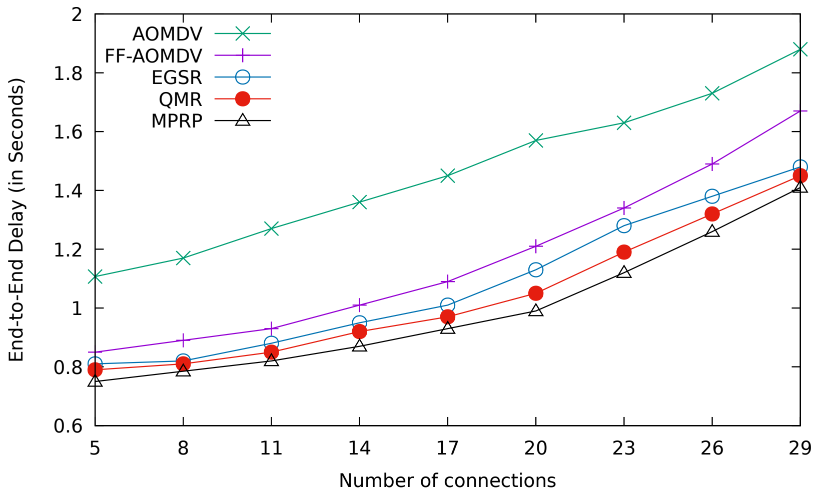

Fig. 4.22: Comparison between AOMDV, FF-AOMDV, EGSR, QMR and proposed protocol MPRP for end-to-end delay with different numbers of OBU nodes receiving data from one RSU.

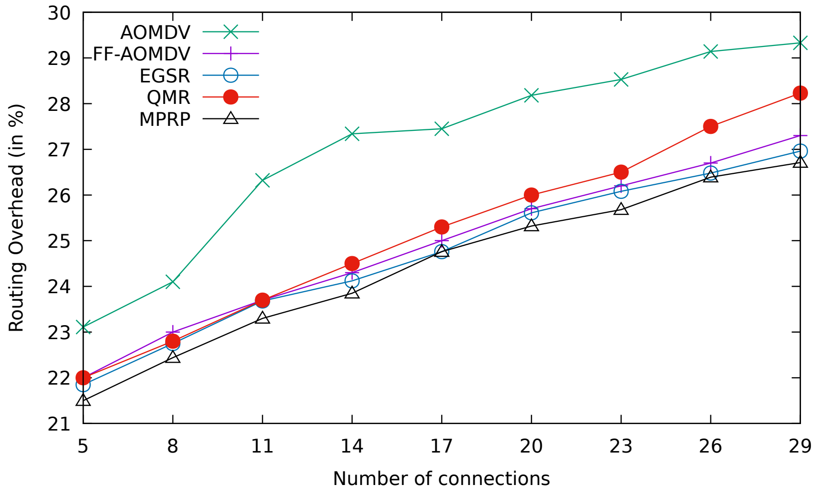

Fig. 4.23: Comparison between AOMDV, FF-AOMDV, EGSR, QMR and proposed protocol MPRP for routing overhead with different numbers of OBU nodes sending data to one RSU.

In Figure 4.23, when the number of OBU nodes increases, the possibility of having more traffic problems increases and hence the link failure occurs, often leading to increasing the routing overhead packets as shown in the rising pattern. MPRP uses the minimum RTT, and packets go through routes with less traffic, and therefore MPRP has the least overhead. This is quite similar with Figure 4.24 that has less overhead as a result of having less amount of data packets coming from only one RSU.

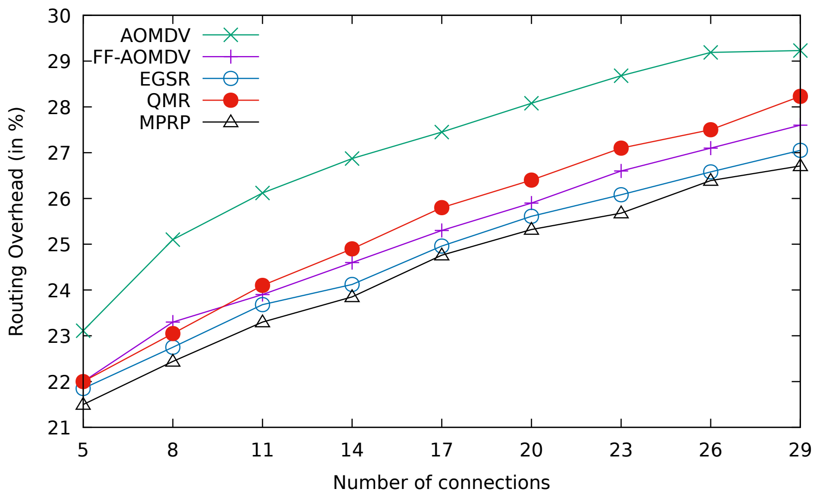

Fig. 4.24: Comparison between AOMDV, FF-AOMDV, EGSR, QMR and proposed protocol MPRP for routing overhead delay with different numbers of OBU nodes receiving data from one RSU

4.3.1.3 Assessment of the simulation results on the basis of network load:

In tests of this section, we consider different packet sizes to identify the data load size with the highest throughput. Next, we use that selected packet size in the remaining tests.

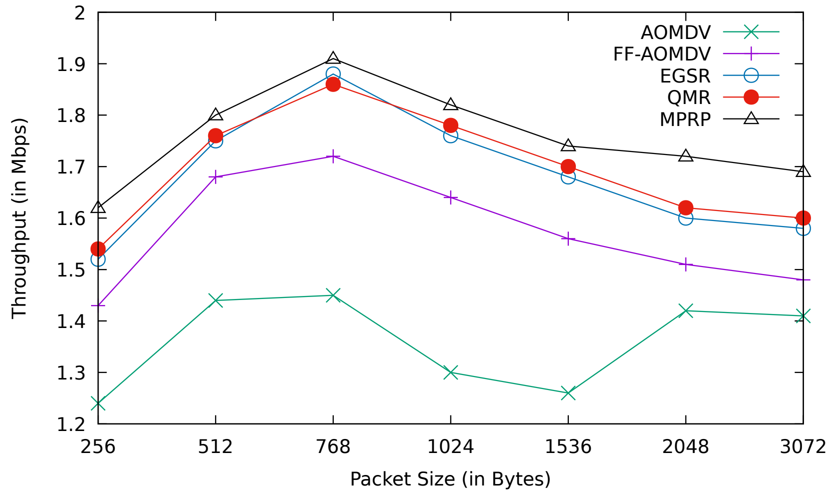

Fig. 4.25: Comparison between AOMDV, FF-AOMDV, EGSR, QMR and proposed protocol MPRP for throughout with different Packet sizes.

In Figure 4.25, the throughput has been calculated based on (3.3) which shows that the throughput increases with the size of the packets until it reaches 768 bytes. Following that, the throughput decreases as the network starts to suffer from data congestion. However, MPRP has the least effect of the congestion on the data transmissions using routes with the minimum RTT, as explained earlier. In overall, MPRP improves the throughput with various packet sizes by 29.2, 11.6, 4.5, 3.7 percent in comparison with AOMDV,FF-AOMDV, EGSR and QMR, respectively.

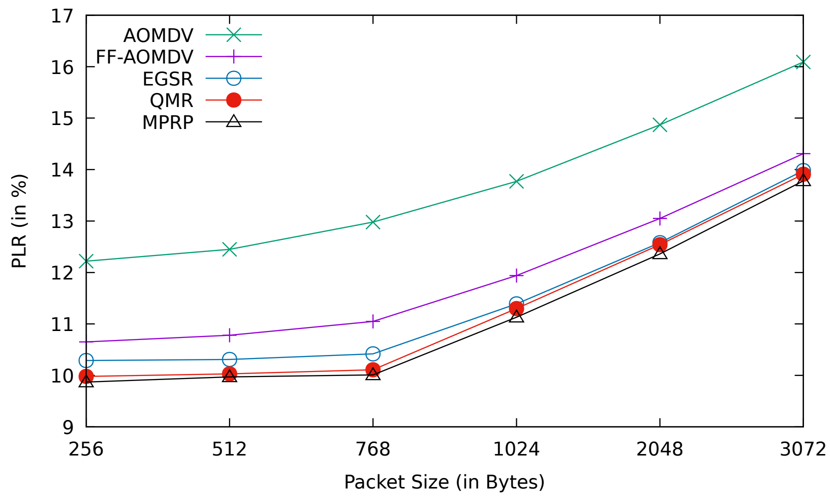

Fig. 4.26: Comparison between AOMDV, FF-AOMDV, EGSR, QMR and proposed protocol MPRP for PLR with different Packet sizes.

In Figure 4.26, MPRP has the least PLR, and this agrees with the throughput result. PLR maintains a steady performance for packet size up to 768 bytes and increases after that. When the packet size increases above 768 bytes, the network may undergo data congestion at the bottle-neck, and as a result, the PLR reduces. Similarly, as a result of having data congestion when the packet size is greater than 768 bytes.

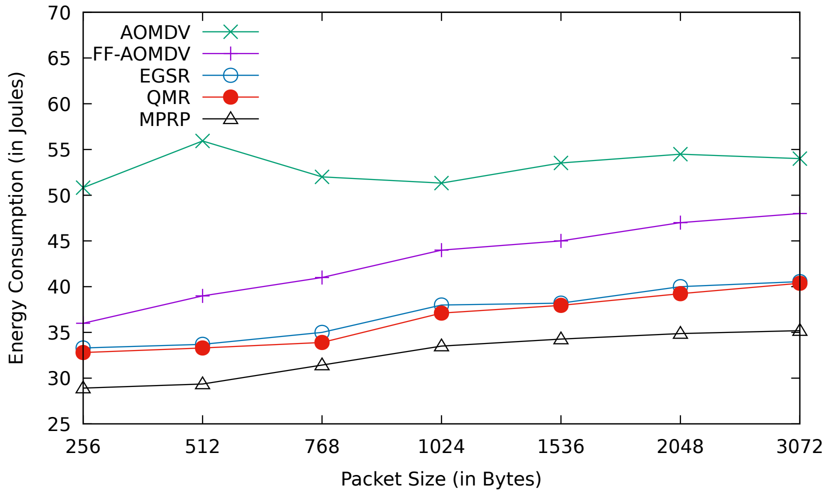

Fig. 4.27: Comparison between AOMDV, FF-AOMDV, EGSR, QMR and proposed protocol MPRP for energy consumption with different Packet sizes.

As shown in Figure 4.27, the energy consumption increases when the transmission delay increases as depicted in Figure 4.28 as a result of the data load size growth. MPRP shows the least energy consumption due to its lowest PLR in this simulation. On the other hand, AOMDV shows the worst result and this is due to having an emerging bottleneck causing a chance of data congestion and collision. The main factor in increasing the end-to-end delay is the queuing time. Avoiding data congestion occurrence is the most promising way to shrink the end-to-end delay. MPRP performance in terms of end-to-end delay is high owing to its data traffic problem detection mechanism in terms of RTT threshold.

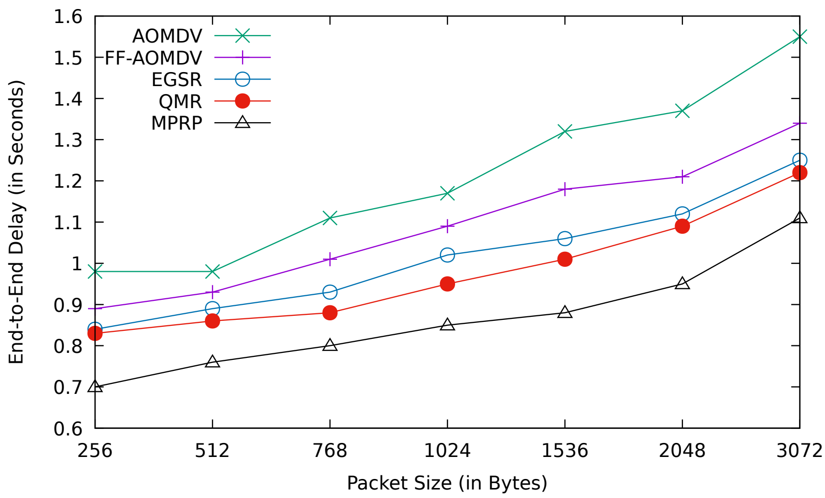

Fig. 4.28: Comparison between AOMDV, FF-AOMDV, EGSR, QMR and proposed protocol MPRP for end-to-end delay with different Packet sizes.

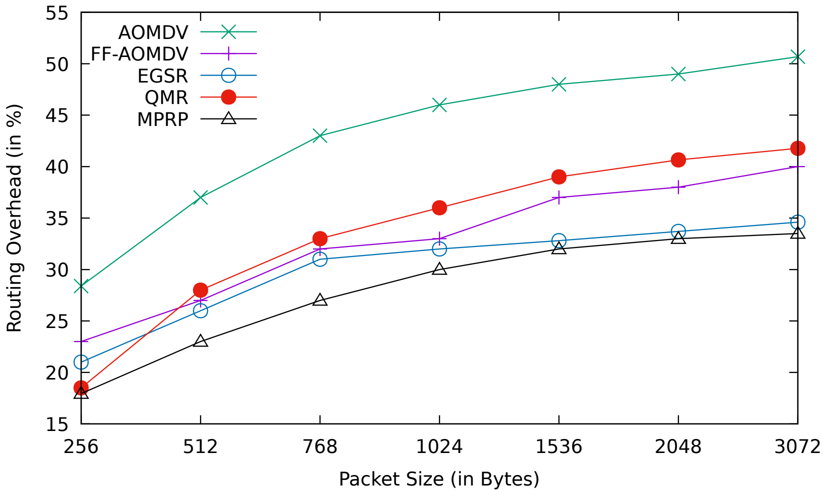

Fig. 4.29: Comparison between AOMDV, FF-AOMDV, EGSR, QMR and proposed protocol MPRP for routing overhead with different Packet sizes.

There will be fewer data packets for the same size of data if the packet size increases. Therefore the ratio of the routing packet to the data packet increases. Additionally, having larger data packets increases the transmission time, increasing the chance of having data collisions. In this case, the data retransmission process may take a longer time than the time of routing data availability in routing tables. As a result, routing discovery packets would increase, as shown in Figure 4.29. However, MPRP has the least routing overhead due to its novel mechanism explained above.

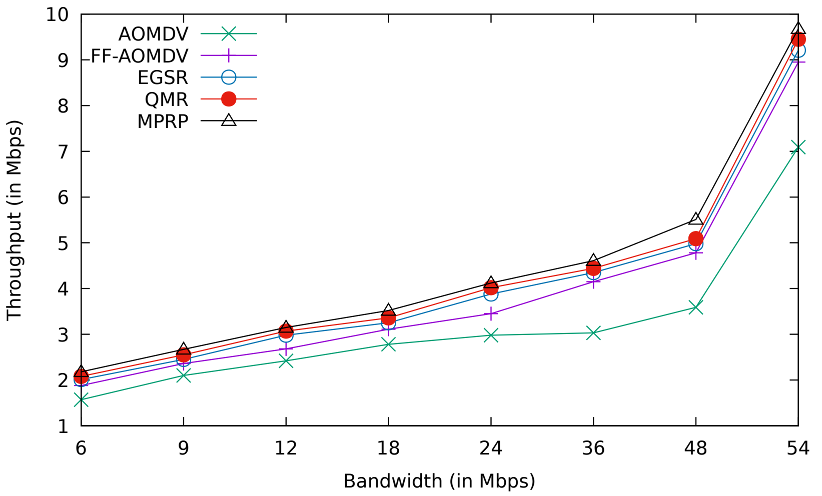

Fig. 4.30: Comparison between AOMDV, FF-AOMDV, EGSR, QMR and proposed protocol MPRP for throughout with bandwidth.

In Figure 4.30, as the bandwidth increases as the throughput increases as a result of the growth in the number of delivered data loads. In other words, the congestion window expands while the data congestion possibility reduces. This, in turn, would diminish the data retransmission rate and accordingly, the end-to-end delay decreases as shown in

Figure 4.31. Also, in this case, the need for routing discovery packets lessens, as shown in Figure 4.32. Despite the fact that the performances of all protocols are close to each other, MPRP shows the best performance.

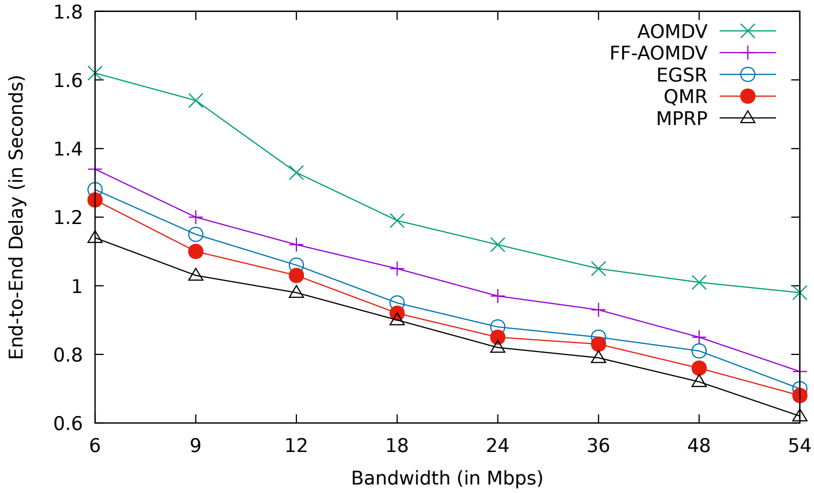

Fig. 4.31: Comparison between AOMDV, FF-AOMDV, EGSR, QMR and proposed protocol MPRP for end-to-end delay with bandwidth.

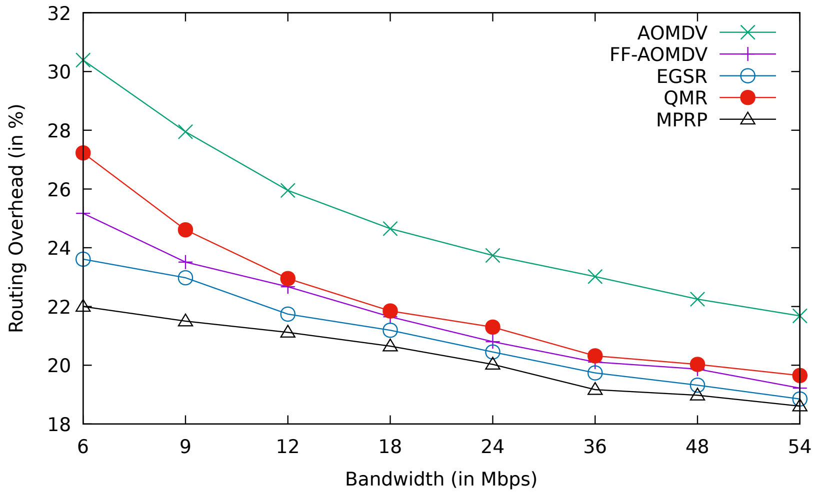

Fig. 4.32: Comparison between AOMDV, FF-AOMDV, EGSR, QMR and proposed protocol MPRP for routing overhead with band width.

4.3.1.4 Assessment of the simulations' result on the basis of nodes' characteristics:

the impact of environmental factors including, faulty node ratio, number of nodes, and mobility speed, has been studied. The results are represented as follows.

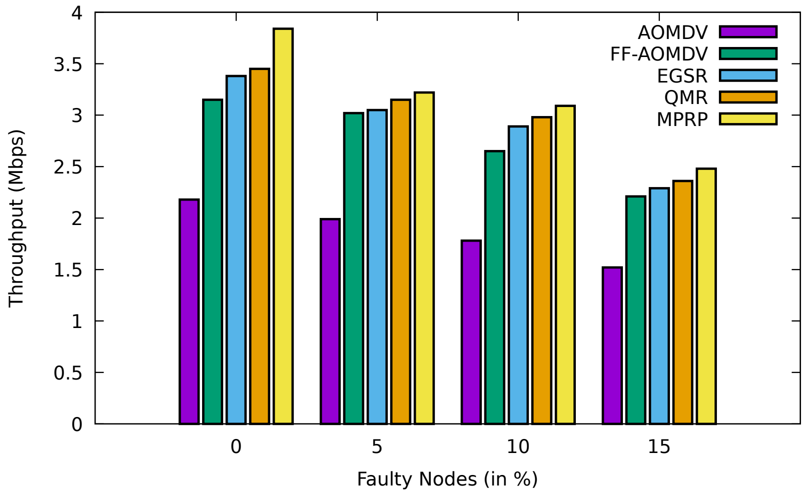

Fig. 4.33: Comparison between AOMDV, FF-AOMDV, EGSR, QMR and proposed protocol MPRP for throughput with faulty node.

We use a threshold value which is the average RTT, to determine if the path can be considered in the MPRP list of available routing paths. If the instant RTT is higher than the average one, this can be a sign of having traffic congestion in a route, as indicated earlier. Also, this can be considered as a sign of having faulty nodes that are functioning improperly because of a malfunction of the software or the hardware of the vehicle. The node can fail during the routing discovery phase, and then the route having such a node will be easily dropped. However, the node might fail during the data transmission, so we study this here in our results. In Figure 4.33, we considered the percentage of faulty nodes to be 0, 5, 10, and 25. As the number of faulty nodes increases, the throughput decreases because of the data loss during the transition period between the routes in the case of multi-path algorithms. On the contrary, the transmission will halt during the route discovery phase for each node failure. Minimum RTT involves the minimum number of nodes and the shortest distance, so the effect of a node failure, which results in data loss during transmission, will be less with MPRP, and this leads to a higher throughput.

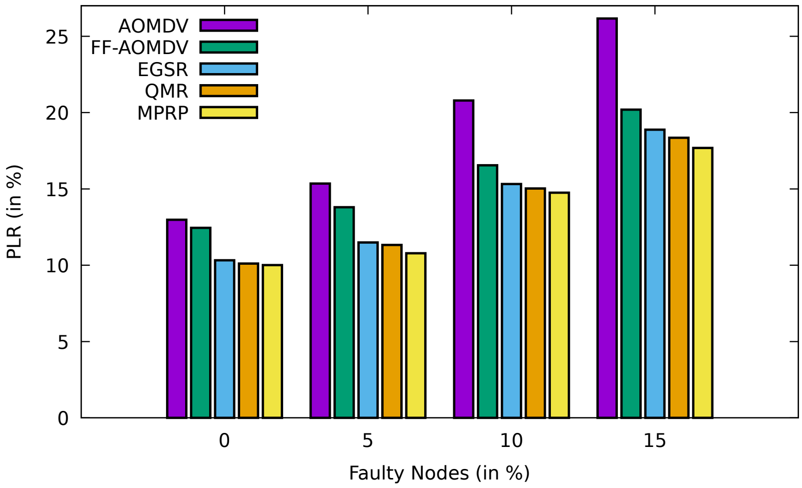

Fig. 4.34: Comparison between AOMDV, FF-AOMDV, EGSR, QMR and proposed protocol MPRP for PLR with faulty node.

More data loss will happen, and less number of data load delivered to destination end when the rate of faulty nodes increases, and therefore the PLR Increases as shown in Figures 4.34, MPRP still outperforms other protocols as it avoids going through an excessive number of nodes in the selected multiple routes in contrary with other shown protocols.

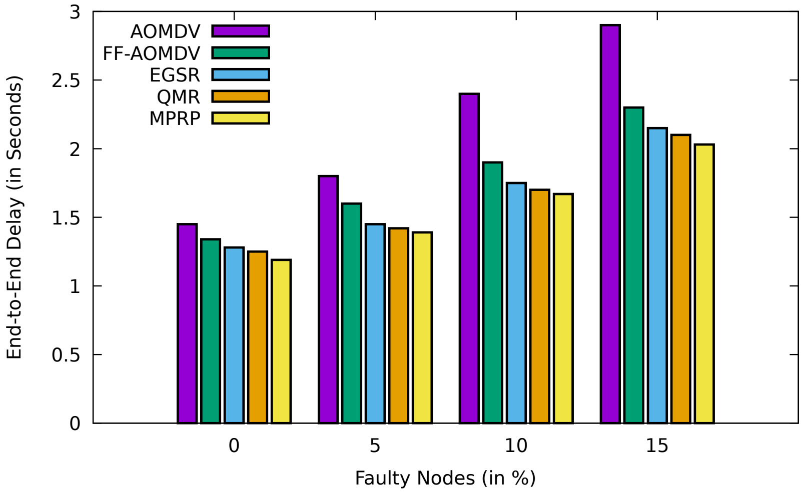

Fig. 4.35: Comparison between AOMDV, FF-AOMDV, EGSR, QMR and proposed protocol MPRP for end-to-end delay with faulty node.

In Figure 4.35, with having faulty nodes increases, the time delay will be longer because the source node (RSU) has to receive an ICMP error message indicating node failure or wait for a timeout without receiving an acknowledgment and hence the RSU has to switch between alternative routes.

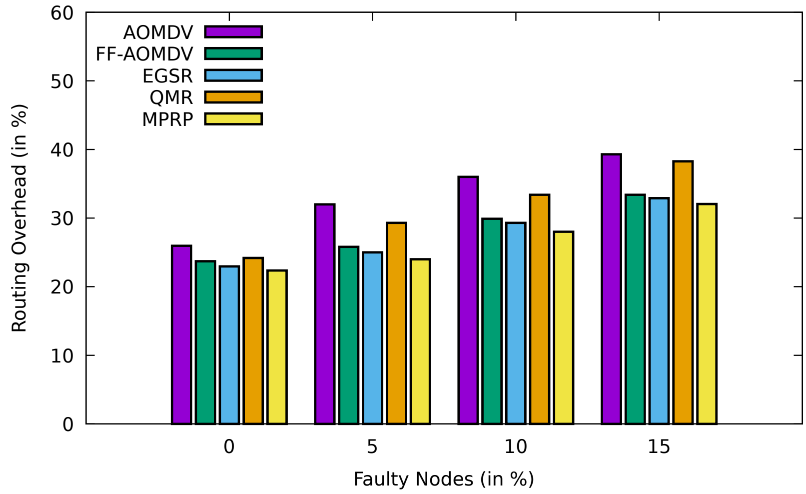

Fig. 4.36: Comparison between AOMDV, FF-AOMDV, EGSR, QMR and proposed protocol MPRP for routing overhead with faulty node.

In Figure 4.36, the higher faulty node rate increases the chance of having link failures. As a consequence of growth in the chance of link failure, the network goes through the route discovery phase more frequently.

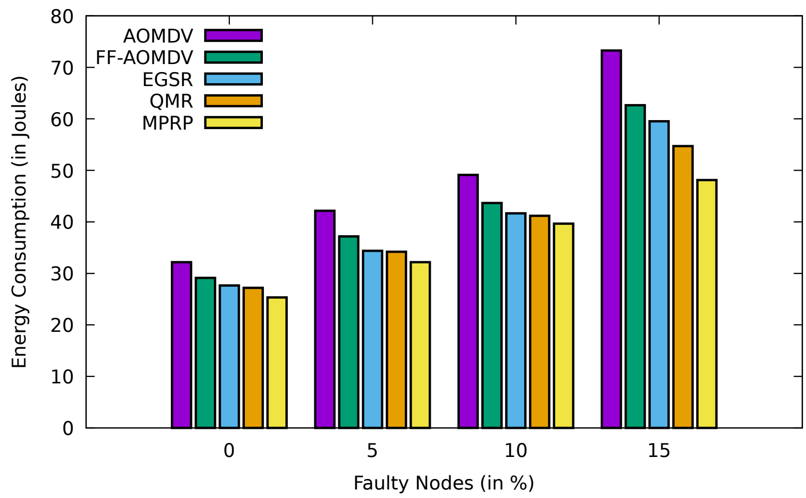

Fig. 4.37: Comparison between AOMDV, FF-AOMDV, EGSR, QMR and proposed protocol MPRP for energy consumption with faulty node.

In Figure 4.37, increasing the amount of energy consummation is an outcome of the growth in the ratio of faulty nodes. With a higher faulty nodes rate, the PLR increases obviously, and this, in turn, increases the number of data re-transmission packets. In this case, the network needs more routing packets to keep the network connectivity. Such extra data loads consume an excessive amount of nodes' energy.

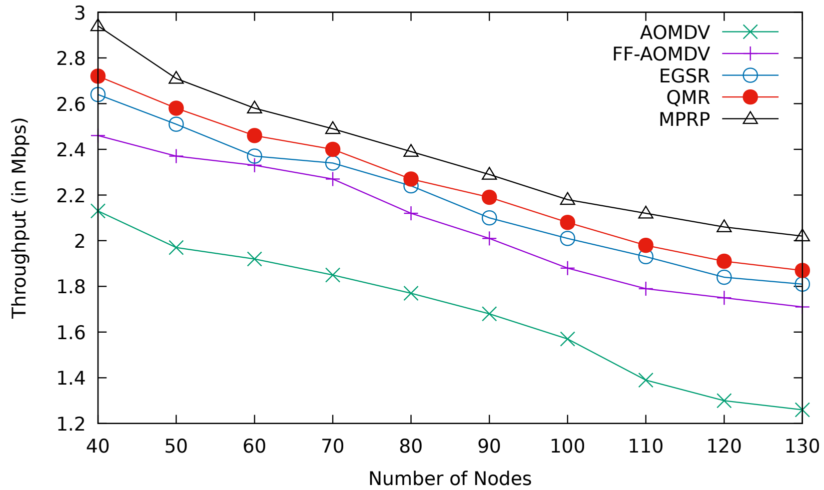

Fig. 4.38: Comparison between AOMDV, FF-AOMDV, EGSR, QMR and proposed protocol MPRP for throughput with number of nodes.

Table 4.3: Number of nodes vs. throughput

#node	AOMDV	FF-AOMDV	EGSR	QMR	MPRP
40	2.13	2.46	2.64	2.72	2.94
50	1.97	2.37	2.51	2.58	2.71
60	1.92	2.33	2.37	2.46	2.58
70	1.85	2.27	2.34	2.4	2.49
80	1.77	2.12	2.24	2.27	2.39
90	1.68	2.01	2.1	2.19	2.29
100	1.57	1.88	2.01	2.08	2.18
110	1.39	1.79	1.93	1.98	2.12
120	1.3	1.75	1.84	1.91	2.06
130	1.26	1.71	1.81	1.87	2.02
sum	16.84	20.69	21.79	22.46	23.78
gain (%)	41.21	14.93	9.13	5.88	

The throughput is high compared to other protocols, as shown in Figure 4.38. MPRP selects the path that has the minimum RTT, and hence it increases the number of packets delivered to the destination node in a given time. Additionally, the route selected based on this mechanism would avoid the congested nodes, as explained above. Table 4.3 shows improvement of MPRP by 41.21, 14.93, 9.13 and 5.88 percent compared to AOMDV, FF-AOMDV, EGSR and QMR, respectively.

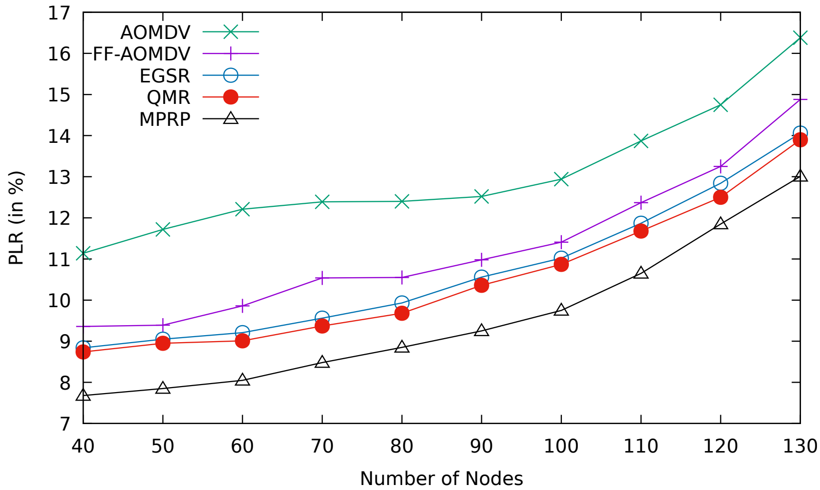

Fig. 4.39: Comparison between AOMDV, FF-AOMDV, EGSR, QMR and proposed protocol MPRP for PLR with number of nodes.

In Figure 4.39, it is visible that as the number of nodes increases, the number of packets delivered decreases. This is owing to the congested traffic where the obvious amount of data will be dropped and lost. On the other hand, and as indicated earlier, MPRP selects the path based on its reliability, so it outperforms other protocols. Additionally, MPRP uses the threshold mechanism, and as a result, the packet loss decreases.

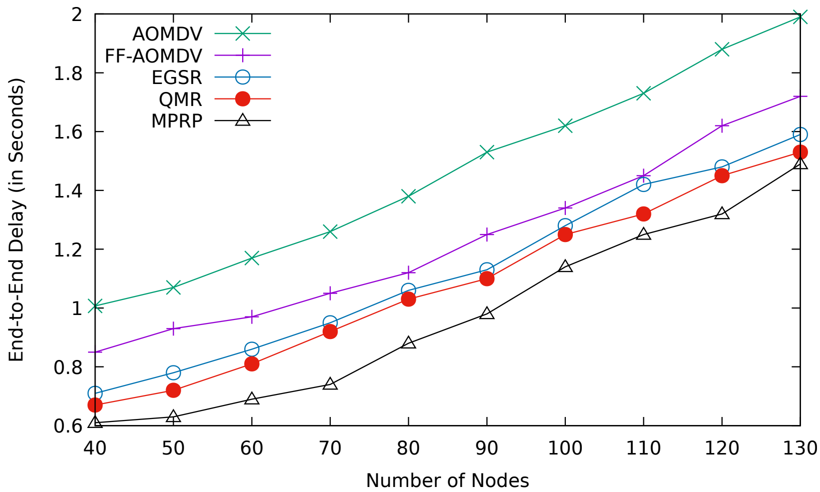

Fig. 4.40: Comparison between AOMDV, FF-AOMDV, EGSR, QMR and proposed protocol MPRP for end-to-end delay with number of nodes.

Table 4.4: Number of nodes vs. end-to-end delay

#node	AOMDV	FF-AOMDV	EGSR	QMR	MPRP
40	1.007	0.85	0.71	0.67	0.61
50	1.07	0.93	0.78	0.72	0.63
60	1.17	0.97	0.86	0.81	0.69
70	1.26	1.05	0.95	0.92	0.74
80	1.38	1.12	1.06	1.03	0.88
90	1.53	1.25	1.13	1.1	0.98
100	1.62	1.34	1.28	1.25	1.14
110	1.73	1.45	1.42	1.32	1.25
120	1.88	1.62	1.48	1.45	1.32
130	1.99	1.72	1.59	1.53	1.49
sum	14.637	12.3	11.26	10.8	9.73
saving (%)	33.5	20.9	13.6	9.9	

In Figure 4.40, increasing the number of nodes as the processing time to find the efficient route among several possible routes, increases, and therefore the end-to-end delay augments. In the case of multi-path protocols, the delay is shorter as alternative paths are always available if a link fails. MPRP algorithm can detect and select the least congested link, so the queuing delay will be minimal, and as a result, the end-to-end delay will be relatively short compared to other protocols. The corresponding data is noted in table 4.4. MPRP reduces the end-to-end delay by 33.5, 20.9, 13.6 and 9.9 percent compare to AOMDV, FF-AOMDV, EGSR and QMR, respectively.

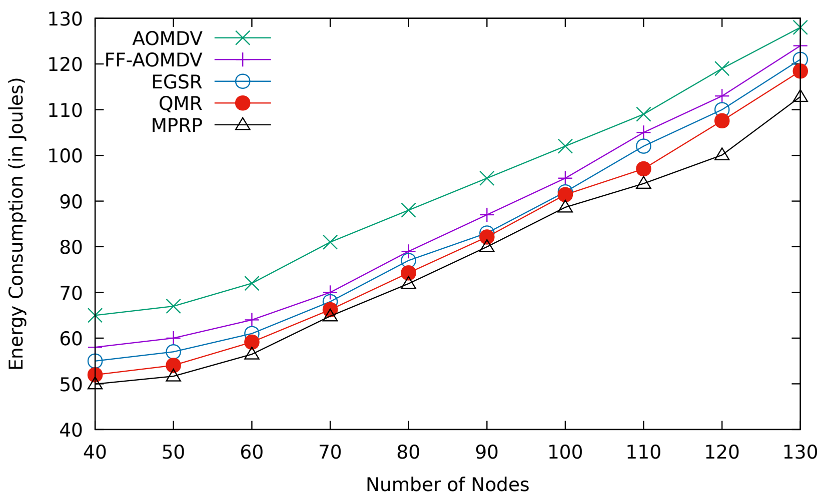

Fig. 4.41: Comparison between AOMDV, FF-AOMDV, EGSR, QMR and proposed protocol MPRP for energy consumption with number of nodes.

A consequence of involving more nodes in data transmission is that more amount of energy is going to be used. Every node may receive routing packets and forward them. In this case, the number of neighboring nodes to the sender would increase and consequently, the energy depletion of the MANET nodes is faster. The result of the energy consumption with the number of nodes is depicted in Figure 4.41.

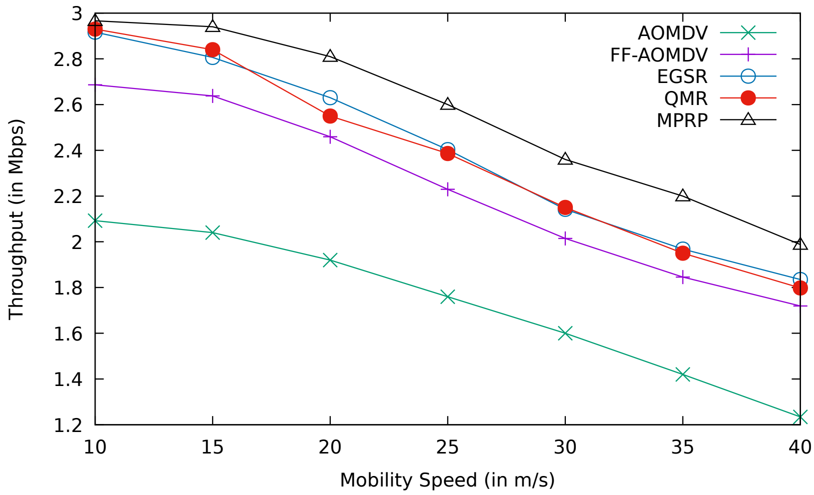

Fig. 4.42: Comparison between AOMDV, FF-AOMDV, EGSR, QMR and proposed protocol MPRP for throughput with mobility speed.

Table 4.5: Mobility speed vs. throughput

speed	AOMDV	FF-AOMDV	EGSR	QMR	MPRP
10	2.0924	2.6864	2.9164	2.93	2.9664
15	2.04	2.638	2.806	2.8396	2.94
20	1.92	2.4592	2.63	2.55	2.8096
25	1.76	2.2292	2.4028	2.386	2.6
30	1.6	2.0144	2.142	2.15	2.36
35	1.42	1.8456	1.968	1.95	2.2
40	1.2344	1.7192	1.8352	1.798	1.988
sum	12.0668	15.592	16.7004	16.6036	17.864
gain (%)	48.04	14.57	6.97	7.59	

When the mobility speed of the vehicles increases, links incur more instability which in turn would lose more data packets, and this agrees with [73]. Accordingly, fewer packets would be delivered successfully to the destination node, and as a result, the throughput will be diminished. Minimum RTT, utilized in the MPRP mechanism, may include less number of nodes and also a shorter distance where packets are traveling. Also, minimum RTT implies less congested routes where the possibility of having data loss is low, leading to more stable paths. This would minimize the number of nodes that have a high speed in the selected stable route. Therefore, the negative impact of vehicle mobility on the route stability is reduced, and this accordingly enhances the throughput of the MPRP protocol compared to other protocols as shown in Figure 4.46. At speed zero (non-moving vehicles such as parked ones), MPRP has a better throughput than other protocols as well as when the mobility speed is higher. MPRP improves throughput by 48.04, 14.57, 6.97 and 7.59 percent compared to AOMDV, FF-AMODV, GSR and QMR, respectively.

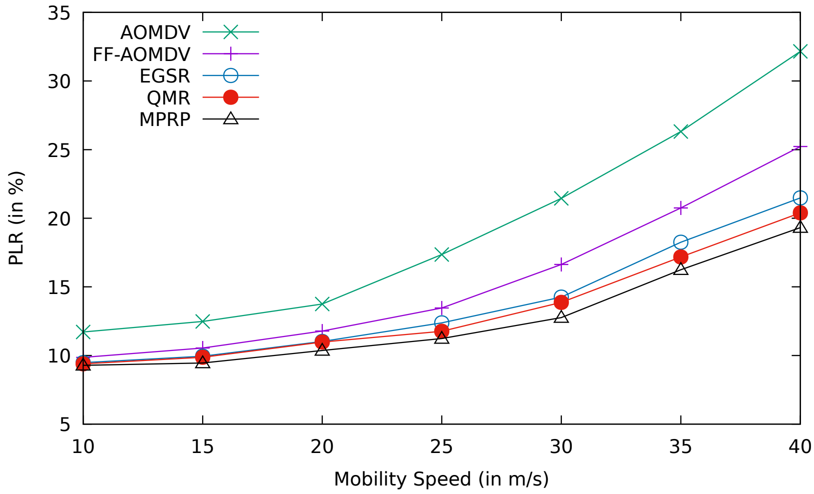

Fig. 4.43: Comparison between AOMDV, FF-AOMDV, EGSR, QMR and proposed protocol MPRP for PLR with mobility speed.

In Figure 4.43, PLR for different protocols performs similarly as throughput versus mobility speed. At 40 m/s (144 km/h) speed, MPRP loses just about 13% out of the sent packets, which are still within the accepted range compared to other protocols. The stability of the selected route in terms of packet loss is vital, particularly with link failure caused by node mobility and this is achieved in the MPRP algorithm.

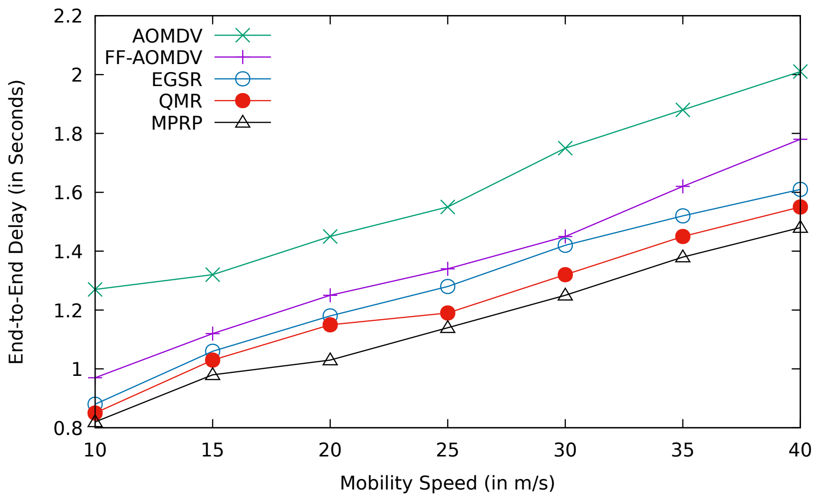

Fig. 4.44: Comparison between AOMDV, FF-AOMDV, EGSR, QMR and proposed protocol MPRP for end-to-end delay with mobility speed.

In Figure 4.44, MPRP protocol experiences low time delay as if the current link fails, the available path in the routing table that has the second least RTT will be adopted.

Whereas FF-AOMDV adopts the alternative path that consumes less energy to reach the destination, and AOMDV, on the other hand, picks the next available path based on the hop count. In these two later protocols, the time delay is long as the route distance might be further away than that in the case of MPRP. EGSR is a protocol designed for urban areas with a lower mobility speed, and that is why it has low performance compared to MPRP. On the contrary, QMR is highly adaptable to high mobility speed.

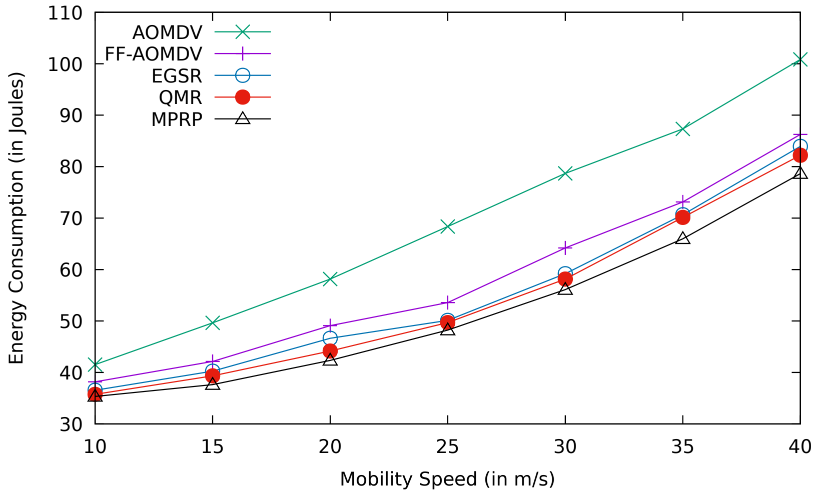

Fig. 4.45: Comparison between AOMDV, FF-AOMDV, EGSR, QMR and proposed protocol MPRP for energy consumption with mobility speed.

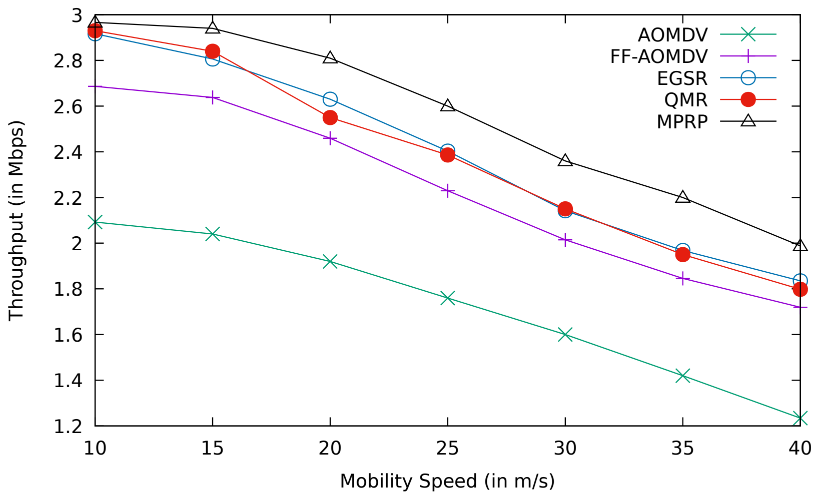

Fig. 4.46: Comparison between AOMDV, FF-AOMDV, EGSR, QMR and proposed protocol MPRP for throughput with mobility speed.

Table 4.6: Mobility speed vs. energy consumption

speed	AOMDV	FF-AOMDV	EGSR	QMR	MPRP
10	41.54	38.19	36.54	35.75	35.35
15	49.65	42.15	40.25	39.35	37.65
20	58.15	49.11	46.65	44.16	42.35
25	68.36	53.58	50.13	49.7	48.23
30	78.68	64.19	59.19	58.16	56.11
35	87.32	73.13	70.65	70.13	65.98
40	100.84	86.25	83.95	82.21	78.64
sum	484.54	406.6	387.36	379.46	364.31
saving (%)	24.81	10.40	5.95	3.99	

Energy consumption is a metric impacted by PLR. As the nodes, mobility speed increases, as the PLR enlarges, resulting in more data retransmissions. This, in turn would consume more energy as shown in Figure 4.45. MPRP saves energy by 24.81, 10.40, 5.95 and 3.99 percent compared to AOMDV, FF-AMODV, GSR and QMR, respectively according to table 4.6.

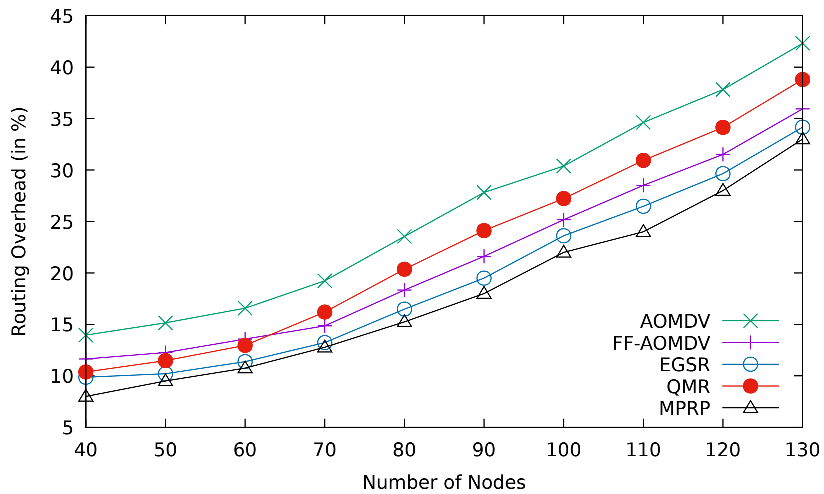

Fig. 4.47: Comparison between AOMDV, FF-AOMDV, EGSR, QMR and proposed protocol MPRP for routing overhead with mobility speed.

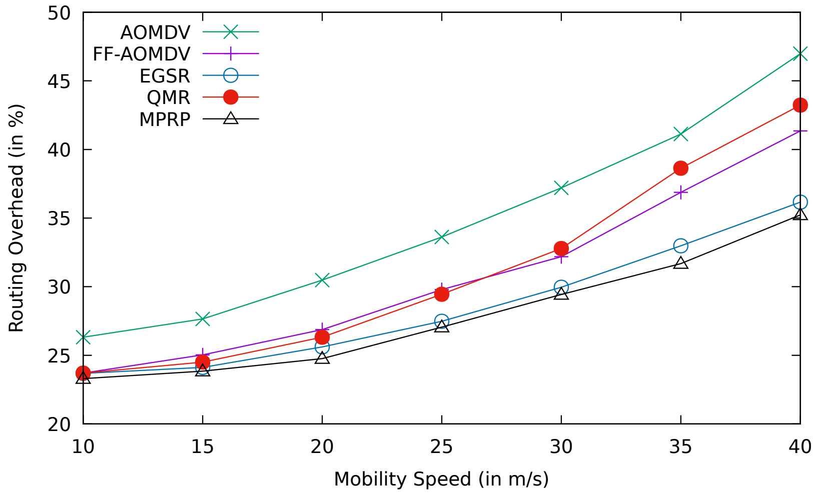

Fig. 4.48: Comparison between AOMDV, FF-AOMDV, EGSR, QMR and proposed protocol MPRP for routing overhead with mobility speed.

Figures 4.47 and 4.48 show the routing overhead for different protocols. It is demonstrated that AODV has the least routing overhead because it is a single path routing protocol, and therefore the amount of route discovery and maintenance packets is limited. On the other hand, the multi-path protocols undergo a higher routing overhead. These protocols seek to find alternate routes in case of having link failure or faulty nodes to reduce end-to-end delay and increases packet delivery rate. FF-AOMDV routes are calculated based on less energy, so it will be updating its routes quite often, and this, in turn, increase the number of overhead packets. Similarly, AOMDV selects the route based on the hop-count, which would require more routing packets to find alternative routes. MPRP has the least routing overhead among those multi-path protocols. RSU sends RREQ to all nodes in its range, and once the RREP is received, routes are determined based on the minimum RTT. Therefore the control packets are limited, and hence the routing overhead is relatively low.

4.3.1.5 Assessment of the simulations' result on the basis of deviation error margin:

To have a better understanding of the performance enhancement that MPRP could achieve, we present results using error bars. As it was shown in the results conducted earlier, MPRP outperforms AOMDV and FF-AOMDV with a large margin so we remove them in the forthcoming results to eliminate any possible ambiguity in the sense of bars overlapping.

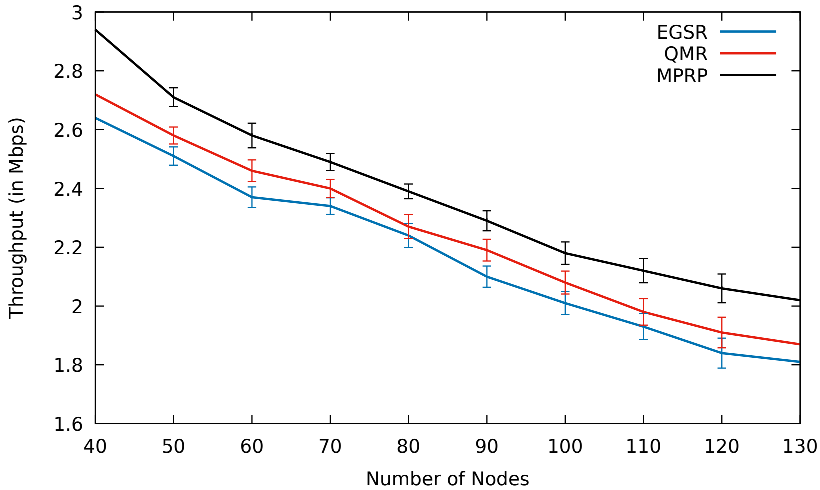

Fig. 4.49: Comparison between EGSR, QMR and proposed protocol MPRP for throughput including error bars with number of nodes.

Figure 4.49 shows that the deviation error of MPRP is not crossing or overlapping the performance of the others. It proves that the proposed protocol shows promising improvement in comparison with other studied protocols.

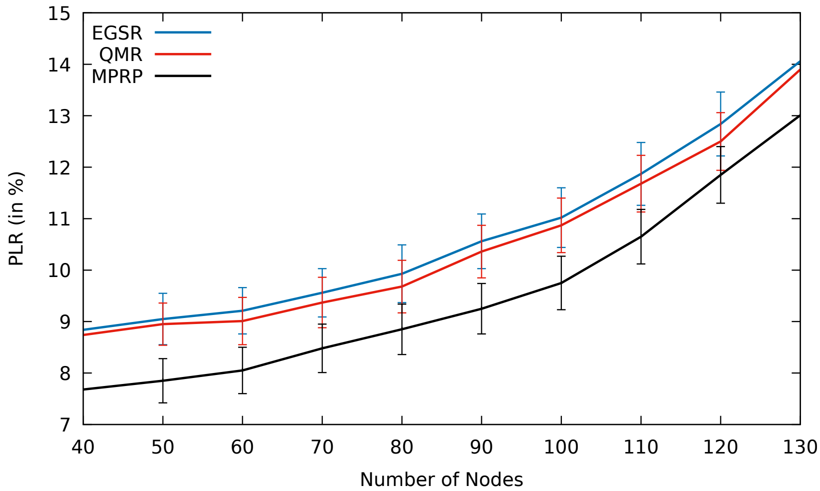

Fig. 4.50: Comparison between EGSR, QMR and proposed protocol MPRP for PLR including error bars with number of nodes.

Similarly, in Figure 4.50, MPRP error bars are not passing the performance line of other protocols in terms of PLR. Additionally, EGSR and QMR error bars are not close to the MPRP performance line, especially for lower number of nodes.

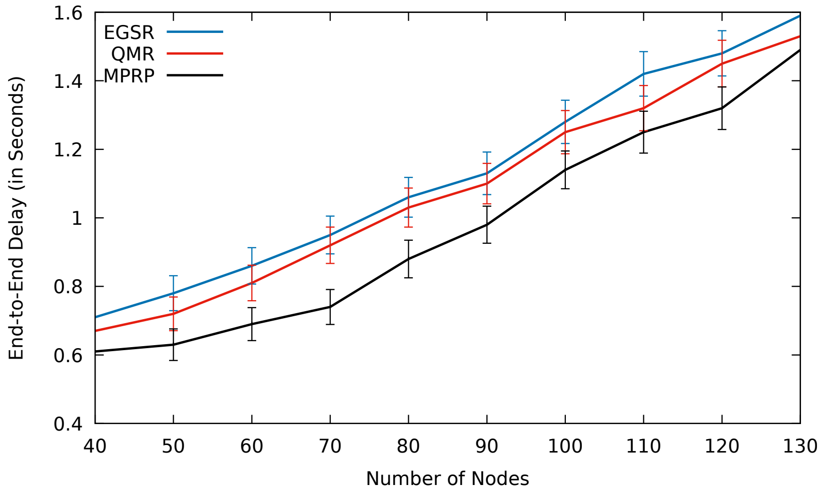

Fig. 4.51: Comparison between EGSR, QMR and proposed protocol MPRP for end-to-end delay including error bars with number of nodes.

The MPRP performance is distinguished in end-to-end delay considering error bars as illustrated in Figure 4.51.

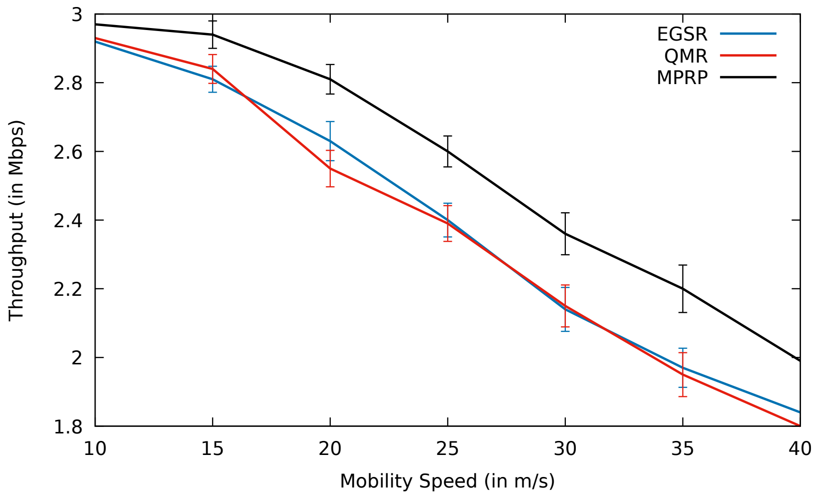

Fig. 4.52: Comparison between EGSR, QMR and proposed protocol MPRP for throughput including error bars with mobility speed.

With increasing the mobility speed, error bars in Figure 4.52 depict the efficiency of MPRP for highways environments. No error bar overlapping is observed for MPRP's throughput where EGSR and QMR are performing tightly.

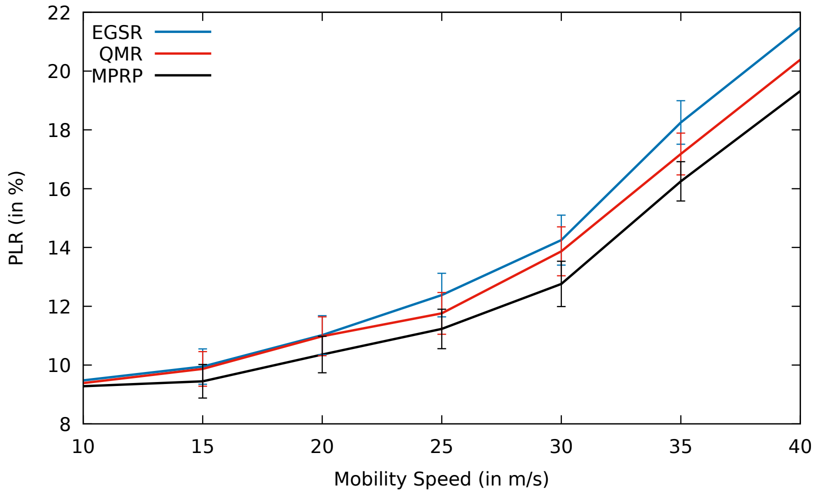

Fig. 4.53: Comparison between EGSR, QMR and proposed protocol MPRP for PLR including error bars with mobility speed.

The error margin is widening as the mobility speed increases in Figure 4.53. The error bars crossing each other only with the lower mobility speed. When the speed increases, the crossing of the error bar becomes negligible.

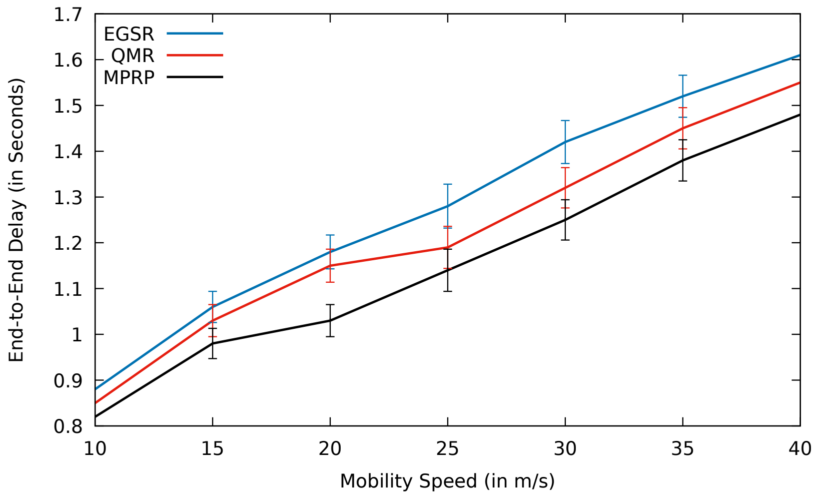

Fig. 4.54: Comparison between EGSR, QMR and proposed protocol MPRP for end-to-end delay including error bars with mobility speed.

A slight overlapping between MPRP and QMR error bars is observed which is audible in Figure 4.54.

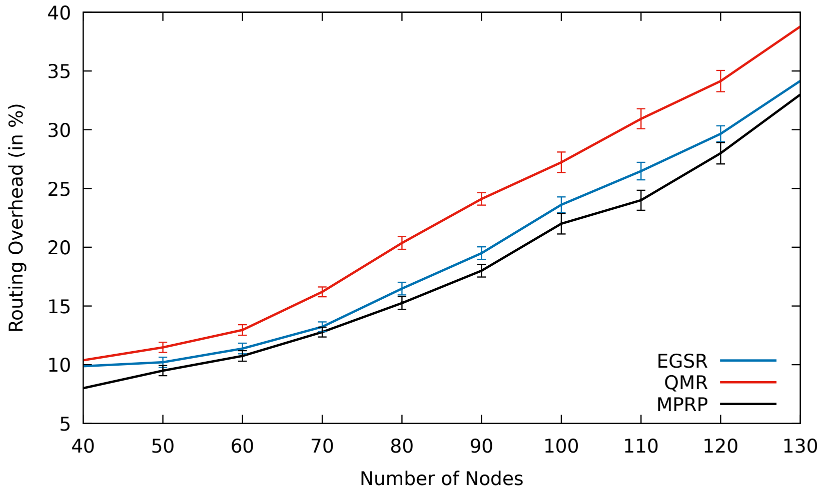

Fig. 4.55: Comparison between EGSR, QMR and proposed protocol MPRP for outing overhead including error bars with number of nodes.

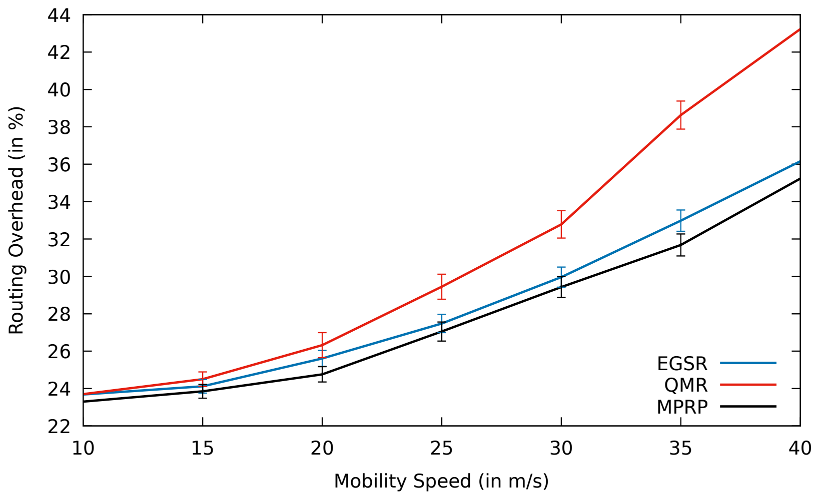

Fig. 4.56: Comparison between EGSR, QMR and proposed protocol MPRP for outing overhead including error bars with mobility speed.

QMR is showing a quite low performance for routing overhead ratio in Figures 4.55 and 4.56. The EGSR and MPRP are close on this matter; however, MPRP error bars mostly do not overlap the EGSR error bar in a wide range.

4.3.2 The results of scenario 2

In the following simulation, the sender and receiver OBUs are located in different road segments; therefore, there is no pair of sender and receiver whose road segments are the same. An exemplification of the given scenario is provided in Figure 4.57. Simulator selected sender and receiver nodes randomly. ISR algorithm was designed to work appropriately for the given scenario; therefore, we compare QMR and ISR with MPRP in this scenario with nine simulation runs to acquire more accurate results.

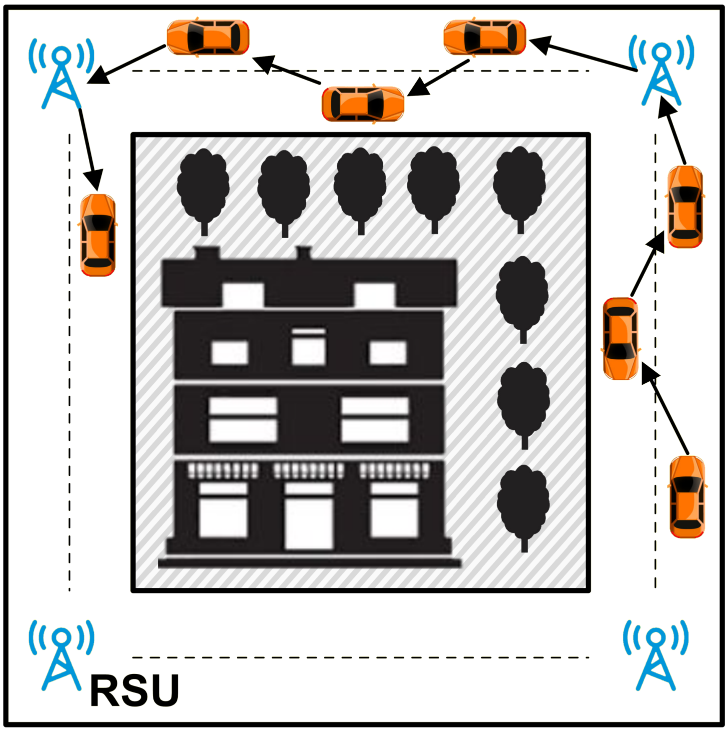

Fig. 4.57: Scenario 2: data communications in multiple road segments.

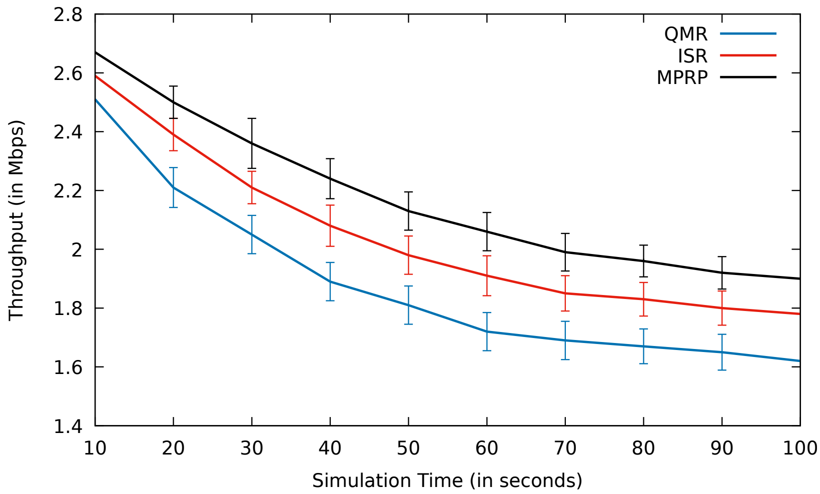

Fig. 4.58: Comparison between EGSR, ISR and proposed protocol MPRP for throughput including error bars with simulation time.

The performance of all the protocols drops in terms of throughput as simulation time goes ahead in Figure 4.58. MPRP shows the highest performance where it is not crossed by other protocols error bars. Selecting the efficient route based on the minimum RTT in MPRP algorithm implies avoiding links with high traffic congestion and this leads to such promising performance. Similarly, MPRP's PLR is the lowest in Figure 4.59, proving its novel performance. The threshold mechanism of MPRP in algorithm 3 selects routes whose RTTs are lower than the average RTT value. Hence, lengthy routes are dropped and therefore, the possibility of having links failure is reduced.

4.3.2.1 Assessment of the simulation results on the basis of simulation time:

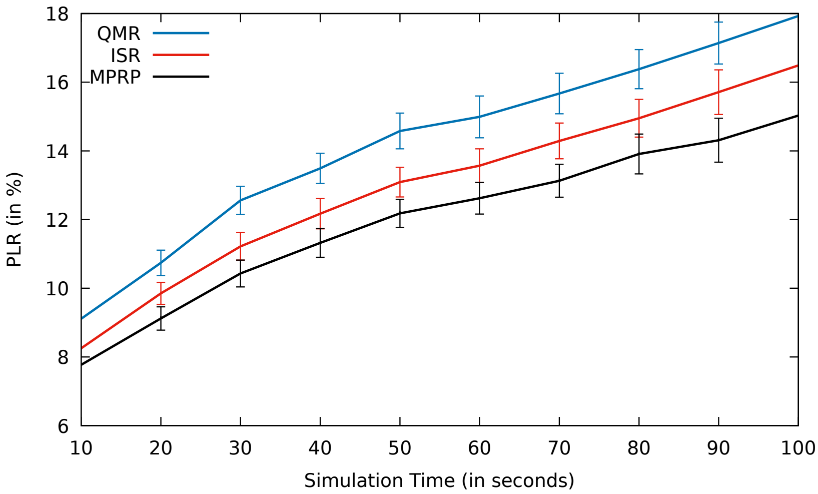

Fig. 4.59: Comparison between EGSR, ISR and proposed protocol MPRP for PLR including error bars with simulation time.

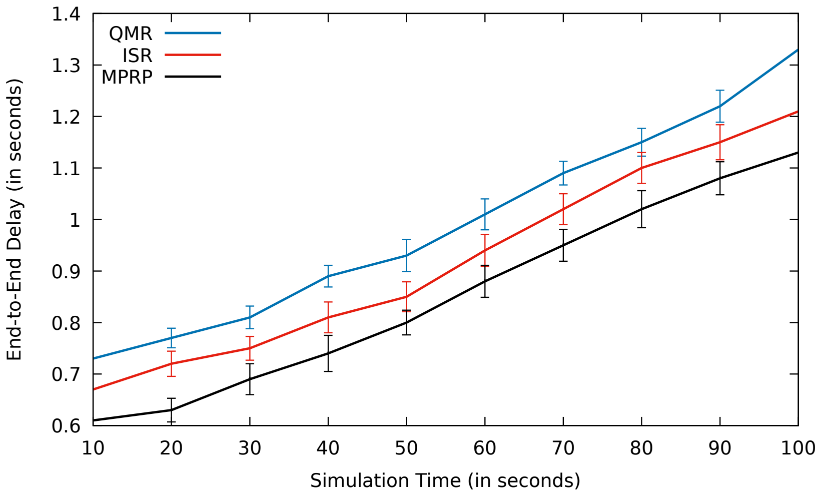

Fig. 4.60: Comparison between EGSR, ISR and proposed protocol MPRP for end-to-end delay including error bars with simulation time.

Through time, the network gets more congested and consequently, the end-to-end delay increases which is the case in Figure 4.60; however, MPRP has the lowest delay due to its route selection mechanism.

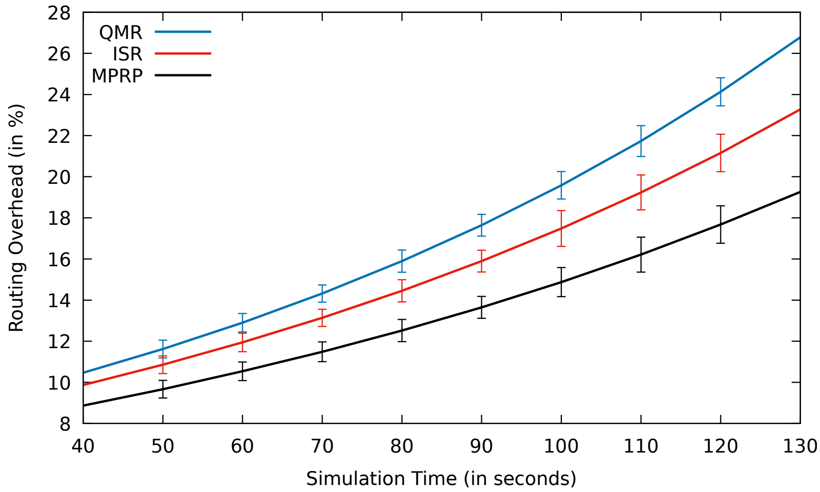

Fig. 4.61: Comparison between EGSR, ISR and proposed protocol MPRP for routing overhead including error bars with simulation time.

The routing protocol needs to go through the route discovery phase when the PLR increases. MPRP has the lowest PLR; therefore, the route discovery phase is initiated at a lower rate than other protocols. This, in turn, reduces the routing overhead ratio as shown in Figure 4.61. Additionally, an excessive amount of routing packets are sent to collect information about the network status such as head nodes selection in case of ISR and the next node in case of QMR. These routing packets are not used in the MPRP and, therefore, QMR and ISR have worse routing overhead performance than MPRP.

4.3.2.2 Assessment of the simulation results on the basis of mobility speed:

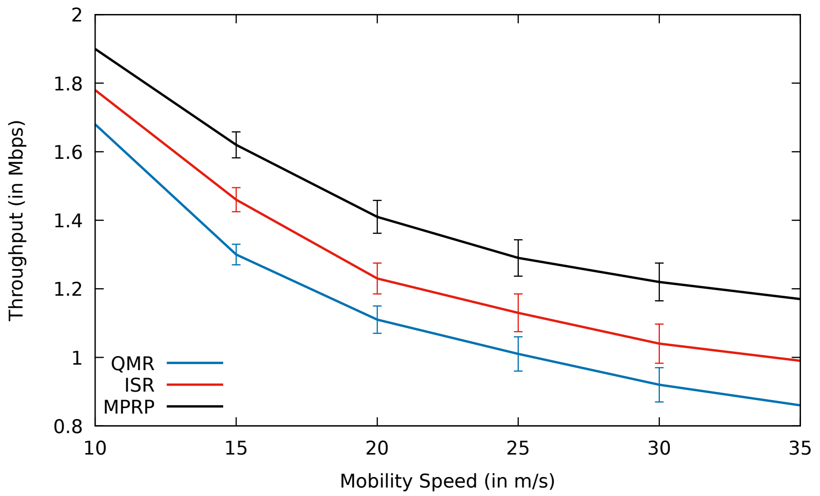

Fig. 4.62: Comparison between QMR, ISR and proposed protocol MPRP for throughput including error bars with mobility speed.

The network topology is prone to change when at mobility speed increases. Consequently, the performance of protocols drops, as it is depicted in Figures 4.62 and 4.63. When vehicles move with high speed, channels disconnect and PLR increases. RSU has a wider transmission range than OBU and, therefore, RSU can find more alternative routes using MPRP than OBU.

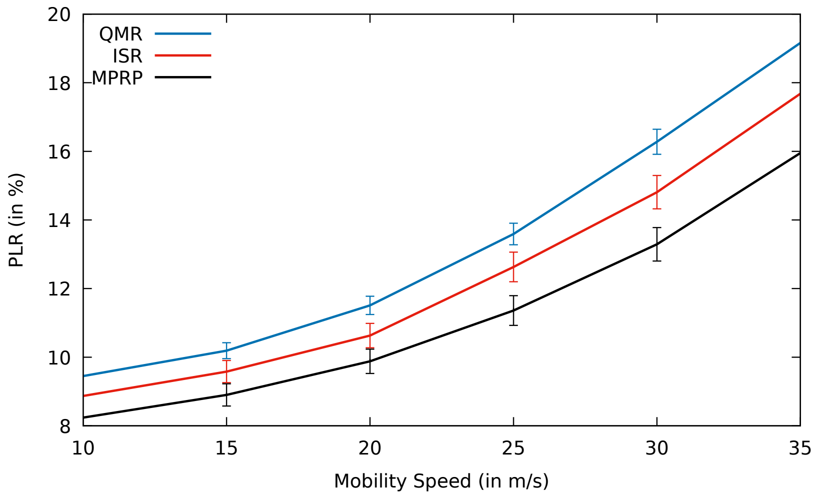

Fig. 4.63: Comparison between QMR, ISR and proposed protocol MPRP for PLR including error bars with mobility speed.

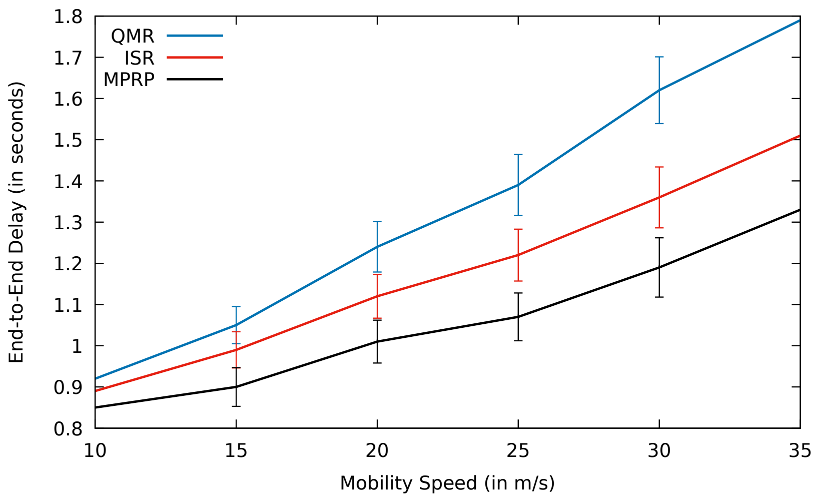

Fig. 4.64: Comparison between QMR, ISR and proposed protocol MPRP for end-to-end delay including error bars with mobility speed.

The average end-to-end delay increases when mobility speed increases due to link failure and retransmission of data. The given justification is proven in Figure 4.64. As the result of the route selection mechanism based on the minimum RTT in MPRP, the lowest end-to-end delay emerged for MPRP, followed by ISR and QMR. The resulting error bars are not overlapping significantly with the higher mobility speeds.

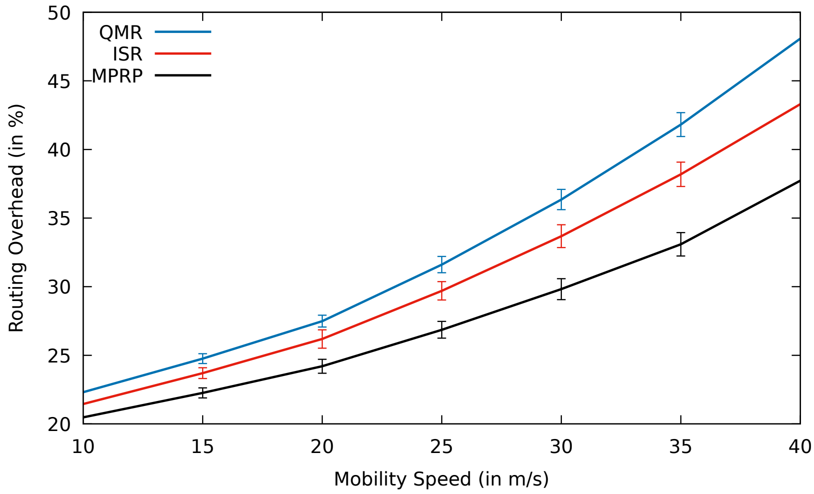

Fig. 4.65: Comparison between QMR, ISR and proposed protocol MPRP for routing overhead including error bars with mobility speed.

According to equation (3.4), the routing overhead is the result of two parameters: data and routing packets. Therefore, when the PLR increases, the number of successfully delivered data packets drops. Therefore, the routing overhead ratio increases. Additionally, the routing protocol has to go through the routing discovery phase in case of link failure, which produces more routing packets. The MPRP has the lowest routing overhead in Figure 4.65, which proves the throughput and PLR result. With increasing mobility speed, the ISR and QMR routing overhead is distinguishable from MPRP. No error bars overlapping in this case.

4.3.2.3 Assessment of the simulation results on the basis of number of nodes:

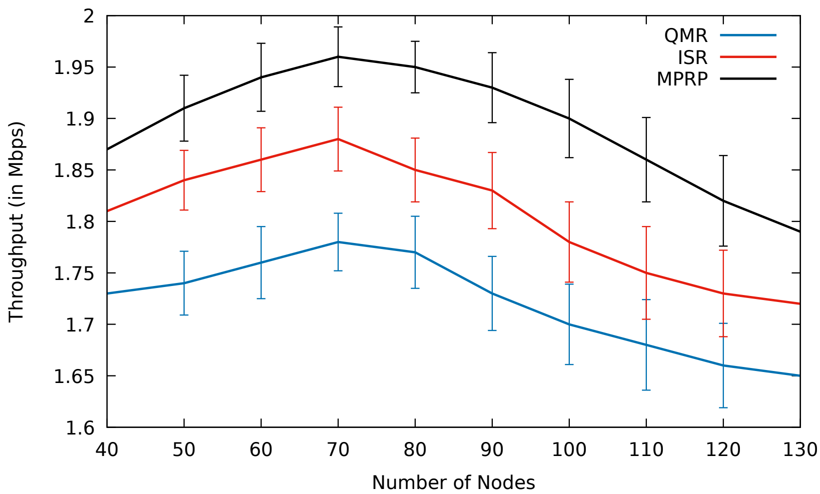

Fig. 4.66: Comparison between QMR, ISR and proposed protocol MPRP for throughput including error bars with number of nodes.

The network connectivity depends on the number of nodes in each area. Therefore, when the number of nodes increases, the network is more connected. However, it results in having more data congestion and collision, especially when network nodes frequently broadcast emergency messages or cooperative awareness messages (CAM). In Figures 4.66 and 4.67, increasing the number of nodes would improve the utilization of the network. This continues until the number of nodes reaches 70 which is the optimum. Beyond that optimum number of nodes, more data packets will result in traffic data jams and hence the performance degrades monotonically. Also, we notice having no error bars overlapping.

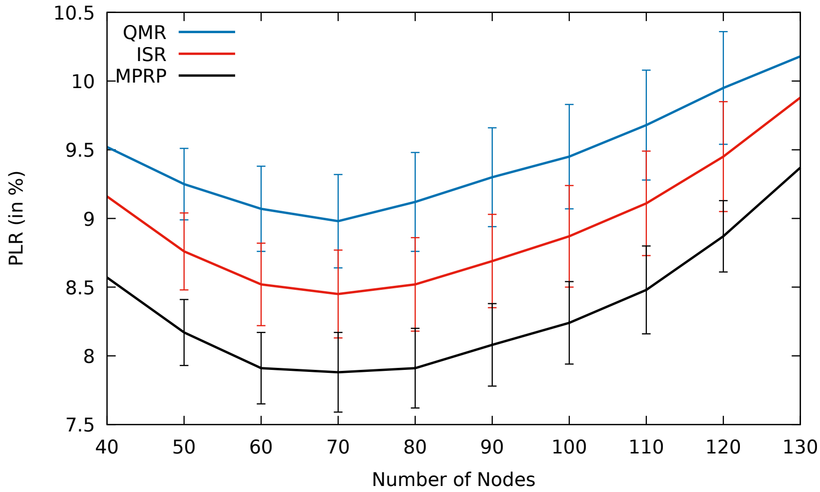

Fig. 4.67: Comparison between QMR, ISR and proposed protocol MPRP for PLR including error bars with number of nodes.

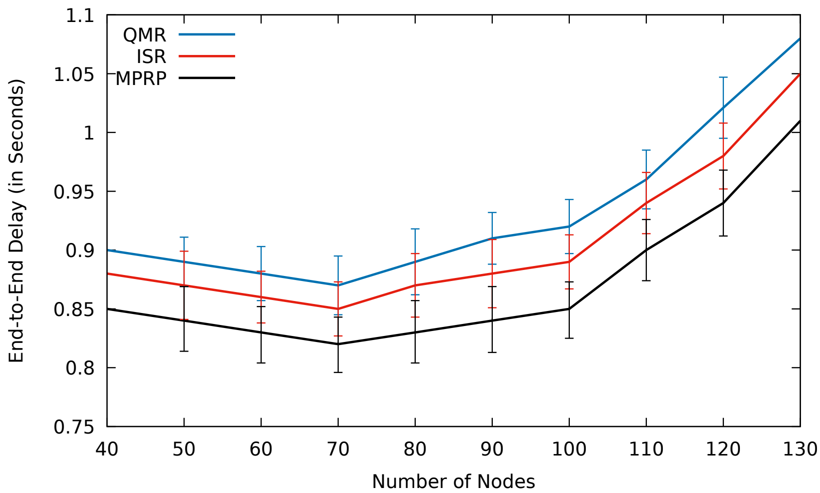

Fig. 4.68: Comparison between QMR, ISR and proposed protocol MPRP for end-to-end delay including error bars with number of nodes.

The end-to-end delay increases drastically when the number of nodes goes beyond the optimum value as depicted in Figure 4.68. The chance of having lengthy routes increases when there are lots of intermediate nodes. MPRP mechanism drops those lengthy routes and, therefore, end-to-end delay is minimal.

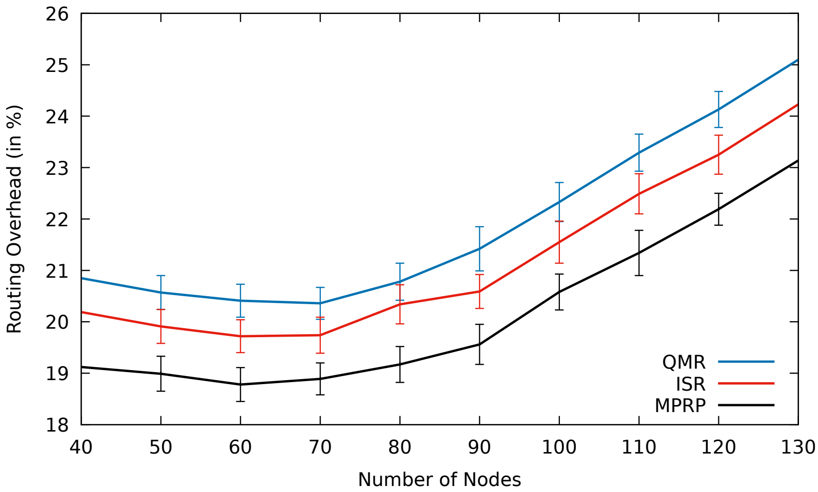

Fig. 4.69: Comparison between QMR, ISR and proposed protocol MPRP for routing overhead including error bars with number of nodes.

In Figure 4.69, the routing overhead increases slightly with the number of nodes because the throughput in this range increases. When the number of nodes is greater than the optimum number, the throughput diminishes due to the traffic problems occurrence. In this range, data retransmissions increase and accordingly more routing packets are sent to accommodate those retransmissions. We can see no error bars are overlapping.

4.4 Routing Protocol Analysis

In VANETs, energy consumption is not a challenge due to the availability of a significant source of energy. The network nodes could use the vehicle battery. As a result, methods that use energy consumption to measure the traffic condition of the network, such as ETE [74] and FF-AOMDV, are not accurate and do not achieve high performance in VANETs. Moreover, using other methods that rely on successful data delivery probabilities, such as the ETX method would impose high overhead on the network in terms of sending an excessive amount of link probe packets (LPP) [75]. This, in turn would add more traffic load to the network, which causes traffic problems such as data packet congestion. On the other hand, RTT measures the status of the network and, therefore, routes can be selected, avoiding those congested paths without the need to add extra overhead. In addition, the route optimization process based on RTT is impressible to frequent topological change in VANETs, which is not the case with using ETX and ETE methods. This feature is more obvious with vehicles having high mobility speeds.

The data path from the sender node to the receiver end may encounter congestion or collision. Algorithms designed on the basis of one-way delay such as [76–79] rely on the delay only in the reverse path, which may be vulnerable to various traffic challenges compared to the forwarding path. On the other hand, RTT consist of both forwarding and reverse-path delays and this provides more accuracy. The main difficulty with the routing protocols designed based on the delay to represent the state of the links' condition is their dependency on the clock synchronization [80]. The clock of all the nodes should be synced in order to calculate the accurate RTT; otherwise, the performance could be impacted by the accuracy of the calculated RTT.

Another difficulty is the placement of the RSU devices in the network. To optimize the network performance, the number and position of RSU nodes need to be determined precisely. RSU devices play a key role in the network topology, and it is more likely to be placed where there is a physical obstacle to provide steady coverage as well as where vehicles are operating at a high mobility speed [72].

Table 4.7 provides the required characteristics for each protocol. In this comparison, protocols such as EGSR, QMR and TIHOO are dependant on the GPS, which may cause a bigger routing packet size. Additionally, it may impose computation load on nodes. Several pieces of research do not consider computing energy requirements in terms of energy consumption. With limited resource devices, it could be time and energy consuming. As an exemplification, EGSR considered that each node has sufficient computation resources, which is not always the case. Regarding scalability, road segments in MPRP are limited by the average RTT threshold between OBU nodes and RSU nodes. In EGSR, the road connecting two adjacent intersections is considered as the road segment.

4.4.1 Routing protocol time-complexity

To understand the time-complexity of the route discovery phase, we consider three different scenarios as depicted in Figure 4.70. In this regard, we consider that there is n number of intermediate node in the network.

According to the scenario, all the intermediate nodes are receiving the RREQ packet simultaneously, and all of them forward it to the destination. Therefore the order of RREQ rebroadcasting is $O(n)$. However, in a worst-case scenario, each node may receive RREQ for n times; therefore, the entire network deals with the time-complexity of $O(n^2)$ on receiving RREQ. The total number of discovered routes at the most is n.

In contrast with scenario a, in scenario b the intermediates nodes are arranged serially. Despite the node arrangement, the RREQ rebroadcasts n time to reach the destination. Therefore the order of RREQ redistribution is the same. In this scenario, each node receives RREQ from the previous and the next node. Therefore the time-complexity of receiving RREQ is $O(2n)$. In this case, the network discovers only one route.

As to scenario c, if all the intermediate nodes are included in a route, then the time-complexity of RREQ remain $O(n)$. Based on the network topology the RREQ receiving

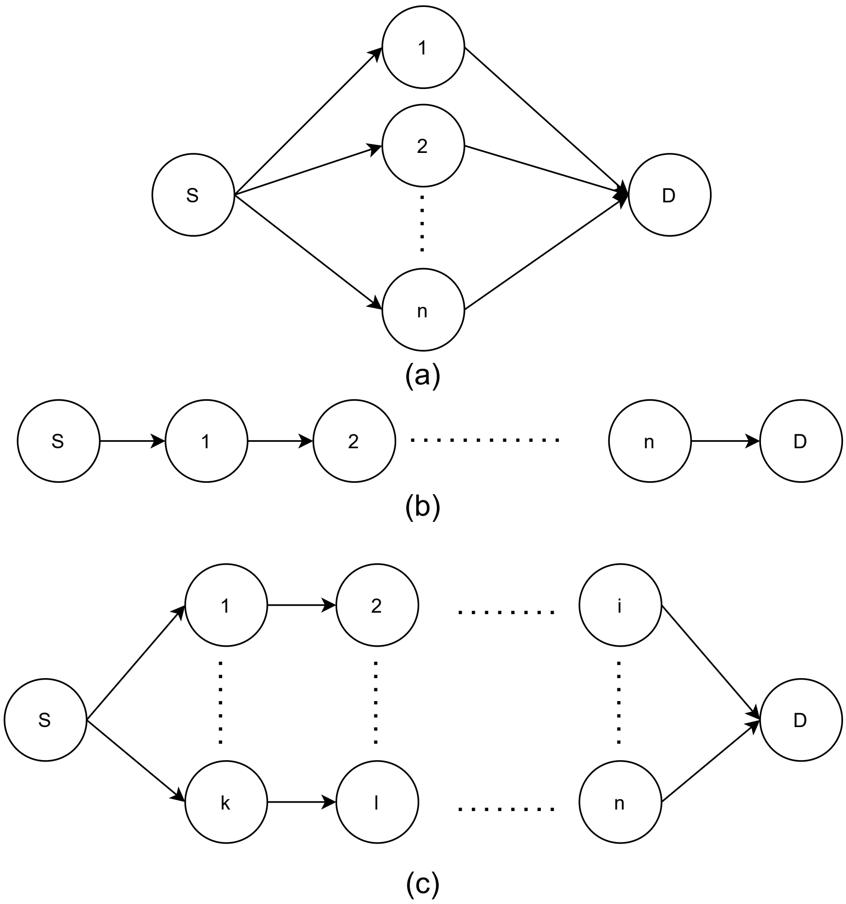

Fig. 4.70: scenarios of time-complexity study.

complexity vary between $O(1) \leq O \leq O(n)$.

Considering all the assumed scenarios the time complexity of RREQ rebroadcasting is $O(n)$ for each route discover. The number of times that a network require to goes through route discovery is dependent on the network configuration and network topology. Additionally, in the worst-case scenario RREQ receiving has a time complexity of $O(n^2)$.

The most possible number of discovered routes is n. Considering the worst-case scenario for sorting algorithms such as bubble sort and insertion sort, the complexity of route selection is $O(n^2)$.

Characteristics	MPRP	EGSR [36]	QMR [12]	FF-AOMDV [21]	TIHOO [20]	AOMDV
Clock Synchronization	Yes	Yes	No	No	No	No
GPS	No	Yes, Required as it is geographic aware protocol	Yes, Acquire position	NO	Yes, Required for positioning the neighbour and their mobility	No
Energy optimization	No	No	Yes	Yes	No	No
Scalability approach	Road segmentation	Road segmentation	No	No	No	No
Routing Discovery	Reactive protocol	Proactive protocol, based on t_{ant}	Hybrid protocol, Q-learning with variable α and γ	Reactive Protocol	Reactive Protocol	Reactive protocol
RTT	Yes	NO	NO	NO	NO	NO

Table 4.7: Routing protocol characteristics comparison

Chapter 5

Multi-Path Routing Protocol based on GA in VANETs (MPRP-GA)

5.1 Proposed Protocol

5.1.1 Problem statement

The adaption of MANETs' reactive topological routing protocols such as AODV, AOMDV, DSR and temporally ordered routing algorithm (TORA) in VANETs [81] faces several limitations caused by characteristics of VANETs, including high mobility speed, road segment node density and diversity of applications. The mobility speed of each node on the network changes in the different road segments. Also, the node density change on each segment of the road due to many reasons such as intersection signal, urban rush hours and vehicular congestion. Despite the fact that the issues arise due to topological changes in the network, The succession of data packet delivery on time is vital VANETs must be guaranteed, especially when it turns into emergency and driver assistance messages. Therefore, the data packets must be transferred via intermediate nodes with the lowest chance of topological change and network congestion to accommodate the data transmission objective.

5.1.2 Proposed solution

The MPRP routing protocol uses round trip time (RTT) as the route selection metric. MPRP generates a route request packet (RREQ) to discover possible routes from source to destination. By receiving the route request packet (RREQ), the receiver can calculate the

RTT. The sender node receives multiple RREPs based on which several routes establish from source to destination. MPRP eliminates the routes with an RTT greater than the RTT threshold that is average RTT. MRPR does not have an explicit mechanism for evaluating the quality of the selected route. We proposed a new fitness function to address the characteristics mentioned above. Also, in our fitness function, we consider the network congestion as a route quality metric. Based on the introduced fitness function, we proposed a routing protocol named MPRP-FFn, which employs the fitness function in the MPRP. In the next step, we proposed a genetic algorithm-based routing protocol of MPRP-GA to optimize the MPRP-FFn. When the route discovery phase is over in the proposed protocols, the sender eliminates routes having RTT greater than the threshold. Then the route having the lowest mobility, data congestion and the highest neighbor optimized density is selected. The metrics that our fitness function consider are noted as follow:

- The mobility speed of every intermediate vehicle for each discovered route,
- the density and the number of neighbouring nodes for each discovered route,
- Data Congestion for each discovered route,
- Distinguishing random loss and congestion loss

5.1.3 System model

The system model is similar to the system model explained in 4.1.3. The main difference is the method of route discovery in which we used the link-disjoint mechanism instead. In this algorithm, routes from a particular source and destination can not share a similar intermediate link. As an exemplification, in Figure 5.1, if two routes of S-A-B-C-D and S-E-B-F-D are already discovered, we can not have the route of S-A-B-F-D, which overlaps some links from the routes existing.

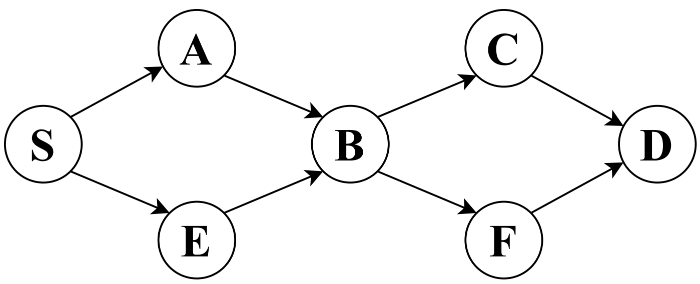

Fig. 5.1: Link-disjoint mechanism.

5.1.4 Fitness function

The explanation and specifications of the proposed fitness function are provided in the following. The first metric we considered in our fitness function is velocity. The nodes with a lower mobility speed are more likely to be selected.

$$F_v = \begin{cases} 1, & \text{if } v \leq 1 \\ \frac{1}{\sqrt{v}}, & \text{otherwise} \end{cases} \tag{5.1}$$

In equation (5.1) the variable v represents the mobility speed of the current node; if the vehicle speed is less than one meter per second, we assign 1 to the velocity function; otherwise, it is calculated as noted. The trend of F_v changes through various mobility speeds is illustrated in Figure 5.2. When vehicles (nodes) have a slower speed, channels would be more stable and consequently routing will not undergo frequent breakage that occurs when nodes' mobility is high. Accordingly, F_v should tend to be high at low speeds and vice versa.

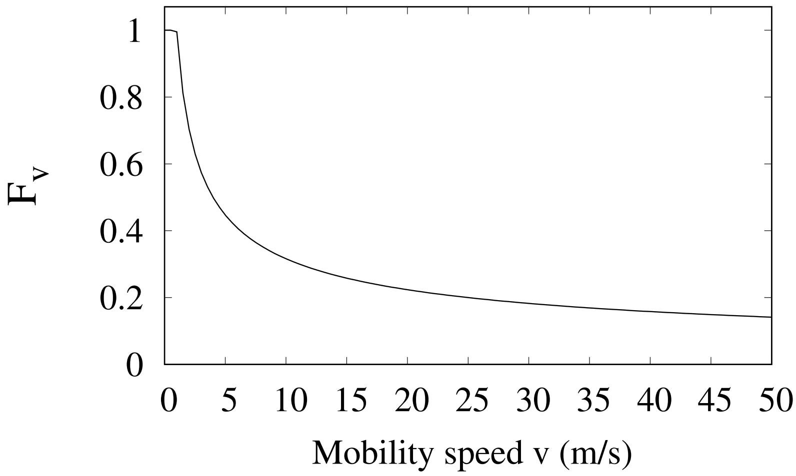

Fig. 5.2: Velocity function versus mobility speed

The second impacting factor that we included in our fitness function is node density. The node density is the average number of the neighbouring and intermediate nodes in the region between the source and the destination during the data communication time including the route discovery period. Selected routes would go through those neighbouring nodes. In equation (5.2), the F_d represents the fitness component for a node density. The e is Euler's number, σ is the deviation function, n_a is the average number of nodes through time, and n_i is the instant number of neighbouring and intermediate nodes.

$$F_d = e^{-\sigma(n_i - n_a)^2} \tag{5.2}$$

We use equation (5.3) to calculate the average number of neighbouring and intermediate nodes. Here t is the number of times we recorded numbers of adjacent nodes, and n_j is the number of neighbor nodes recorded at jth time. Table 5.1 illustrates a comparison of neighbor list length and corresponding average neighbor list size. The provided data in the table results from the simulation for three randomly selected nodes to compare the number of instant neighbor nodes and the average number of the neighbouring node.

Time	n_{i1}	n_{a1}	n_{i2}	n_{a2}	n_{i3}	n_{a3}
1	5	5	4	4	3	3
2	7	6	9	6.5	7	5
3	10	7.3	7	6.6	8	6
4	9	7.75	11	7.75	6	6
5	8	7.8	9	8	4	5.6

Table 5.1: Neighbor length versus average neighbor length

$$n_a = \frac{\sum_{j=1}^{t} n_j}{t} \tag{5.3}$$

In equation (5.4), the σ notation represents the deviation function. RTT_i is the instant RTT and the notation n represents the number of intermediate hops traversed in an arbitrary route.

$$\sigma = \frac{RTT_i}{(n+1)} \tag{5.4}$$

The density function trend is depicted in Figure 5.3. Accordingly, the highest fitness is observed when the number of neighbouring nodes is equal to the average number of neighbouring nodes. The fitness increases exponentially when the number of nodes increases and reaches near n_a because of the better connectivity available. Similarly, having a higher number of nodes than n_a increases the chance of having data congestion and data collision; therefore, the function drops exponentially.

The last component of our fitness function is the data congestion at the intermediate nodes. In this regard, we refer to TCP CERL+ [16] as the method of our calculation. Equation (5.5) provides the congestion avoidance calculus, where L is queue length and B is buffer size.

$$F_c = \begin{cases} 1 - \frac{L}{B}, & \text{if } L \leq N \\ 0, & \text{otherwise} \end{cases} \tag{5.5}$$

Equation (5.6) introduces the calculation for the queue length at the bottleneck of each node. The notation T represents the minimum RTT and BW denotes the bandwidth at the channel between a couple of nodes. Every time a node receives an RREP packet, the value of L is updated.

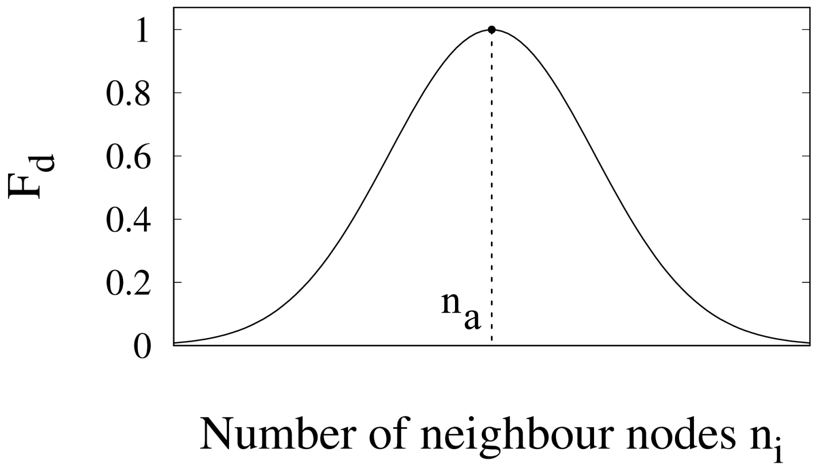

Fig. 5.3: density function versus the number of neighbor nodes.

$$L = (RTT - T) \times BW \tag{5.6}$$

In TCP CERL+, we use parameter N as the dynamic queue length threshold. The calculation of N is denoted in equation (5.7), where l_{max} represents the most significant value calculated for the variable L. The parameter A is the threshold.

$$N = A \times l_{max} \tag{5.7}$$

TCP CERL+ calculates the threshold by equation (5.8), where RTT_{avg} is calculated every time an RREP packet is received.

$$A = \frac{RTT_{avg}}{T} \tag{5.8}$$

The developed fitness function is introduced in equation (5.9) where the three components are used.

$$F = F_v + F_d + F_c \tag{5.9}$$

F is applied on the routes returned by the MPRP protocol. The route with the highest fitness is more likely used for data transmission.

5.2 Methodology

The main contribution in developing MPRP is route discovery based on RTT, selecting the route with the smallest RTT to diminish the data transmission delay. Additionally, MPRP specifies a threshold value based on which the MPRP eliminates the routes with the RTT larger than the threshold to avoid routes with long end-to-end delay. Figure 5.4 provides an overview of steps that MPRP-GA goes through for route discovery and route selection.

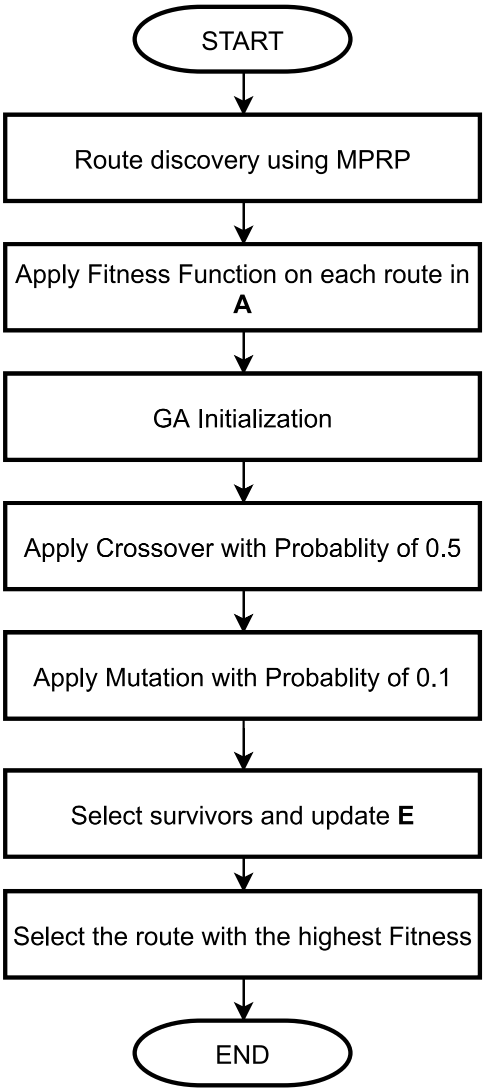

Fig. 5.4: A brief steps of MPRP-GA.

5.2.1 Methodology Flow

1. **MPRP:** it is a routing protocol proposed to evaluate each route based on the RTT. MPRP has four essential functions: route discovery, threshold determination, and route elimination based on the threshold and route selection. MPRP omits the routes having RTT larger than the threshold.

    - **A:** It is an array of routes in which the MPRP stores the selected routes.

2. **Neighbour discovery:** it is a mechanism used with many routing protocols, including DCFP [19], TA-AOMDV [63] and GTLQR [52], for neighbour exploration and link availability evaluation between two neighbour nodes. In this regard, every node periodically generates and broadcasts a hello packet. After receiving a reply

for the respective hello, the sender node can update the routing table and add the receiving node to the neighbour list.

3. **Genetic Algorithm:**

   (a) Initialization: It refers to the initialization part of the algorithm 4. It provides the parameters and explanation for GA as below:

   - **Population:** The discovered set of routes for a particular source and destination by the MPRP is called population.
   - **Chromosome:** Every individual route in a population is known as a chromosome.
   - **Genes:** it is a number of distinct nodes in a discovered routes.
   - **PopSize:** It is the size of the array A discovered by MPRP.
   - $\mathbf{P_c}$**:** A constant probability value indicates the chance of crossing for every pair of routes in array A.
   - $\mathbf{P_m}$**:** It is a designated probability value for mutation of the routes after crossing.
   - **Efficient routes:** It is an array of routes selected by the GA. It is denoted by $E_r[]$.

   (b) Crossover: This is the essential phase in a genetic algorithm. In this regard, the genetic algorithm tries to find an elite gene (intermediate node) in the selected and mated chromosomes (parent routes). Then the algorithm crosses the genes from both the parents' routes and reproduces two new offspring.

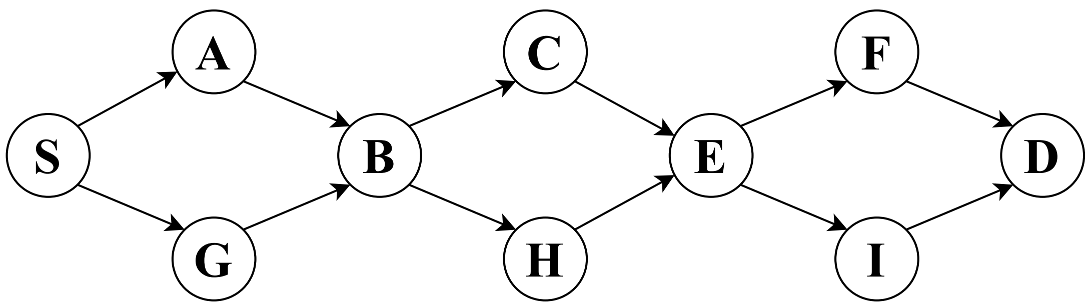

Fig. 5.5: Possible routes from S to D.

Hereafter an example for the crossover is provided. We assume two discovered routes of S-A-B-C-E-F-D and S-G-B-H-E-I-D by MPRP in the range of the RTT threshold according to the Figure 5.5. The GA finds node B as the gene B in both routes. Then the GA crosses two routes, but the similar gene remains the same in both the produced offspring routes. The offspring routes would be S-A-B-H-E-I-D AND S-G-B-C-E-F-D.

(c) Mutation: This is the last step of the genetic algorithm in which each gene in the route may toggle by the possibility of P_c. The elite nodes in the route remain the same. In the given example the genes at the fourth position get muted. Therefore the final generated routes would be S-A-B-C-E-I-D AND S-G-B-H-E-F-D..When an offspring route went through the mutation, it would be evaluated by the fitness function. If a child's route show improvement over its parents, it would be added to the array of the efficient routes (E_r).

(d) Survivor Selection: the fitness function evaluates the efficiency of the generated route. If an offspring route has fitness greater than its parents', it is an efficient route and would be added to E_r. Otherwise, the generated route would be omitted through the survivor selection phase.

(e) Termination term: It is a condition under which the GA could generate no more new routes.

4. **Fitness Function:** The combination of three mathematical components of node mobility speed, nodal density and network congestion constitutes the fitness function to score each intermediate node in a route. The introduced protocols of MPRP-FFn and MPRP-GA use the introduced fitness function in section 5.1.4 as the optimization mechanism.

The algorithm 4 receives an array of the discovered route obtained by MPRP. The $A[]$ denotes these routes. Two constant variables of P_c and P_m are designated to indicate the probability of crossover and mutation. We used notations of P_a and P_b for mated parents in the process of child route reproduction. The notation POP (population) is an array of routes constituted by discovered routes in A and all the routes generated through crossover and mutation phase which is known as population. Accordingly, F_r represents the respective fitness value for each route in POP. Finally, E_r is the selected efficient routes, including discovered and generated routes.

Algorithm 5 calculates fitness for every route, either it is a discovered route obtained by MPRP or a generated route as the result of GA. The RREP packet carries information such as mobility speed, density and congestion details of each intermediate node in the discovered route. The GA task takes place in the source node.

5.3 Experiment Setup and Performance Analysis

We used ns-3.32 on Ubuntu 20.04.2 LTS version as our operating system to scrutiny the performance of MPRP-GA and MPRP-FFn as our proposed protocols. Additionally, we

Algorithm 4 MPRP-GA Routing Algorithm.

Const : $P_c = 0.5$
$P_m = 0.1$
input : $POP \leftarrow$Array $A[]$ returned by MPRP.
$F_r[] = null$
output: Efficient routes in array of E_r.

while *(all routes in the* POP*)* **do**
  foreach $(P_a, P_b \in POP)$ **do**
    $C \leftarrow$ Crossover $(P_a,\ P_b,\ P_c)$
    $M \leftarrow$ Mutation $(P_a,\ P_b,\ C,\ P_c)$
    $POP \leftarrow$ Add M
    $F \leftarrow$ Fitness (M)
    $F_r \leftarrow$ Add F
  end
end
foreach $(r \in POP)$ **do**
  if $(F_r(r) \geq F_r(P_a)\&F_r(P_b))$ **then**
    $E_r \leftarrow r$
  else
    drop (r)
  end
end
Sort_Desc(E_r)
return(E_r)

Algorithm 5 Fitness Function Algorithm.

input : Route R.
output: Fitness R

Function `Fitness`(R)**:**
  $F = 0$ **foreach** $Node$ **C** $\in R$ **do**
    $F_v \leftarrow$ eq(5.1)
    $F_d \leftarrow$ eq(5.2)
    $F_c \leftarrow$ eq(5.5)
    $F+ = (F_v + F_d + F_c)$
  end
return(F)

used SUMO-1.9.2 as the traffic simulator. Various QoS metrics of throughput, packet loss ratio (PLR), end-to-end delay (E2E), routing overhead and energy consumption are measured and compared. In this regard, we considered different simulation scenarios and configurations, including various simulation times, different numbers of nodes, mobility speed, various amounts of random loss and packet size to evaluate the performance of the proposed protocols. The vehicular traffic simulator distributes vehicles randomly on 5 streets with a length of 1.5 km each, similar to figure 5.6. The road map contains intersections equipped with nine RSU node at each intersection or middle of road sections. The parameters and the respective default values used for this simulation are available in table 5.2 unless it is noted.

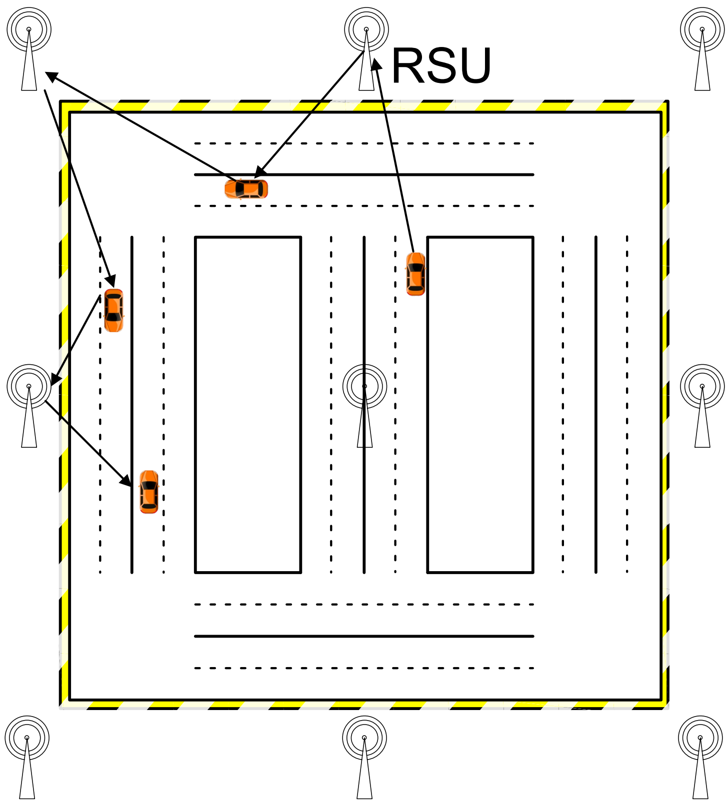

Fig. 5.6: Simulation road map.

5.3.1 Results

5.3.1.1 Evaluation of the simulation results based on time variable:

We assess the performance of the given protocol with different simulation periods and compare the result of each protocol based on designated graphs. As the data load on the network increases over time, as the chance of having data congestion and collision increases. Therefore, the network performance degrades during simulation time.

Table 5.2: Simulation Parameters

Parameter Type	Parameter Value
Network Simulator	ns-3.32
Traffic Simulator	SUMO 1.9.2
Wireless Protocol	IEEE 802.11p
MAC and Physical Layer standard	OFDM rate 6Mbps
Protocols	TA-AOMDV, EHO-AOMDV, MPRP, MPRP-FFn, MRPP-GA
Topology size	1500m × 1500m
Crossover Probability	0.5
Mutation Probability	0.1
Number of runs	5
Simulation Time	100 seconds
Number of nodes	100
Mobility speed	10 m/s
Data payload	768 bytes/packet
Initial Energy Source	100 Joules
Transmission Energy	0.2 watt
Receiving Energy	0.1 watt
Propagation Model	Free space propagation model
Traffic Type	CBR

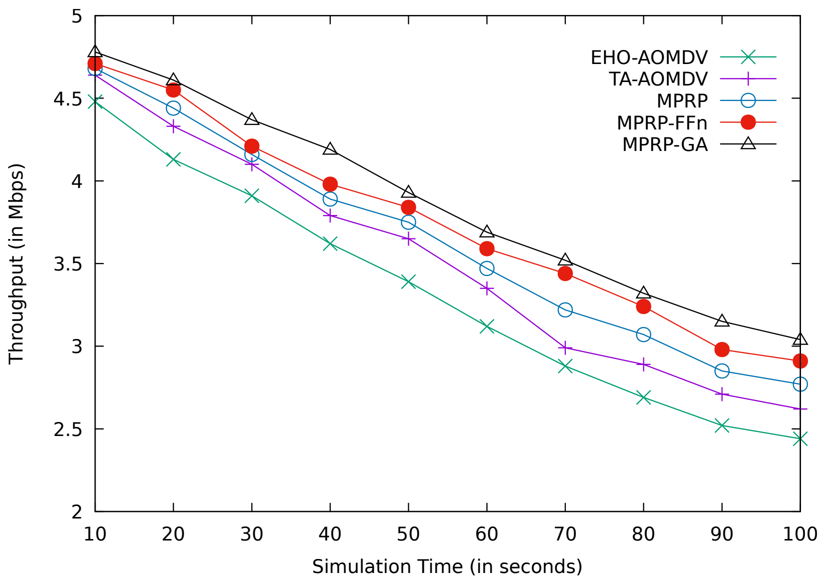

Fig. 5.7: Comparison between the proposed protocols of MPRP-GA and MPRP-FFn with MPRP, TA-AOMDV and EHO-AOMDV for throughput over various simulation times.

Table 5.3: Simulation time vs. throughput

time	EHO-AOMDV	TA-AOMDV	MPRP	MPRP-FFn	MPRP-GA
10	4.48	4.64	4.68	4.71	4.78
20	4.13	4.33	4.44	4.55	4.61
30	3.91	4.1	4.16	4.21	4.37
40	3.62	3.79	3.89	3.98	4.19
50	3.39	3.65	3.75	3.84	3.93
60	3.12	3.35	3.47	3.59	3.69
70	2.88	2.99	3.22	3.44	3.52
80	2.69	2.89	3.07	3.24	3.32
90	2.52	2.71	2.85	2.98	3.15
100	2.44	2.62	2.77	2.91	3.04
sum	33.18	35.07	36.30	37.45	38.60
gain (%)	16.34	10.07	6.34	3.07	

In Figure 5.7, the proposed protocols of MPRP-FFn and MPRP-GA are showing an enhancement in terms of throughput. The MPRP selects routes with the least RTT; therefore, it performs better than TA-AOMDV and EHO-AOMDV. Additionally, The RTT is containing queueing time and processing time. Hence, a route with a shorter RTT is possibly less congested. MPRP-FFn algorithm selects the most fitted route out the routes returned by MPRP. Therefore, the selected route goes through the least congested nodes with a lower mobility speed avoiding topological change. Additionally, the selected route has the most optimized density, which guarantees topological consistency and minimizes collision occurrence. The MPRP-GA has the same functionally as FFn with an additional GA optimization mechanism that generates new possible routes that provide comparatively better performance. Table **??** indicates that MPRP-GA improves throughput by 3.07, 6.34, 10.07 and 16.34 percent compared to MPRP-FFn, MPRP, TA-AOMDV and EHO-AOMDV, respectively.

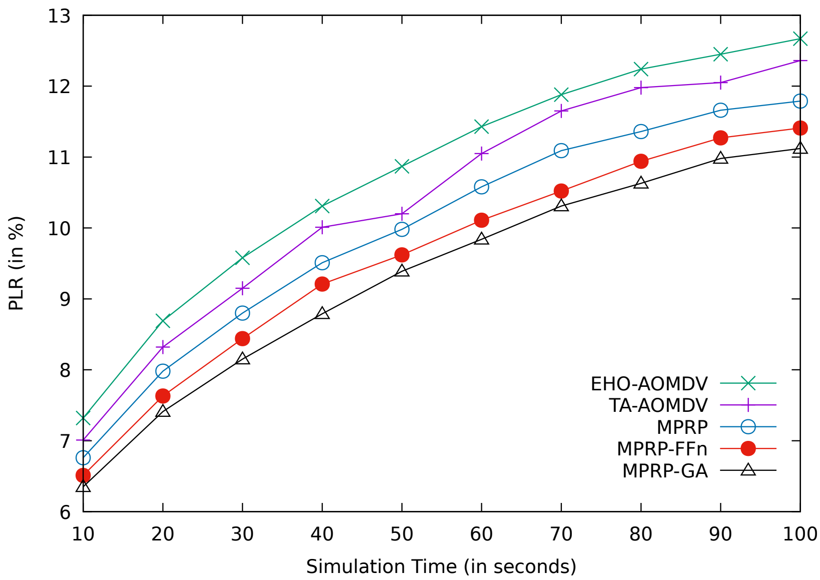

Fig. 5.8: Comparison between the proposed protocols of MPRP-GA and MPRP-FFn with MPRP, TA-AOMDV and EHO-AOMDV for PLR over various simulation times.

Over time the amount of data load increases on the network. Therefore the chance of having data congestion and collision increases. In this regard, the PLR for all the given protocols increased over time in Figure 5.8. The promising performance of MPRP-GA and MPRP-FFn is the result of their congestion control method. Using RTT as the route optimization metric in MPRP improves performance over AOMDV based protocols by partially avoiding data congestion and collisions. However, TA-AOMDV optimizes the buffer size, but the proposed buffer control mechanism is not sufficient to minimize the occurrence of data collision and congestion.

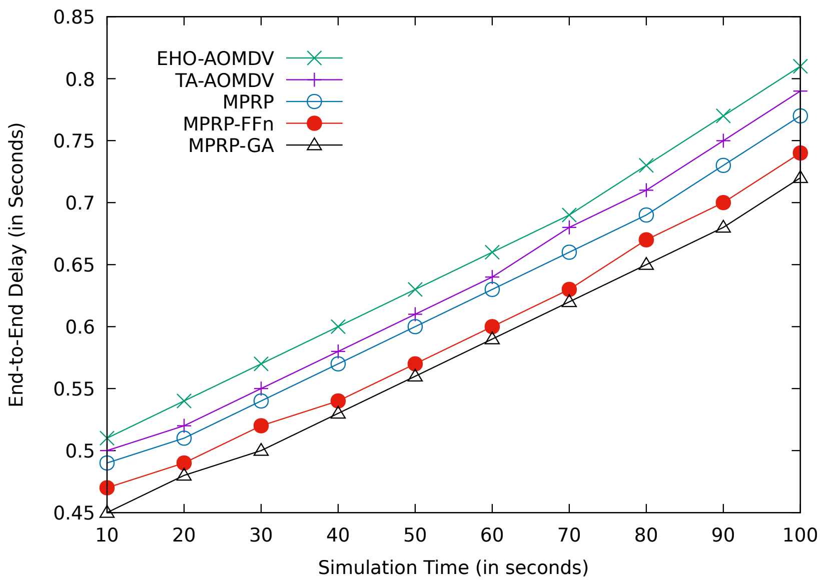

Fig. 5.9: Comparison between the proposed protocols of MPRP-GA and MPRP-FFn with MPRP, TA-AOMDV and EHO-AOMDV for average E2E over various simulation times.

Various factors constitute the end-to-end delay, such as route discovery delay, processing delay and queueing delay. To minimize the E2E, we need to minimize all the given factors. In Figure 5.9, all the studied protocols are reactive topological protocols with a similar mechanism of route discovery by employing RREQ and RREP. Therefore route discovery delay could be the same. The proposed protocols of MPRP-GA and MPRP-FFn select the less congested routes to minimize data congestion. Additionally, The selected routes are more topological consistent due to selection routes with lower mobility speed of its nodes. Therefore the chance of link failure reduces due to topological change, and consequently, the algorithm goes through the route discovery phase less frequently.

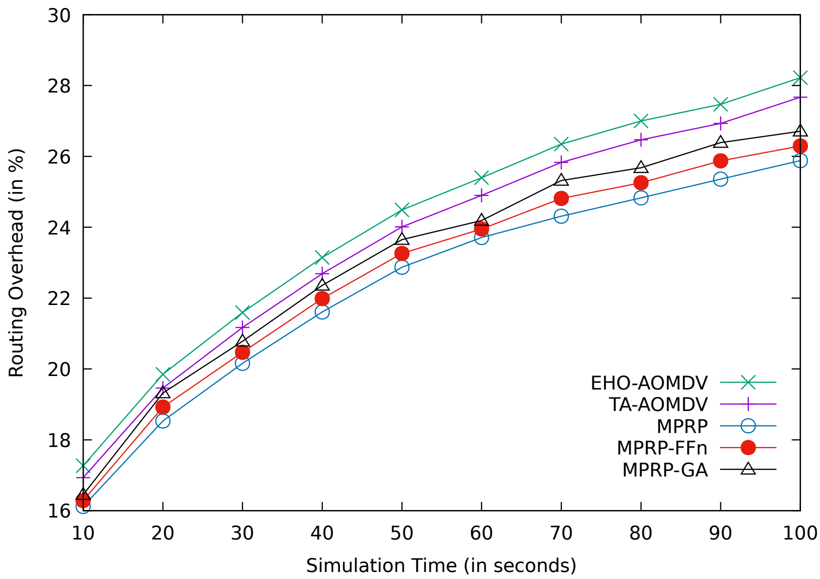

Fig. 5.10: Comparison between the proposed protocols of MPRP-GA and MPRP-FFn with MPRP, TA-AOMDV and EHO-AOMDV for routing overhead over various simulation times.

The overhead routing ratio results from two incidents; those are the times a protocol goes through the route discovery phase, and the number of replicas regenerates in each. The MPRP has the lowest routing discovery. In MPRP, each intermediate OBU node appears only in one route to avoid having a loop; therefore, the number of generated replicas degrades. On the contrary, an intermediate node may appear in multiple routes in GA and FFn. Figure 5.10 shows the superiority of MPRP over other protocols.

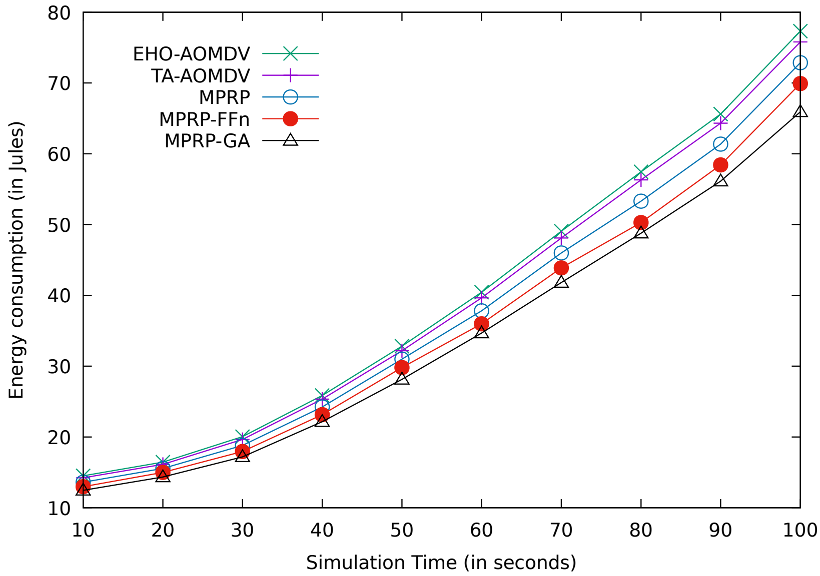

Fig. 5.11: Comparison between the proposed protocols of MPRP-GA and MPRP-FFn with MPRP, TA-AOMDV and EHO-AOMDV for energy consumption over various simulation times.

The main objective in TA-AOMDV and EHO-AOMDV is to increase the network's lifetime by engaging the nodes having higher residual energy in data transmission. More energy is consumed due to the given mechanism to provide longer battery life for all the nodes in the network. In Figure 5.11 the TA-AOMDV and EHO-AOMDV are showing the highest energy consumption. However, the network's lifetime is not a matter of study in this thesis due to the energy independence characteristic of VANETs. MPRP based routing protocols are showing less energy consumption.

5.3.1.2 Evaluation of the simulation results based on mobility speed variable:

The high mobility speed is the most crucial factor in VANETs. By increasing speed, the chance of topological change increases. Two vehicles with a communication range of 250 meters and a speed of 30 m/s in opposite directions may communicate only for 6 seconds. Therefore, the study of various mobility speeds is vital in VANETs.

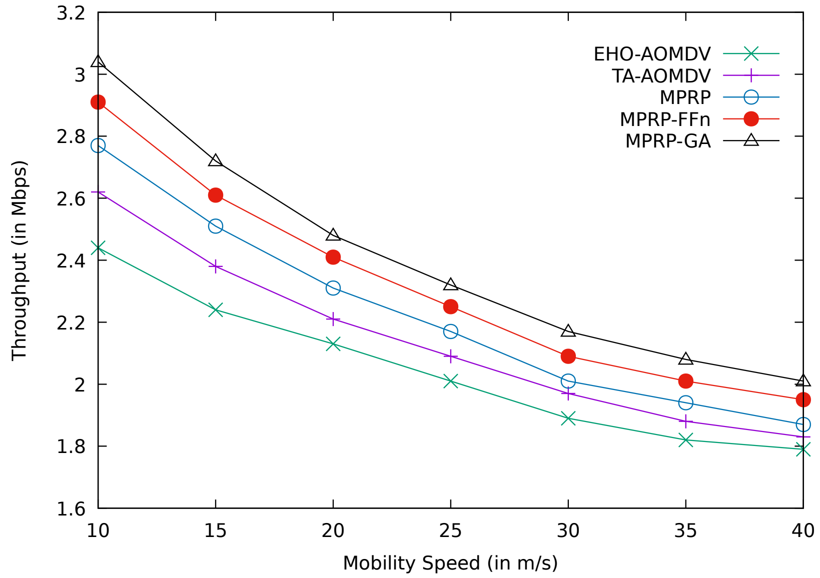

Fig. 5.12: Comparison between the proposed protocols of MPRP-GA and MPRP-FFn with MPRP, TA-AOMDV and EHO-AOMDV for throughput over various mobility speeds.

Table 5.4: Mobility speed vs. throughput

speed	EHO-AOMDV	TA-AOMDv	MPRP	MPRP-Ffn	MPRP-GA
10	2.44	2.62	2.77	2.91	3.04
15	2.24	2.38	2.51	2.61	2.72
20	2.13	2.21	2.31	2.41	2.48
25	2.01	2.09	2.17	2.25	2.32
30	1.89	1.97	2.01	2.09	2.17
35	1.82	1.88	1.94	2.01	2.08
40	1.79	1.83	1.87	1.95	2.01
sum	14.32	14.98	15.58	16.23	16.82
gain (%)	17.46	12.28	7.96	3.64	

The MPRP-GA and MPRP-FFn consider the intermediate node with lower mobility speed as a candidate node for data communication. In Figure 5.12 these two protocols are showing better performance due to the reason mentioned earlier. The MPRP-GA generates new routes out of discovered routes to discover routes having a higher fitness. Accordingly, in Figure 5.13 the MPRP-GA shows the lowest PLR followed by MPRP-FFn. According to the table 5.4, MPRP-GA improves throughput by 17.46, 12.28, 7.96 and 3.64 percents compared to EHO-AOMDV, TA-AOMDV, MPRP and MPRP-FFn, respectively.

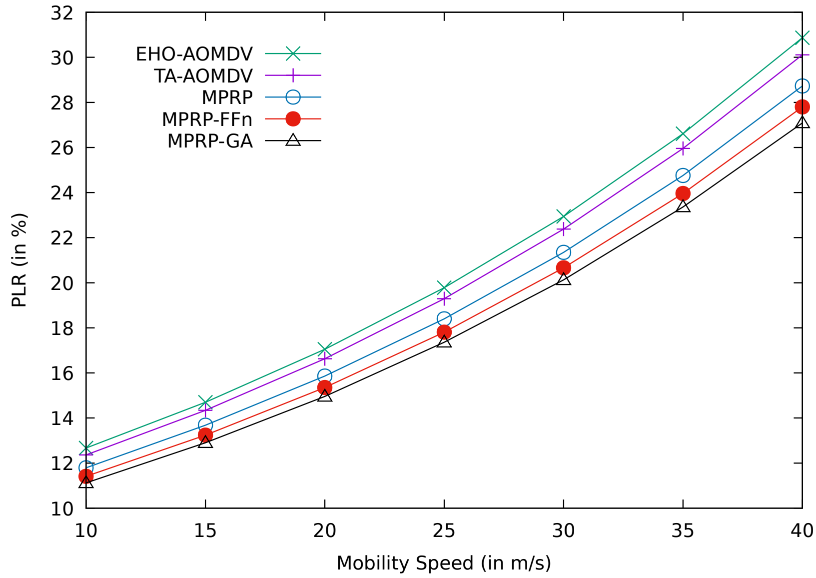

Fig. 5.13: Comparison between the proposed protocols of MPRP-GA and MPRP-FFn with MPRP, TA-AOMDV and EHO-AOMDV for PLR over various mobility speeds.

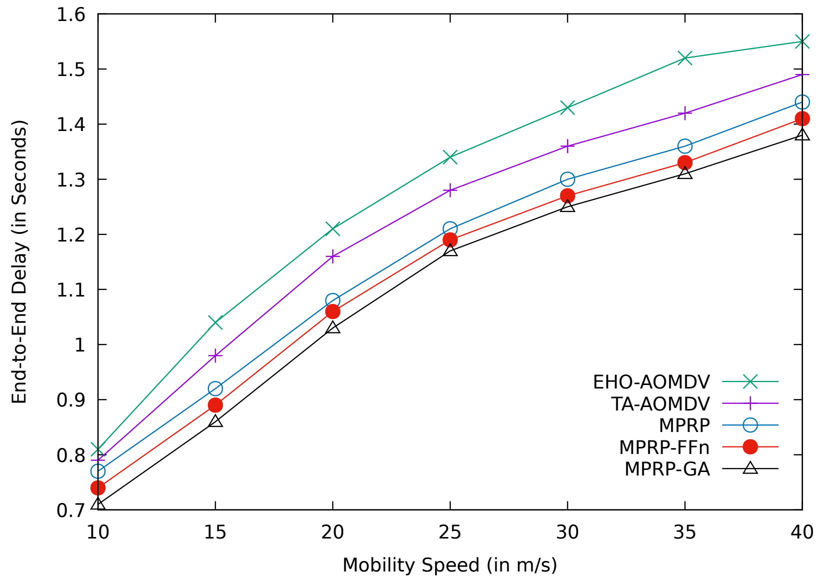

Fig. 5.14: Comparison between the proposed protocols of MPRP-GA and MPRP-FFn with MPRP, TA-AOMDV and EHO-AOMDV for average E2E over various mobility speeds.

Table 5.5: Mobility speed vs. end-to-end delay

speed	EHO-AOMDV	TA-AOMDV	MPRP	MPRP-FFn	MPRP-GA
10	0.81	0.79	0.77	0.74	0.71
15	1.04	0.98	0.92	0.89	0.86
20	1.21	1.16	1.08	1.06	1.03
25	1.34	1.28	1.21	1.19	1.17
30	1.43	1.36	1.3	1.27	1.25
35	1.52	1.42	1.36	1.33	1.31
40	1.55	1.49	1.44	1.41	1.38
sum	8.90	8.48	8.08	7.89	7.71
saving (%)	13.37	9.08	4.58	2.28	

With more stable links, fewer times a routing protocol goes through the route discovery phase. Therefore, MPRP-GA minimizes the delay caused by route discovery and retransmission of data loads. In Figure 5.14 the MPRP-GA and MPRP-FFn are showing the best performance for E2E delay due to their route selection method. MPRP-GA shorten the end-to-end delay by 13.37, 9.08, 4.58 and 2.28 percents compared to EHO-AOMDV, TA-AOMDV, MPRP and MPRP-FFn, respectively, as it is noted in table 5.5.

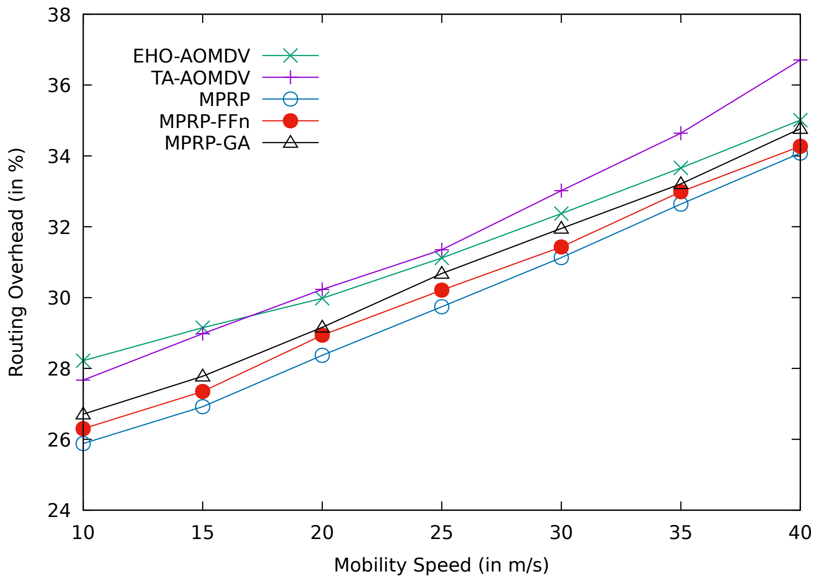

Fig. 5.15: Comparison between the proposed protocols of MPRP-GA and MPRP-FFn with MPRP, TA-AOMDV and EHO-AOMDV for routing overhead over various mobility speeds.

In Figure 5.15, TA-AOMDV produces more routing overhead to maintain the link connectivity. Therefore, by increasing the speed, TA-AOMDV routing overhead ratio overtakes others. MPRP shows the lowest Routing overhead due to the designated loop avoidance mechanism and link stability. However, MPRP-GA and MPRP-FFn provide loop-free routes, but a particular intermediate node may appear in several distinct routes, causing growth in routing overhead.

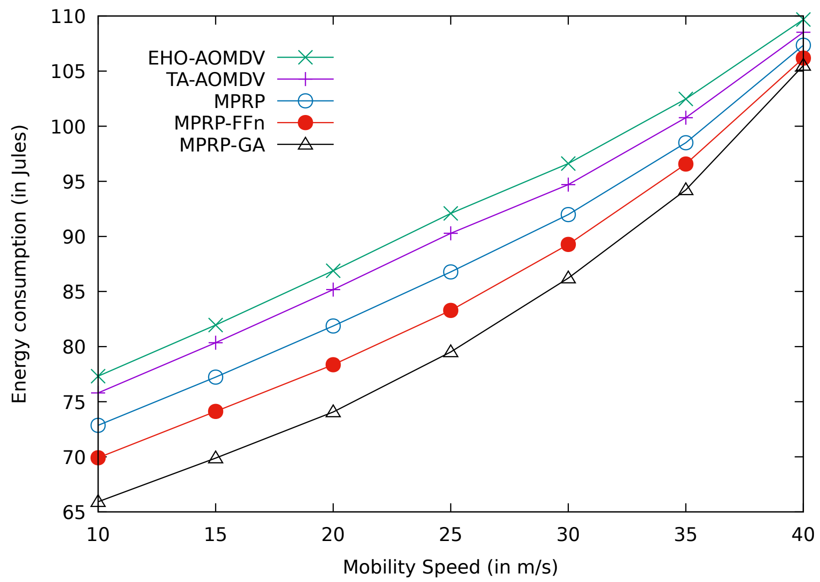

Fig. 5.16: Comparison between the proposed protocols of MPRP-GA and MPRP-FFn with MPRP, TA-AOMDV and EHO-AOMDV for energy consumption over various mobility speeds.

Each node consumes energy during data transmission (sending and receiving), including data and routing packets either they have been delivered successfully or fail. Therefore, the more network involves in data communication, the more energy consumes. Having a higher PLR and routing overhead increases energy consumption. Therefore, in Figure 5.16 the lowest energy consumption belongs to MPRP-GA and MPRP-FFn, respectively, followed by MPRP. The AOMDV based protocols show the higher energy consumption due to the higher ratio of PLR and routing overhead.

5.3.1.3 Evaluation of the simulation results based on number of nodes variable:

Increasing the number of nodes may increase the network's connectivity, but in contrast, it increases the chance of having more data collision and congestion. Node density is one of the components of our advanced fitness function. Thus, we studied the impacts of the number of nodes in our simulation. In the following results, we observed the best performance with the number of nodes equal to seventy. This number is the result of the simulator configuration. Therefore with different configurations, we may have different results. In the setup with seventy nodes, the protocol has the most optimum density in which the network is connected and not congested.

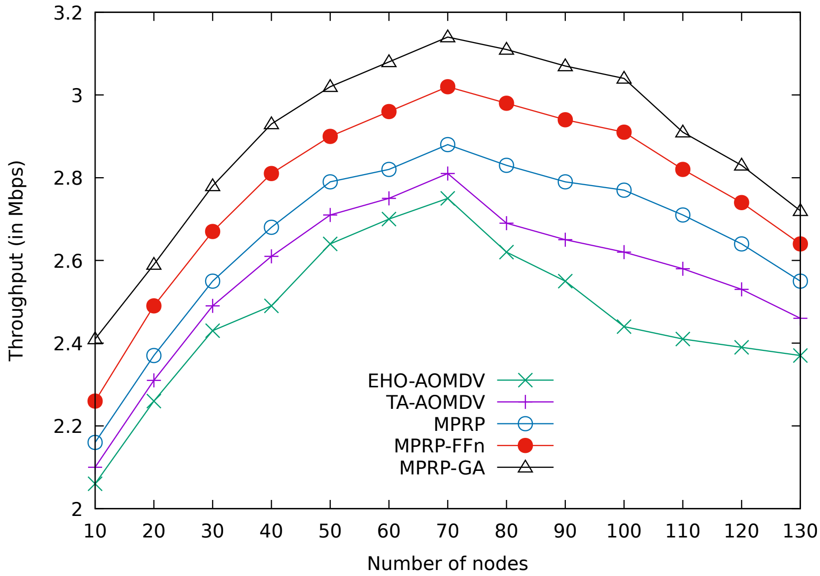

Fig. 5.17: Comparison between the proposed protocols of MPRP-GA and MPRP-FFn with MPRP, TA-AOMDV and EHO-AOMDV for throughput over various number of nodes.

In Figure 5.17, the high performance of MPRP-GA is because of the route generation mechanism from the discovered routes obtained by MPRP. Similarly, the performance of MPRP-FFn is a result of the stable route selection. MPRP-GA and MPRP-FFn both select the routes in which the intermediate nodes have the optimum number of neighbouring nodes. MPRP uses RTT as the metric of route optimization; therefore, its mechanism partially avoids highly congested routes.

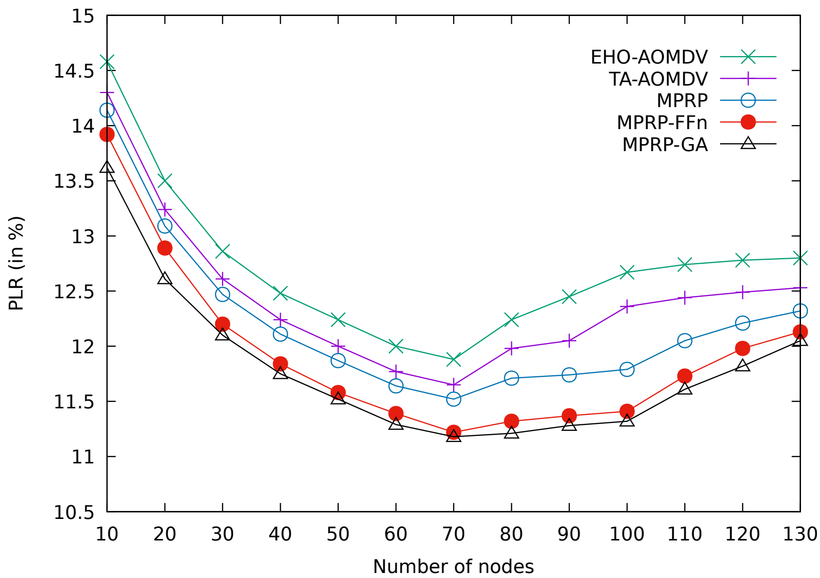

Fig. 5.18: Comparison between the proposed protocols of MPRP-GA and MPRP-FFn with MPRP, TA-AOMDV and EHO-AOMDV for PLR over various number of nodes.

Figure 5.18 provides proof of the importance of the neighbouring node. In a low-density environment, the chance of data loss due to lack of connectivity increases. On the contrary, the chance of having data congestion and data collision in a high-density environment is high. MPRP-GA and MPRP-FFn select the intermediate nodes with near-optimized neighbouring nodes.

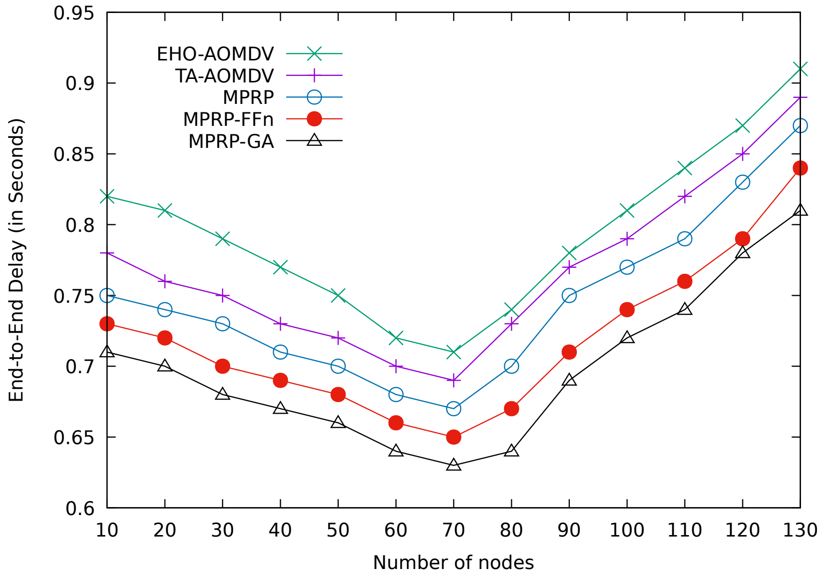

Fig. 5.19: Comparison between the proposed protocols of MPRP-GA and MPRP-FFn with MPRP, TA-AOMDV and EHO-AOMDV for average E2E over various number of nodes.

In a low-density environment, the delay due to route discovery may increase due to a lack of connectivity between the two ends. Oppositely, when the environment is highly dense, a data packet faces a long queuing time in each intermediate node. According to Figure 5.19, MPRP-GA is more successful in optimizing the routes in both scenarios followed by MPRP-FFn. The inbuilt density mechanism in both introduced protocols provides superiority over other protocols.

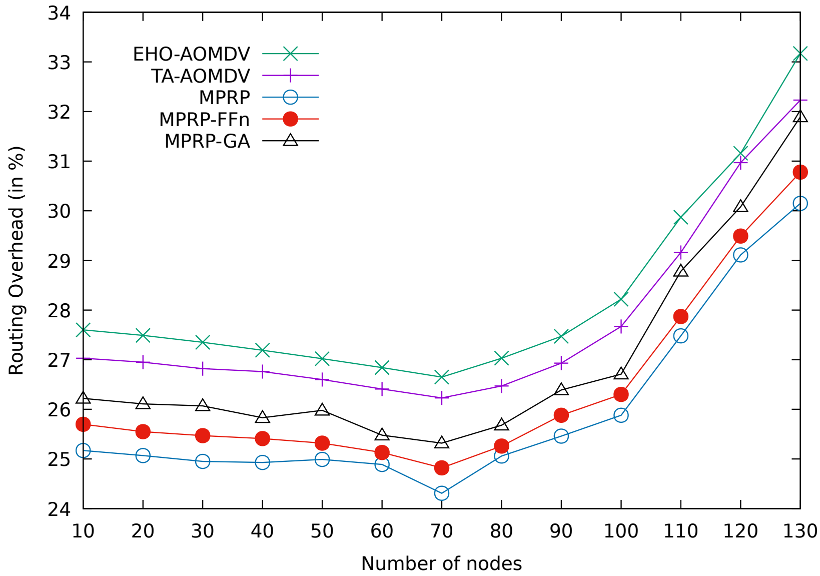

Fig. 5.20: Comparison between the proposed protocols of MPRP-GA and MPRP-FFn with MPRP, TA-AOMDV and EHO-AOMDV for routing overhead over various number of nodes.

In two scenarios, a protocol produces more routing overhead: a high level of link failure and a high number of routing packet replicas. In Figure 5.20 the load impose for find a route increases when the number of nodes increases. A more number replica for each routing packet may produce when there are more nodes in the path. Similarly, When the protocol can not find proper routes between two ends, it goes through the discovery phase more frequently. The low-density environment has a slight impact on the performance of the network in the routing overhead term.

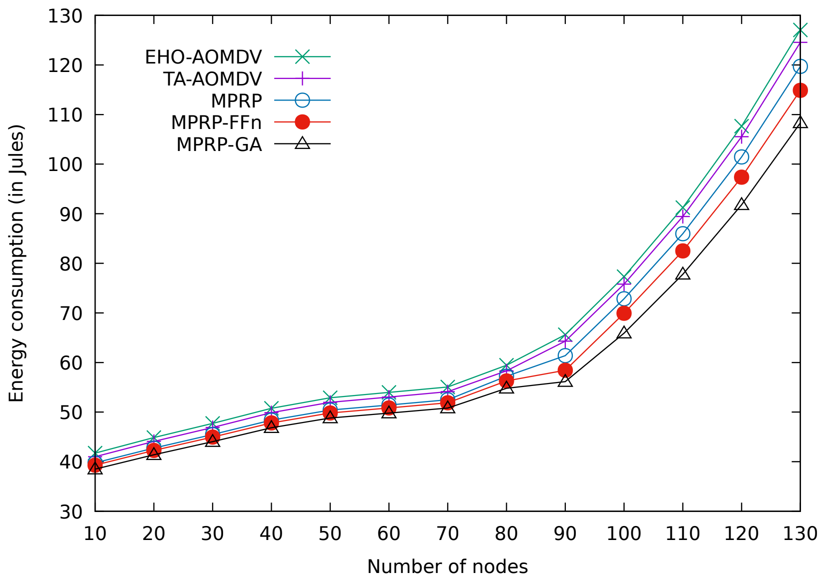

Fig. 5.21: Comparison between the proposed protocols of MPRP-GA and MPRP-FFn with MPRP, TA-AOMDV and EHO-AOMDV for energy consumption over various number of nodes.

Table 5.6: Number of node vs. energy consumption

#node	EHO-AOMDV	TA-AOMDV	MPRP	MPRP-FFn	MPRP-GA
70	55.07	54.11	52.48	51.87	50.81
80	59.45	58.32	57.24	56.29	54.79
90	65.61	64.32	61.38	58.43	56.14
100	77.32	75.8	72.86	69.92	65.92
110	91.24	89.44	85.97	82.51	77.79
120	107.66	105.54	101.45	97.36	91.79
130	127.04	124.54	119.71	114.88	108.31
sum	583.39	572.07	551.09	531.26	505.55
saving (%)	15.40	13.16	9.01	5.09	

Having a higher energy consumption is the result of having more nodes in Figure 5.21. Every node is a receiver and a forwarder of routing packets whether or not they participate in data transmission. When there are more neighbouring the more nodes receive and forward the routing packet, which requires more energy. According to table 5.6, MPRP-GA saves 15.40, 13.16, 9.01 and 5.09 compared to EHO-AOMDV, TA-AOMDV, MPRP and MPRP-FFn, respectively.

5.3.1.4 Evaluation of the simulation results based on random loss variable:

There are several reasons for random loss occurs in a wireless environment, including noise, signal attenuation and fading, hardware malfunction, high bit error rate and the hidden and exposed node.

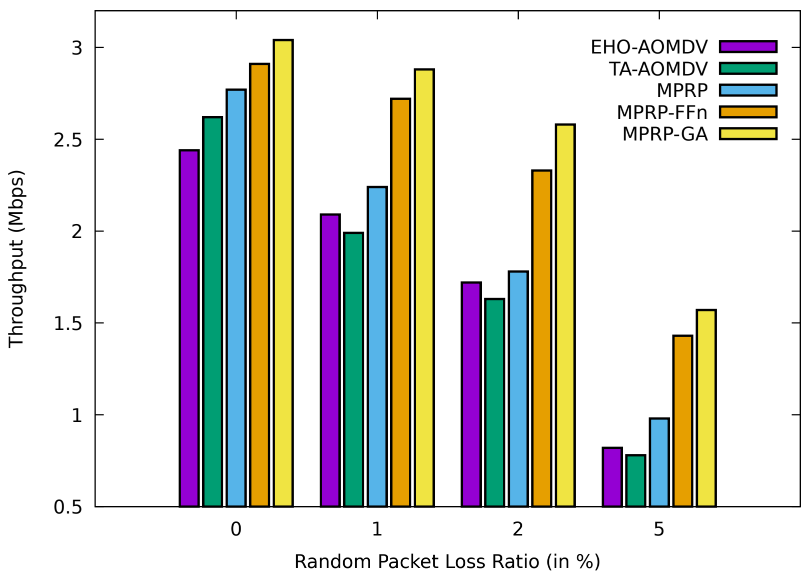

Fig. 5.22: Comparison between the proposed protocols of MPRP-GA and MPRP-FFn with MPRP, TA-AOMDV and EHO-AOMDV for throughput over various random loss ratio.

Figure 5.22 compares the performance of routing protocols in terms of throughput. The simulation and the study took place for scenarios when the random loss is 0%, 1%, 2% and 5%. Accordingly, with the 5% random loss, the MPRP-GA provides the highest gain of 91%, 101%, 60%, and 10% compared with EHO-AOMDV, TA-AOMDV, MPRP and MPRP-FFn. TCP CERL+ as the congestion control component of our fitness function discriminates the random loss and data congestion loss resulting in the promising performance of MPRP-GA and MPRP-FFn.

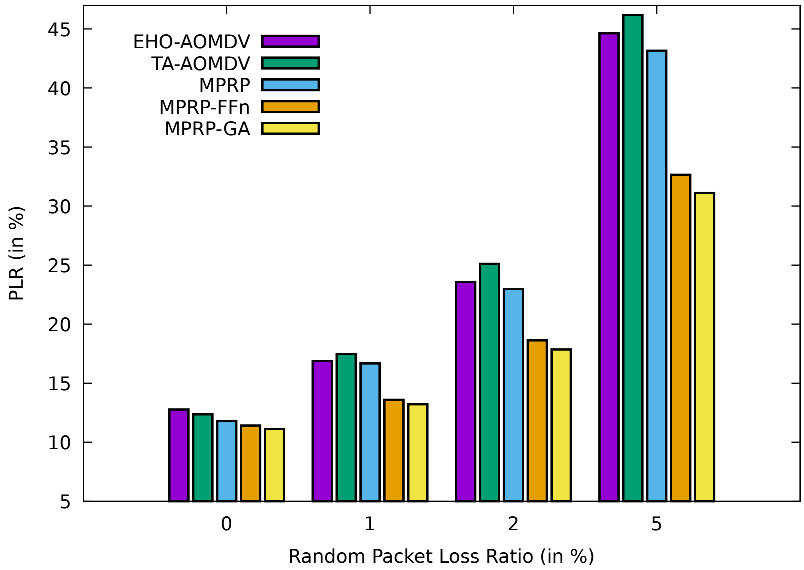

Fig. 5.23: Comparison between the proposed protocols of MPRP-GA and MPRP-FFn with MPRP, TA-AOMDV and EHO-AOMDV for PLR over various random loss ratio.

The MPRP-GA has the lowest PLR according to Figure 5.23. MPRP-GA and MPRP-FFn are equipped with a congestion control mechanism evaluating the probability of having data loss because of random loss in a link. Thus, these two protocols have the best performance. The threshold in MPRP protects packets from long-range fading. Therefore, it partially covers the random loss. The better performance of EOH-AOMDV over TA-AOMDV is the result of its load balancing mechanism.

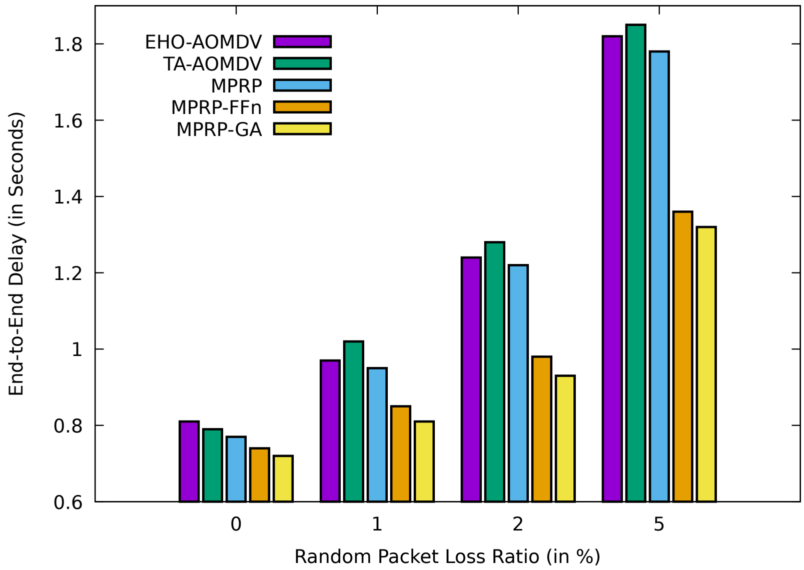

Fig. 5.24: Comparison between the proposed protocols of MPRP-GA and MPRP-FFn with MPRP, TA-AOMDV and EHO-AOMDV for average E2E over various random loss ratio.

In figure 5.24, the MPRP-GA has the lowest end-to-end delay among all the studied protocols. The E2E dropped 38%, 40%, 35% and 3% compared with EHO-AOMDV, TA-AOMDV, MPRP and MPRP-FFn, respectively. MPRP-GA select the less congested routes those having less chance of random loss as well.

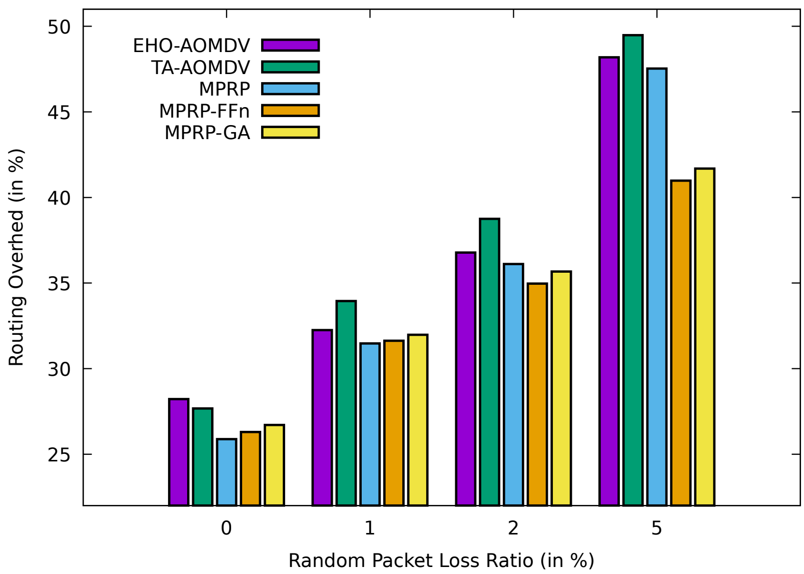

Fig. 5.25: Comparison between the proposed protocols of MPRP-GA and MPRP-FFn with MPRP, TA-AOMDV and EHO-AOMDV for routing overhead over various random loss ratio.

With having more link failure, the routing protocol imposes more routing overhead on the network for route discovery. In Figure 5.25, when we have 0 % and 1% random loss, the MPRP has the lowest routing overhead among the studied protocol. When we increased the ratio of random loss in simulations, the MPRP-FFn shows the best performance because of a large difference in PLR. In the case of MPRP-GA and MPRP-FFn, The network needs to go through the route discovery phase fewer times; therefore, a fewer number of routing packets is generated. In this regard, at 5 % random loss, the MPRP-FFn routing overhead is lowered by 18 %, 21 %, 16 % and 3 % compared with EHO-AOMDV, TA-AOMDV, MPRP and MPRP-FFn, respectively.

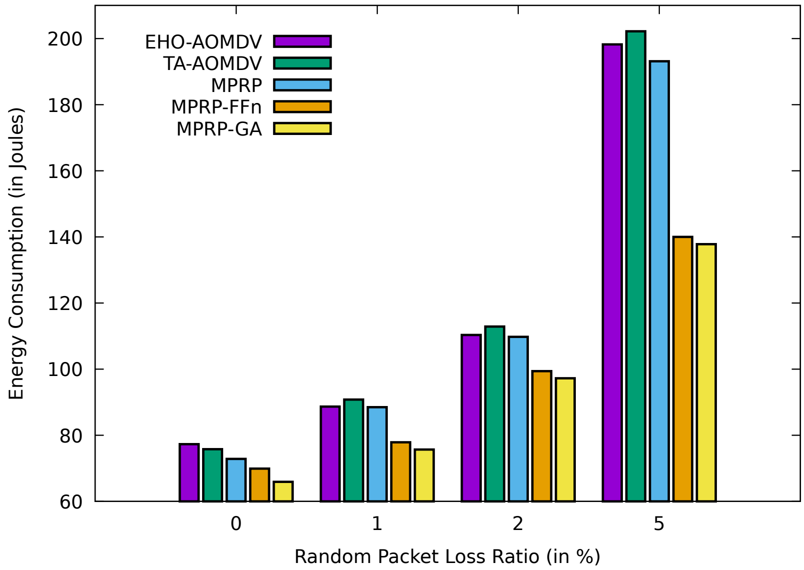

Fig. 5.26: Comparison between the proposed protocols of MPRP-GA and MPRP-FFn with MPRP, TA-AOMDV and EHO-AOMDV for energy consumption over various random loss ratio.

According to Figure 5.26, by increasing the chance of having random loss, the energy consumption increases drastically. The results showed the gains of 156%,167%, 165%, 100% and 109% when we compared them at 0% and 5% for protocols EHO-AOMDV, TA-AOMDV, MPRP, MPRP-FFn and MPRP-GA, respectively.

5.3.1.5 Evaluation of the simulation results based on data load size:

With a fixed size of data, the chance of having random data loss increases when the packet size is small due to data congestion. On the other hand, with a larger data packet size, the possibility of data collision increases. We studied the impact of the network load on the performance of the studied routing protocols by various data packet sizes. The results are depicted in the following. We figure out that a data packet with the size of 768 bytes is the most optimum size for data packets. Therefore, for all the other results in this section, the packet size is considered 768 bytes.

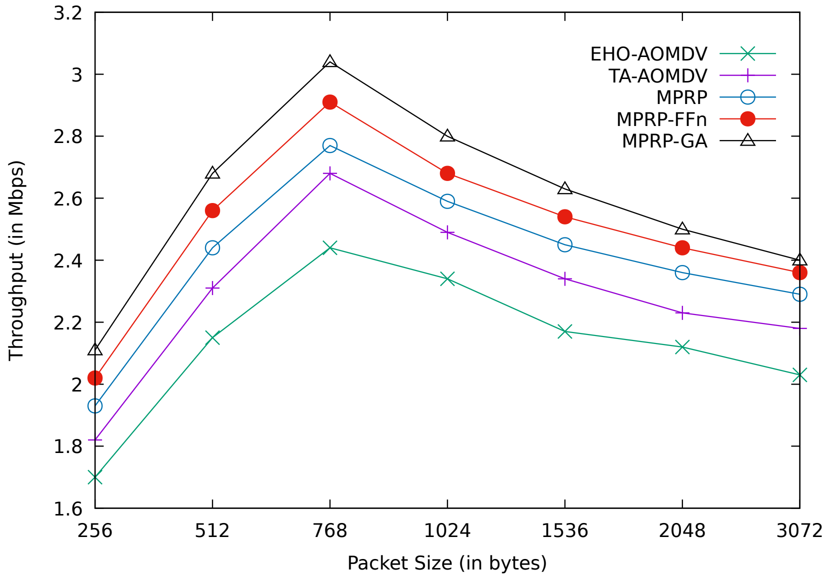

Fig. 5.27: Comparison between the proposed protocols of MPRP-GA and MPRP-FFn with MPRP, TA-AOMDV and EHO-AOMDV for throughput over various packet sizes.

Table 5.7: Packet size vs. throughput

packet size	EHO-AOMDV	TA-AOMDV	MPRP	MPRP-FFn	MPRP-GA
256	1.7	1.82	1.93	2.02	2.11
512	2.15	2.31	2.44	2.56	2.68
768	2.44	2.68	2.77	2.91	3.04
1024	2.34	2.49	2.59	2.68	2.8
1536	2.17	2.34	2.45	2.54	2.63
2048	2.12	2.23	2.36	2.44	2.5
3072	2.03	2.18	2.29	2.36	2.4
sum	14.95	16.05	16.83	17.51	18.16
gain (%)	21.47	13.15	7.90	3.71	

We calculate the throughput with equation (3.3). According to Figure 5.27, with increasing data load size, the throughput increases until it reaches 768 bytes. In this simulation, it is the most optimum packet size discovered. By increasing the size, the channel must be occupied for a more extended time, which can increase the chance of more data collisions. The fitness function in MPRP-GA degrades the effect of congestion and collision. Therefore, the MPRP-GA shows the best throughput performance followed by MPRP-FFn. MPRP-GA throuput improves 21.47, 13.15, 7.90 and 3.71 percent compared to EHO-AOMDV, TA-AOMDV, MPRP and MPRP-FFn, respectively, according to table 5.7.

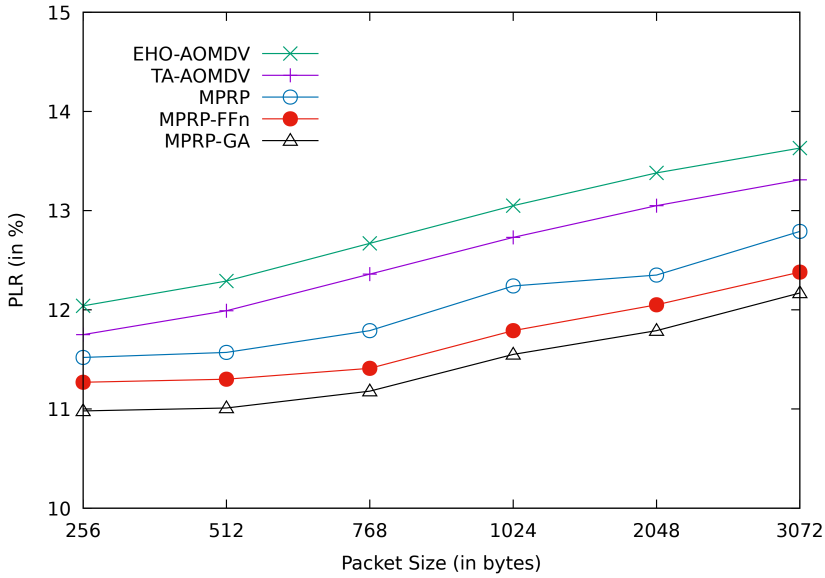

Fig. 5.28: Comparison between the proposed protocols of MPRP-GA and MPRP-FFn with MPRP, TA-AOMDV and EHO-AOMDV for PLR over various packet sizes.

The lowest PLR of MPRP-GA agrees with the throughput performance in Figure 5.28. We use equation (3.2) to calculate PLR. When we have a larger data packet, the number of packets we could transmit is less; therefore, when a packet fails to deliver either by data collision or data congestion, it has a higher impact on PLR.

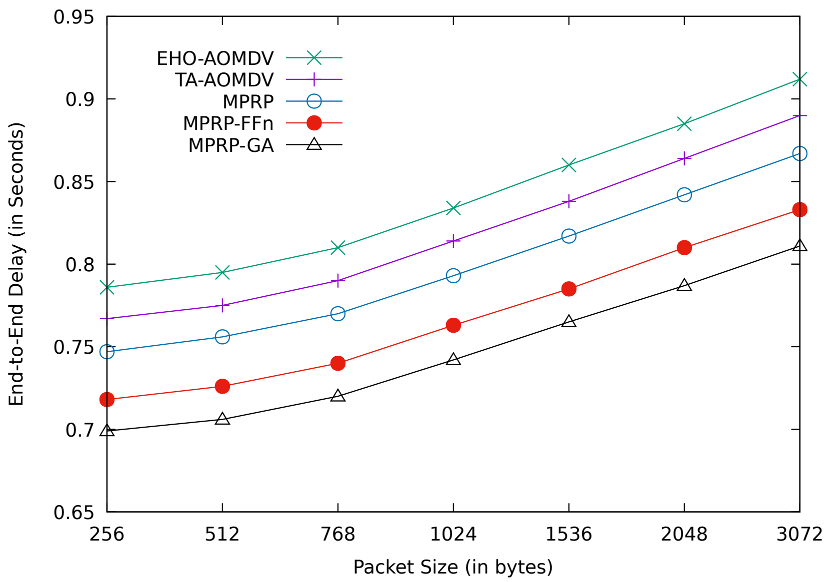

Fig. 5.29: Comparison between the proposed protocols of MPRP-GA and MPRP-FFn with MPRP, TA-AOMDV and EHO-AOMDV for average E2E over various packet sizes.

E2E shows a steady grow in Figure 5.29. When the size of the data packet increases, the queueing time increases. MPRP-GA promises a better e2e delay than others due to using RTT and fitness function as the route optimization mechanism.

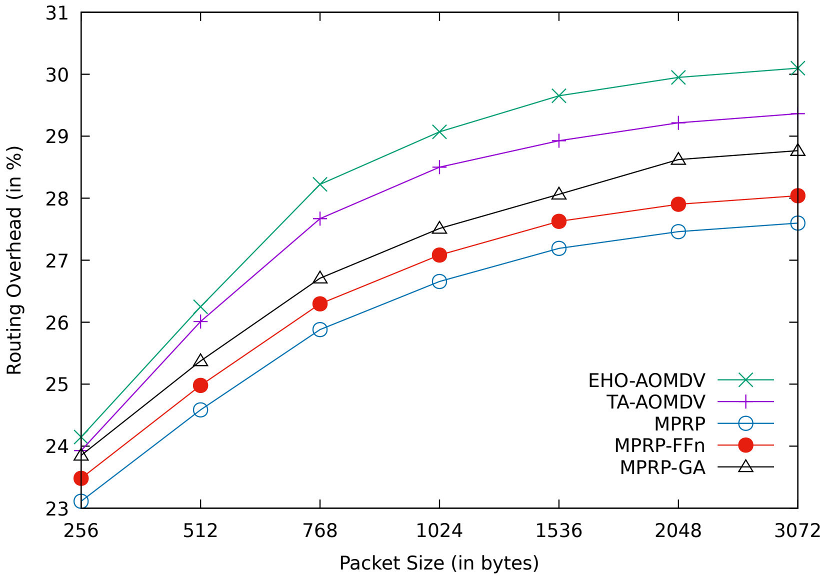

Fig. 5.30: Comparison between the proposed protocols of MPRP-GA and MPRP-FFn with MPRP, TA-AOMDV and EHO-AOMDV for routing overhead over various packet sizes.

Similar to the PLR, routing overhead increases as the packet size grows. A fewer number of data packets is required to transmit the same amount of data. Therefore the ratio of routing loads over data loads increases. Figure 5.30 depicts the explained fact. MPRP has the lowest routing overhead, followed by MPRP-FFn and MPRP-GA. The AOMDV based routing overhead is a result of their route discovery mechanism.

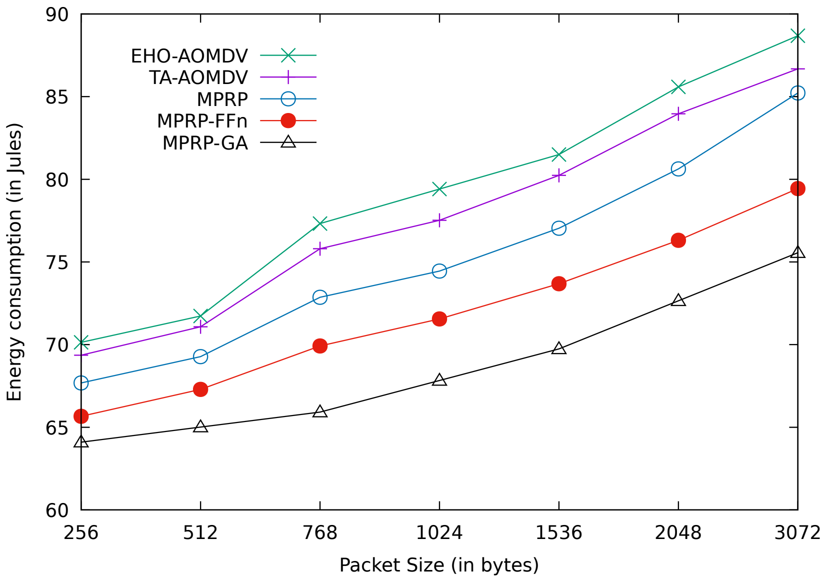

Fig. 5.31: Comparison between the proposed protocols of MPRP-GA and MPRP-FFn with MPRP, TA-AOMDV and EHO-AOMDV for energy consumption over various packet sizes.

More energy is needed when our network is more engaged with data transmission, according to Figure 5.31. MPRP-GA and MPRP-FFn show better performance in energy metrics due to their route stability and avoiding congestion. Additionally, the MPRP based protocols are not optimizing residual energy. In a short period, it provides better performance, but it can affect the network's life-time, which is not a concern For VANETs.

5.4 Routing Protocol Analysis

According to the [82], any general genetic optimization algorithm has a time complexity of $O(n^k)$, where n represents the population length, k represents the chromosome length, and O is the worst-case scenario. Therefore, with a larger size of the input, the genetic algorithm is considered an NP-complete problem. In this regard, we employ GA on MPRP, which implicitly degrades the population size as well as chromosome length by applying a threshold mechanism. In this study, we used the vector data structure to obtain the routes list; therefore, the sorting of efficient routes list also imposes $O(n \times log(n))$ time complexity to the algorithm.

The all the MPRP based protocols rely on RTT, which requires clock synchronization to calculate the exact RTT [80]. The importance of the clock accuracy increases in MPRP-FFN and MPRP-GA due to their dependency on RTT to calculate the deviation mentioned in equation (5.4) of fitness function.

Another crucial matter in the development of routing protocols is protocol heterogeneity. MPRP can work beside AODV as to the similarity of routing packets and data packet header. As to MPRP-FFn and MPRP-GA the structure of routing packets requires alteration to a address the objective of the protocol. However, the proposed protocols can work along side of other routing protocols using standard IP data packet header.

Using the link-disjoint mechanism in MPRP-GA and MPRP-FFn increases the number of routing packets replicas in the network. Therefore, the routing overhead is significantly higher in the MPRP-GA and MPRP-FFn, which is necessary for the proposed genetic algorithm. Having a higher routing overhead for the proposed protocols in this chapter is a trade-off to achieve better performance in other QoS metrics.

Chapter 6

Conclusion and future works

In this thesis, we propose a Multi-Path Routing Protocol called MPRP that makes use of the round trip time (RTT) to perform packet transmission tasks to the destination node in VANETs. The main idea in the MPRP routing protocol is the implementation of centralized network intelligence in one component of the network to reduce the time taken while maintaining the consensus between source and destination for efficient packet data transmission. Most of the data communications between vehicles should go through the Road-Side Unit (RSU) to control packets transmission and reduce the data traffic in the network. MPRP primarily selects the optimum route that has the minimum RTT, and this implies a route that has the least traffic problems such as data congestion and collision. Optimum routes should have RTT that is shorter than a threshold value which is set as the average RTT. This mechanism secures a short route to the RSU. It hence reduces the possibility of having packet loss that may occur with high-speed mobility vehicles getting further away from the RSU. This, in turn, would speed up the transmission of alert messages between vehicles and therefore lessens having vehicle accidents. Moreover, MPRP reduces the data retransmissions, and this minimizes the data traffic load to deliver the normal messages promptly. The performance of the proposed MPRP is assessed by simulations and compared to other protocols. MPRP exhibits an increase in the rate of successfully delivered packets over AOMDV, FF-AOMDV, EGSR, QMR and ISR, respectively. The novelty of our routing algorithm is obvious when error bars are used where overlapping with other protocols does not happen in most of the performance metrics. The overall simulation results show that MPRP can greatly improve the performance of data communications in VANETs even as the number of vehicles increases.

Additionally, this thesis propose a routing protocol optimizing routes based on the developed fitness function MPRP-FFn. The main idea of developing these protocols is to improve the performance of MPRP by introducing a more robust mechanism considering the network's characteristics and VANETs' topological characteristics. Hence, we employ TCP CERL+ to determine the network's data congestion. To evaluate the network topology, we introduce two metrics of density and mobility speed. By considering given metrics, we introduce a fitness function as the optimization mechanism in MPRP-FFn. Then we enhance the proposed protocol by employing the genetic algorithm MPRP-GA. Both the protocols the routes obtained by MPRP within the RTT threshold. This, in turn, eliminates routes with long E2E delays and the possibility of having long-range communication is eliminated. The routing protocols employ the fitness function for each discovered route in MPRP-FFn and the generated routes in the case of MPRP-GA. Then, the routing protocols select the route with the highest fitness for data communication until the link fails and the next one is selected. Both the proposed protocols exhibit improvement of packet delivery ratio compared to MPRP, TA-AOMDV and EHO-AOMDV, respectively. The end-to-end delay significantly improved, resulting from avoiding lengthy routes considering the MPRP threshold and route optimization mechanism.

Despite the significant improvement of the proposed protocol compared to the studied ones, we plan to study these protocols with two new functionality. In our work, we overlook the importance of the load-balancing rule to mitigate network congestion. Therefore it is necessary to add this component to our work. Additionally, a method of link connectivity prediction would help to reduce the chance of link failure. Therefore, if the routing protocol senses a suspicious link, it eliminates the route from the routing table.

Bibliography

References

[1] Z. Lu, G. Qu, and Z. Liu, "A survey on recent advances in vehicular network security, trust, and privacy," *IEEE Transactions on Intelligent Transportation Systems*, 2019.

[2] X. Wen, J. Chen, Z. Hu, and Z. Lu, "A p-opportunistic channel access scheme for interference mitigation between v2v and v2i communications," *IEEE Internet of Things Journal*, 2020.

[3] R. Atallah, M. Khabbaz, and C. Assi, "Multihop v2i communications: A feasibility study, modeling, and performance analysis," *IEEE Transactions on Vehicular Technology*, 2017.

[4] S. Ji, J. Kim, and C. You, "Cadma: collision-avoidance directional medium access for vehicular ad hoc networks," *Wireless Networks*, 2016.

[5] A. A. Aouiz, S. B. Hacene, and P. Lorenz, "Channel busyness based multipath load balancing routing protocol for ad hoc networks," *IEEE Network*, 2019.

[6] R. Tian and B. Zhang, "Routing for vehicular ad hoc networks," 2020.

[7] A. Bhardwaj and H. El-Ocla, "Multipath routing protocol using genetic algorithm in mobile ad hoc networks," *IEEE Access*, vol. 8, no. 1, pp. 177 534–177 548, 2020.

[8] C. Chen, L. Liu, T. Qiu, D. O. Wu, and Z. Ren, "Delay-aware grid-based geographic routing in urban vanets: A backbone approach," *IEEE/ACM Transactions on Networking*, vol. 27, no. 6, pp. 2324–2337, 2019.

[9] S. Kim, "Impacts of mobility on performance of blockchain in vanet," *IEEE Access*, vol. 7, pp. 68 646–68 655, 2019.

[10] M. A. Gawas, M. Mulay, and V. Bhatia, "Cross layer approach for neighbor node selection in vanet routing," in *2018 11th International Symposium on Communication Systems, Networks & Digital Signal Processing (CSNDSP)*. IEEE, 2018, pp. 1–6.

[11] M. Bhagyavathi and V. Saritha, "Energy and velocity-based multipath routing protocol for vanet," *International Journal of Advanced Intelligence Paradigms*, vol. 12, no. 3-4, pp. 239–253, 2019.

[12] J. Liu, Q. Wang, C. He, K. Jaffrès-Runser, Y. Xu, Z. Li, and Y. Xu, "Qmr: Q-learning based multi-objective optimization routing protocol for flying ad hoc networks," *Computer Communications*, vol. 150, pp. 304–316, 2020.

[13] J. Cheng, G. Yuan, M. Zhou, S. Gao, Z. Huang, and C. Liu, "A connectivity-prediction-based dynamic clustering model for vanet in an urban scene," *IEEE Internet of Things Journal*, vol. 7, no. 9, pp. 8410–8418, 2020.

[14] V. V. Chetlur and H. S. Dhillon, "Success probability and area spectral efficiency of a vanet modeled as a cox process," *IEEE Wireless Communications Letters*, vol. 7, no. 5, pp. 856–859, 2018.

[15] W. Ahsan, M. F. Khan, F. Aadil, M. Maqsood, S. Ashraf, Y. Nam, and S. Rho, "Optimized node clustering in vanets by using meta-heuristic algorithms," *Electronics*, vol. 9, no. 3, p. 394, 2020.

[16] T. Saedi and H. El-Ocla, "Tcp cerl+: revisiting tcp congestion control in wireless networks with random loss," *Wireless Networks*, vol. 27, no. 1, pp. 423–440, 2021.

[17] S. A. Alghamdi, "Load balancing maximal minimal nodal residual energy ad hoc on-demand multipath distance vector routing protocol (lbmmre-aomdv)," *Wireless Networks*, vol. 22, 2016.

[18] "Advances in vehicular ad-hoc networks (vanets): Challenges and road-map for future development," 2016.

[19] A. M. E. Ejmaa, S. Subramaniam, Z. A. Zukarnain, and Z. M. Hanapi, "Neighbor-based dynamic connectivity factor routing protocol for mobile ad hoc network," *IEEE Access*, vol. 4, pp. 8053–8064, 2016.

[20] S. R. Yahiabadi, B. Barekatain, and K. Raahemifar, "Tihoo: An enhanced hybrid routing protocol in vehicular ad-hoc networks," *Eurasip Journal on Wireless Communications and Networking*, vol. 2019, 2019.

[21] A. Taha, R. Alsaqour, M. Uddin, M. Abdelhaq, and T. Saba, "Energy efficient multipath routing protocol for mobile ad-hoc network using the fitness function," *IEEE Access*, vol. 5, 2017.

[22] D. Rewadkar and D. Doye, "Multi-objective auto-regressive whale optimisation for traffic-aware routing in urban vanet," vol. 12, 2018.

[23] "Fd-aomdv: fault-tolerant disjoint ad-hoc on-demand multipath distance vector routing algorithm in mobile ad-hoc networks," *Journal of Ambient Intelligence and Humanized Computing*, vol. 10, 2019.

[24] F. Abbas, P. Fan, and Z. Khan, "A novel low-latency v2v resource allocation scheme based on cellular v2x communications," *IEEE Transactions on Intelligent Transportation Systems*, vol. 20, 2019.

[25] J. Liu, F. Ding, and D. Zhang, "A hierarchical failure detector based on architecture in vanets," *IEEE Access*, vol. 7, 2019.

[26] A. S. Awad, K. S. Alheety, and A. N. Rashid, "An optimal path selection using lion optimization routing protocol for mobile ad-hoc network," *Periodicals of Engineering and Natural Sciences (PEN)*, vol. 8, no. 4, pp. 2346–2357, 2020.

[27] M. Macit, V. C. Gungor, and G. Tuna, "Comparison of qos-aware single-path vs. multi-path routing protocols for image transmission in wireless multimedia sensor networks," *Ad hoc networks*, vol. 19, pp. 132–141, 2014.

[28] K. N. Qureshi, S. Din, G. Jeon, and F. Piccialli, "Link quality and energy utilization based preferable next hop selection routing for wireless body area networks," *Computer Communications*, vol. 149, pp. 382–392, 2020.

[29] B. H. Khudayer, M. Anbar, S. M. Hanshi, and T.-C. Wan, "Efficient route discovery and link failure detection mechanisms for source routing protocol in mobile ad-hoc networks," *IEEE Access*, vol. 8, pp. 24 019–24 032, 2020.

[30] S. Sarhan and S. Sarhan, "Elephant herding optimization ad hoc on-demand multipath distance vector routing protocol for manet," *IEEE Access*, vol. 9, pp. 39 489–39 499, 2021.

[31] X. Wang, Y. Weng, and H. Gao, "A low-latency and energy-efficient multimetric routing protocol based on network connectivity in vanet communication," *IEEE Transactions on Green Communications and Networking*, 2021.

[32] D.-G. Zhang, L. Chen, J. Zhang, J. Chen, T. Zhang, Y.-M. Tang, and J.-N. Qiu, "A multi-path routing protocol based on link lifetime and energy consumption prediction for mobile edge computing," *IEEE Access*, vol. 8, pp. 69 058–69 071, 2020.

[33] "Multi-metric geographic routing for vehicular ad hoc networks," *Wireless Networks*, vol. 24, 2018.

[34] I. A. Abbasi, A. S. Khan, and S. Ali, "A reliable path selection and packet forwarding routing protocol for vehicular ad hoc networks," *Eurasip Journal on Wireless Communications and Networking*, vol. 2018, 2018.

[35] G. Sun, L. Song, H. Yu, V. Chang, X. Du, and M. Guizani, "V2v routing in a vanet based on the autoregressive integrated moving average model," *IEEE Transactions on Vehicular Technology*, vol. 68, 2019.

[36] F. Goudarzi, H. Asgari, and H. S. Al-Raweshidy, "Traffic-aware vanet routing for city environments-a protocol based on ant colony optimization," *IEEE Systems Journal*, vol. 13, 2019.

[37] "Opportunistic directional location aided routing protocol for vehicular ad-hoc network," *Wireless Personal Communications*, vol. 110, 2020.

[38] K. N. Qureshi, F. U. Islam, O. Kaiwartya, A. Kumar, and J. Lloret, "Improved road segment-based geographical routing protocol for vehicular ad-hoc networks," *Electronics*, vol. 9, no. 8, p. 1248, 2020.

[39] K. N. Qureshi, A. H. Abdullah, J. Lloret, and A. Altameem, "Road-aware routing strategies for vehicular ad hoc networks: Characteristics and comparisons," *International Journal of Distributed Sensor Networks*, vol. 12, no. 3, p. 1605734, 2016.

[40] D. Lin, J. Kang, A. Squicciarini, Y. Wu, S. Gurung, and O. Tonguz, "Mozo: A moving zone based routing protocol using pure v2v communication in vanets," *IEEE Transactions on Mobile Computing*, vol. 16, 2017.

[41] A. Abuashour and M. Kadoch, "Performance improvement of cluster-based routing protocol in vanet," *IEEE Access*, vol. 5, pp. 15 354–15 371, 2017.

[42] "Time barrier-based emergency message dissemination in vehicular ad-hoc networks," *IEEE Access*, vol. 7, 2019.

[43] J. Wu, M. Fang, H. Li, and X. Li, "Rsu-assisted traffic-aware routing based on reinforcement learning for urban vanets," *IEEE Access*, vol. 8, pp. 5733–5748, 2020.

[44] M. Naseem and C. Kumar, "Congestion-aware fibonacci sequence based multipath load balancing routing protocol for manets," *Wireless Personal Communications*, vol. 84, no. 4, pp. 2955–2974, 2015.

[45] T. Mori, K. Hirata, and M. Yamamoto, "Content-oriented probabilistic routing with measured rtt," in *2016 IEEE International Workshop Technical Committee on Communications Quality and Reliability (CQR 2016)*. IEEE, 2016, pp. 1–6.

[46] L. Hai, Q. Gao, J. Wang, H. Zhuang, and P. Wang, "Delay-optimal back-pressure routing algorithm for multihop wireless networks," *IEEE Transactions on Vehicular Technology*, vol. 67, no. 3, pp. 2617–2630, 2018.

[47] K. Haseeb, N. Abbas, M. Q. Saleem, O. E. Sheta, K. Awan, N. Islam, W. ur Rehman, and T. Salam, "Rcer: Reliable cluster-based energy-aware routing protocol for heterogeneous wireless sensor networks," *PloS one*, vol. 14, no. 9, p. e0222009, 2019.

[48] M. Naseem, G. Ahamad, S. Sharma, and E. Abbasi, "Ee-lb-aomdv: An efficient energy constraints-based load-balanced multipath routing protocol for manets," *International Journal of Communication Systems*, p. e4946, 2021.

[49] L. Zhu, C. Li, B. Li, X. Wang, and G. Mao, "Geographic routing in multilevel scenarios of vehicular ad hoc networks," *IEEE Transactions on Vehicular Technology*, vol. 65, no. 9, pp. 7740–7753, 2016.

[50] X. Yang, M. Li, Z. Qian, and T. Di, "Improvement of gpsr protocol in vehicular ad hoc network," *IEEE Access*, vol. 6, pp. 39 515–39 524, 2018.

[51] T. Qiu, X. Wang, C. Chen, M. Atiquzzaman, and L. Liu, "Tmed: A spider-web-like transmission mechanism for emergency data in vehicular ad hoc networks," *IEEE Transactions on Vehicular Technology*, vol. 67, no. 9, pp. 8682–8694, 2018.

[52] Y. Xia, X. Qin, B. Liu, and P. Zhang, "A greedy traffic light and queue aware routing protocol for urban vanets," *China Communications*, vol. 15, no. 7, pp. 77–87, 2018.

[53] D.-G. Zhang, P.-Z. Zhao, Y.-y. Cui, L. Chen, T. Zhang, and H. Wu, "A new method of mobile ad hoc network routing based on greed forwarding improvement strategy," *IEEE Access*, vol. 7, pp. 158 514–158 524, 2019.

[54] S. H. Bouk, S. H. Ahmed, D. Kim, and H. Song, "Named-data-networking-based its for smart cities," *IEEE Communications Magazine*, vol. 55, no. 1, pp. 105–111, 2017.

[55] R. Hou, S. Zhou, M. Cui, L. Zhou, D. Zeng, J. Luo, and M. Ma, "Data forwarding scheme for vehicle tracking in named data networking," *IEEE Transactions on Vehicular Technology*, vol. 70, no. 7, pp. 6684–6695, 2021.

[56] S. Tiennoy and C. Saivichit, "Using a distributed roadside unit for the data dissemination protocol in vanet with the named data architecture," *IEEE Access*, vol. 6, pp. 32 612–32 623, 2018.

[57] X. Guo, Y. Chen, L. Cao, D. Zhang, and Y. Jiang, "A receiver-forwarding decision scheme based on bayesian for ndn-vanet," *China Communications*, vol. 17, no. 8, pp. 106–120, 2020.

[58] A. Dowling, L. Huie, L. Njilla, H. Zhao, and Y. Liu, "Toward long-range adaptive communication via information centric networking," *Intelligent and Converged Networks*, vol. 2, no. 1, pp. 1–15, 2021.

[59] M. Centenaro, L. Vangelista, A. Zanella, and M. Zorzi, "Long-range communications in unlicensed bands: the rising stars in the iot and smart city scenarios," *IEEE Wireless Communications*, vol. 23, no. 5, pp. 60–67, 2016.

[60] X. Guo, S. Yang, L. Cao, J. Wang, and Y. Jiang, "A new solution based on optimal link-state routing for named data manet," *China Communications*, vol. 18, no. 4, pp. 213–229, 2021.

[61] M. A. K. Saluja and M. S. A. Darg, "A detailed analogy of network simulators ns1, ns2, ns3 and ns4," *International Journal on Future Revolution in Computer Science & Communication Engineering*, vol. 3, no. 12, pp. 291–295, 2017.

[62] D. Krajzewicz, J. Erdmann, M. Behrisch, and L. Bieker, "Recent development and applications of sumo-simulation of urban mobility," *International journal on advances in systems and measurements*, vol. 5, no. 3&4, 2012.

[63] Z. Chen, W. Zhou, S. Wu, and L. Cheng, "An adaptive on-demand multipath routing protocol with qos support for high-speed manet," *IEEE Access*, vol. 8, pp. 44 760–44 773, 2020.

[64] U. F. C. Commission, "Amendment of the commission's rules regarding dedicated short-range communication services in the 5.850-5.925 ghz band (5.9 ghz band)," *Fcc 02-302A1*, vol. 5558, 2002.

[65] X. Guo, Y. Chen, L. Cao, D. Zhang, and Y. Jiang, "A receiver-forwarding decision scheme based on bayesian for ndn-vanet," *China Communications*, vol. 17, no. 8, pp. 106–120, 2020.

[66] Y. L. Morgan, "Notes on dsrc & wave standards suite: Its architecture, design, and characteristics," *IEEE Communications Surveys and Tutorials*, vol. 12, 2010.

[67] "Multicast capacity for vanets with directional antenna and delay constraint," *IEEE Journal on Selected Areas in Communications*, vol. 30, 2012.

[68] D. Mirkovic, G. Armitage, and P. Branch, "A survey of round trip time prediction systems," *IEEE Communications Surveys and Tutorials*, vol. 20, 2018.

[69] B. A. A. Nunes, K. Veenstra, W. Ballenthin, S. Lukin, and K. Obraczka, "A machine learning framework for tcp round-trip time estimation," *Eurasip Journal on Wireless Communications and Networking*, vol. 2014, 2014.

[70] Z. Bian, G. Zhang, and D. Bian, "Modeling the rtt of bundle protocol over asymmetric deep-space channels," *Journal of Communications and Information Networks*, vol. 1, 2016.

[71] W. Du, Y. Liao, N. Tao, P. Geurts, X. Fu, and G. Leduc, “Rating network paths for locality-aware overlay construction and routing,” *IEEE/ACM Transactions on Networking*, vol. 23, 2015.

[72] Z. Ahmed, S. Naz, and J. Ahmed, “Minimizing transmission delays in vehicular ad hoc networks by optimized placement of road-side unit,” *Wireless Networks*, vol. 26, no. 4, pp. 2905–2914, 2020.

[73] Y. Tian, K. Xu, and N. Ansari, “Tcp in wireless environments: Problems and solutions,” *IEEE Communications Magazine*, vol. 43, 2005.

[74] M. Oche, A. B. Tambuwal, C. Chemebe, R. M. Noor, and S. Distefano, “Vanets qos-based routing protocols based on multi-constrained ability to support its infotainment services,” *Wireless Networks*, vol. 26, no. 3, pp. 1685–1715, 2020.

[75] N. J. Jevtic and M. Z. Malnar, “Novel etx-based metrics for overhead reduction in dynamic ad hoc networks,” *IEEE Access*, vol. 7, pp. 116 490–116 504, 2019.

[76] L. Sun, G. Tian, G. Zhu, Y. Liu, H. Shi, and D. Dai, “Multipath ip routing on end devices: Motivation, design, and performance,” in *2018 IFIP networking conference (IFIP networking) and workshops*. IEEE, 2018, pp. 1–9.

[77] A. Boudi and M. Loudini, “Active queue management exploiting the rate information in tcp-ip networks,” *IEEE/CAA Journal of Automatica Sinica*, vol. 5, no. 1, pp. 223–231, 2018.

[78] L. Feltrin, G. Tsoukaneri, M. Condoluci, C. Buratti, T. Mahmoodi, M. Dohler, and R. Verdone, “Narrowband iot: A survey on downlink and uplink perspectives,” *IEEE Wireless Communications*, vol. 26, no. 1, pp. 78–86, 2019.

[79] E. M. Ar-Reyouchi, K. Ghoumid, D. Ar-Reyouchi, S. Rattal, R. Yahiaoui, and O. Elmazria, “d-to-ean accelerated ennd probing protocol for narrowband iot medical devices,” *IEEE Access*, vol. 9, pp. 34 131–34 141, 2021.

[80] C. Lee, C. Park, K. Jang, S. Moon, and D. Han, “Dx: Latency-based congestion control for datacenters,” *IEEE/ACM Transactions on Networking*, vol. 25, no. 1, pp. 335–348, 2016.

[81] M. Altayeb and I. Mahgoub, “A survey of vehicular ad hoc networks routing protocols,” *International Journal of Innovation and Applied Studies*, vol. 3, no. 3, pp. 829–846, 2013.

[82] B. Rylander, T. Soule, and J. Foster, “Computational complexity, genetic programming, and implications,” pp. 348–360, 2001.